THE PHYSICAL PROPERTIES (SEDIMENTATION, DIFFUSION AND COAGULATION) OF AEROSOLS.

Thesis

Submitted for the Degree of

Doctor of Philosophy in the

Faculty of Science, University

of London.

by

Eric R. Wooding B. Sc. A.R.C.S.

Department of Chemical Engineering
and Applied Chemistry,

Imperial College of Science and Technology,

London, S.W.7

June, 1953

Acknowledgements.

The author wishes to express his gratitude to Professor D.M. Newitt F.R.S. for supervision of the work, to Dr. J.H. Burgoyne for general guidance and to Dr. J.F. Richardson for continued advice and encouragement.

He is grateful to Messrs. J. Locke and C. Morse for their assistance in construction of the apparatus.

The author is also indebted to the British Shipbuilding Research Association for sponsoring the investigation.

CONTENTS.

		Figures	(i)
		Tables	(ii)
		Abstract	(iii)
Chapter	I	Introduction	1
	II	The physical properties of an aerosol	4
	III	Preliminary experiments	17
	IV	Review of previous work	27
	V	Theory of concentration changes	35
	VI	Formation of a monodisperse aerosol	47
	VII	The photographic observations	55
	VIII	The photometric technique	102
	IX	Measurement of mass concentration	121
	X	Discussion of coalescence	127
	XI	Conclusion	141
Appendix	A1	Relaxation solution of equations derived in chapter V.	
Appendix	A2	Sedimentation of polydisperse aerosols	
		Nomenclature	
		References	

FIGURES

		Following Page.
3.1	General arrangement of apparatus in preliminary experiments.	17
3.2	The aerosol generator.	17
3.3	The sedimentation cell.	18
3.4	The sampling valve.	19
3.5	The projection microscope.	20
3.6	The spread factor.	21
3.7	Typical size distribution in polydisperse aerosols.	21
3.8	Distribution of particles over microscope slide.	23
5.1	The numerical concentration caused by sedimentation of an aerosol in a closed vessel.	35
5.2	The numerical concentration caused by diffusion of an aerosol in a closed vessel.	35
5.3	The numerical concentration caused by sedimentation and diffusion of an aerosol in a closed vessel.	35
5.4	The numerical concentration caused by sedimentation, diffusion and coagulation of an aerosol in a closed vessel.	35
5.5	Values of ϕ_c in the Z T plane	45
6.1	The monodisperse aerosol generator.	49
6.2	The nucleus source.	50
6.3	Temperature distribution in the condensation tube	51

6.4	Electron micrograph of nuclei.	52
6.5	Mass concentration of dinonyl phthalate aerosol.	53
6.6	Numerical concentration for a given current in the nucleus source.	53
6.7	Numerical concentration as function of mass concentration.	54
7.1	General arrangement of apparatus used in photographic observations.	55
7.2	The parameter α .	56
7.3	The parameter γ .	56
7.4	General view of apparatus.	57
7.5	Details of the observation cell.	58
7.6	Exploded view of the cell.	59
7.7	Principle of the cell.	59
7.8	Detail of the slides.	59
7.9	Method of filling the cell.	59
7.10	Details of the slit.	60
7.11	Cross section of the beam.	60
7.12	Profile of the beam.	60
7.13	Photomicrograph of initial concentration.	62
7.14	Photomicrograph of zero of experiment.	62
7.15	Photomicrograph of particle size.	62
7.16	Photomicrograph of concentration.	62
7.17	Photomicrograph of particle size.	62
7.18	Photomicrograph of concentration.	62
7.19	Photomicrograph of concentration.	62
7.20	Photomicrograph of concentration.	62

7.21	Photomicrograph of dimensions of beam.	70
7.22	Elements of volume of observation cell.	70
7.23	The error caused by overlapping of images.	78
7.24	Typical concentration distributions in the cell.	92a
7.25	Experimental values of the parameter α .	100
8.1	Diagram of the photometric apparatus.	102
8.2	Circuit diagram of the photometer.	103
8.3	Details of the photometer.	104
8.4	Optical system of the photometer.	105
8.5	Angle of acceptance of the photometer.	105
8.6	Linearity of the photometer. Facing Page	110
8.7	Angular distribution of light scattered by the aerosol - theoretical.	113
8.8	Angular distribution of light scattered by the aerosol - experimental.	113
8.9	Position of maxima for different radii.	114
8.10	Variation of concentration of the aerosol with time and position.	118
8.11	Variation of concentration with time.	119
8.12	Compensation for flicker of the arc.	120
9.1	Apparatus for the determination of mass concentration.	122
9.2	The condensation coil.	123
9.3	Quick release valve.	124
A1.1	The relaxation network.	A1.1
A1.2	The relaxation operator.	A1.2

TABLES.

		Page
3.1	Distance of particles from leading edge of microscope slide in sedimentation cell	23
4.1	Investigation of diffusion in a field of force	31
6.1	Characteristics of materials used	54a
7.1	The photographs used in a typical observation	64
7.2	Number of particles observed in each element of the cell	67
7.3	Determination of particle size	68
7.4	The unsmoothed value of n	72
7.5	Smoothed values of the numerical concentration n	74
7.6	The first differences of c	75
7.7	Values of the relative concentration c	76
7.8	Results of a typical experiment A 126	79
7.9	Typical values and their accuracy	92a
7.10	Characteristics of aerosols observed	99a
8.1	Particle size measured by photometer technique	116
9.1	Examination of filter media	123
10.1	Proportion of each type of collision in a charged aerosol	134

ABSTRACT

The physical changes which affect the concentration of an aerosol have been investigated. In a monodisperse aerosol of particle size 0.1 to 2 microns and of high concentration, the changes due to the combined effects of sedimentation, diffusion and coagulation have been observed experimentally. A differential equation has been developed which relates the concentration of particles with time and position and comparisons havebbeen made between calculated and experimental values.

The aerosol was produced by the condensation of a vapour on suitable nuclei under controlled conditions and the observations were made in an ultramicroscope cell 2 millimetres deep and of such diameter that changes in the vertical direction predominated.

Two methods of observations were used. In the first, the measurements were made on photomicrographs; particle size was determined by measuring the distance which a particle fell in 5 seconds and numerical concentration was determined at intervals of 10 to 30 seconds using a short exposure. This method was limited to concentrations of less than 10^7 particles per cubic centimetre where individual particles could be distinguished.

For higher concentrations a photometer was used. This consisted of a photomultiplier, a narrow band-width amplifier and an ammeter. Particle size was determined from the angular

distribution of the scattered light and concentration changes were followed by measuring the intensity of light scattered at a fixed angle.

Experimental results were compared graphically and numerically and satisfactory agreement was obtained. Further, a relation has been obtained for the efficiency of coagulation in an electrically charger aerosol.

CHAPTER I.

INTRODUCTION.

An aerosol is a dispersion of a large number of small particles or droplets in a gas. It is an unstable two phase system and an investigation of certain physical phenomena which cause changes in its properties is described in this thesis. The work is complementary to an investigation of the combustion characteristics of oil mists and more particularly of those mists which are responsible for explosions which sometimes occur in the crankcase of marine diesel engines. Explosions of this kind are propagated in an oil mist formed by the evaporation of lubricating oil from an overheated surface in the crankcase with subsequent condensation of the vapour in a cooler region. It has been shown that the mist is combustible if the concentration of oil is sufficiently high but further information is required concerning the changes in its concentration with time and certain characteristic properties, such as coagulation.

A preliminary study of oil mists produced by condensation showed that they contained large numbers of liquid droplets of radii in the range 0.2 to 5 microns; further, at the lower limit of inflammability, the concentration was about 10^{-4} grams. of oil per cubic centimetre of gas.

In the past, much research has been carried out on the

physics of aerosols, but most of the systems examined have been too complex to permit of adequate control of the variables. Numerous physical phenomena affect the concentration and it is frequently impossible to separate their effects completely, so that it is necessary to consider the interaction of two of them. The important causes of concentration changes in an aerosol are sedimentation, diffusion, coagulation and to some extent, phase changes. The variation of concentration with time at any point is given by two differential equations: in one, the aerosol may be considered to be so dilute that the probability of binary collisions of the particles is negligible, and in the other, a term is introduced to account for such collisions.

The first equation was derived by von Smoluchowski (1915) and relates the concentration in a dilute aerosol to the effect of sedimentation and diffusion. Davies (1949) has published solutions subject to certain boundary conditions but it does not appear that they have been subjected to experimental verification. The second equation, for a more concentrated aerosol makes use of von Smoluchowski's (1916) theoretical equation. Its derivation appears on page 4C.

The two relations have been examined experimentally using monodisperse aerosols formed from liquids of low vapour pressure so that phase changes were inappreciable. The measurements were

made in a specially designed cell where the environment of the aerosol could be very carefully controlled. At low concentrations, measurements were carried out with the aid of photomicrographs obtained with an ultramicroscope. More concentrated aerosols were studied with a photometer.

CHAPTER II

THE PHYSICAL PROPERTIES OF AN AEROSOL.

II. 1 The characteristics of an aerosol.

The more important characteristics of an aerosol are particle size and shape, concentration and the physical properties of the two phases. The range of particle size may vary considerably and can be represented by a distribution function; for most purposes however, it is adequate to use the dispersion $\mathcal{D}$ which is defined as the ratio of the standard deviation $\sigma(a)$ of the particle radius a to the arithmetic mean radius $\bar{a}$.

$$\text{i.e.} \qquad \mathcal{D} = \frac{\sigma(a)}{\bar{a}} \qquad (1)$$

When the dispersion is less than 0.1, the aerosols are referred to as monodisperse and when it is greater than 0.1, as polydisperse (La Mer 1952).

In this thesis, the aerosols considered are dispersions of small spherical drops produced by condensation of involatile liquids.

II. 2 The physical phenomena which occur in an aerosol.

There are two types of physical process which may be observed in an aerosol; those which are intrinsic properties and those which may be induced. Some of them cause irreversible changes

in the particle concentration or changes in particle size, while others cause no observable change whatsoever.

The various phenomena may conveniently be discussed under the following headings :-

1. Those which are the result of motion of the gas molecules.
2. The dynamical properties of the small particles.
3. Phase changes.
4. Those produced by electromagnetic radiation.

II. 2. 1. The physical properties resulting from the molecular motion of the gas.

The molecules of a gas are in continuous random motion and if a particle of radius comparable with the mean free path of a gas molecule is introduced, it is subjected to bombardments which cause an irregular motion, called the Brownian Motion. The velocities of the particles obey the Maxwell-Boltzman Law and the probability $\omega(u)$ of a velocity u is :-

$$\omega(u) = \frac{m}{(2\pi kT)^{\frac{3}{2}}} \exp \frac{-m|u|^2}{2kT} \qquad (2)$$

The result of the random motion is to cause diffusion, and according to Fick's Law (1885), the rate at which particles pass through unit area, normal to the concentration gradient $\text{grad}_r\, n$ is:-

$$\frac{dn}{dt} = -D \, \text{grad}_r \, n$$

(3)

Einstein (1906) showed the diffusivity to be

$$D = \frac{kT}{6\pi\eta a}$$

(4)

As the radius of the particles is comparable with the mean free path of the gas molecules, they behave as if the medium is discontinuous and equation (4) is modified by the 'slip factor' F.

$$D = \frac{kT}{6\pi\eta a} F$$

(5)

Knudsen and Weber (1911) showed this factor to have a value given by

$$F = 1 + \frac{\lambda}{a}\left[0.882 + 0.28 \exp\left(-1.57 \frac{a}{\lambda}\right)\right] \quad (6)$$

The rate at which the numerical concentration increases in a small element of volume is given by Fick's second law of diffusion:-

$$\frac{dn}{dt} = D \nabla^2 n$$

(7)

From equation (4) it is seen that the diffusivity is inversely

proportional to the radius of a particle. Eventually the particles impinge on the walls of their container and may adhere. The boundary conditions in diffusion problems can be represented by the conditions :-

$n = 0$ at the wall for particles which are completely absorbed.

and $\frac{\partial n}{\partial r} = 0$ if perfect reflection occurs.

The brownian motion also causes particles to collide with one another and if coalescence occurs, two particles of radius a form one of radius $2^{1/3}a$. Von Smoluchowski (1916) derived a relation for the rate of change of concentration due to coagulation, namely :-

$$\frac{dn}{dt} = -8\pi D a n^2 \tag{8}$$

$$= -Kn^2 \tag{9}$$

Substituting from equation (4), it is seen that the coagulation coefficient K is given by

$$K = \frac{4}{3}\frac{kT}{\eta} F \tag{10}$$

In deriving this relationship it was assumed that all the particles coalesced on collision; an assumption which will be discussed further in Chapter X.

It is seen that the rate of coagulation increases as the square

of the concentration and is related to the particle radius only through the slip factor.

Some less important consequences of the molecular motion in the gaseous phase are rotation of the droplets, coagulation in a streaming aerosol and the drift of a particle in a temperature gradient.

II. 2.2. The dynamical properties of the particles.

If a particle in a fluid is acted upon by a force, it will be accelerated to a velocity at which the resistive force $6\pi\eta a v$ is equal to the accelerating force. This expression is valid provided that the flow is streamline, that the fluid behaves as a continuum and that there is no interfenence from other particles or from the walls of the container.

If the radius of the particles is comparable with the mean free path of the gas molecules the resistance is reduced by the slip factor F.

In the gravitational field, the accelerating force is

$$\frac{4}{3}\pi a^3 (\rho - \rho_0) g \qquad (11)$$

so that the terminal velocity is given by

$$v = \frac{2}{9}\frac{a^2}{\eta} g (\rho - \rho_0) F \qquad (12)$$

Davies (1947) showed that this relation had an error of less than 1 % for radii up to 17 microns and for $(\rho - \rho_0)$ equal to 1gm.cm^{-3}.

The terminal velocity increases as the square of the radius. It is unaffected by other particles unless the concentration is considerably greater than 10^{-4} gm.cm.$^{-3}$. The effect of neighbouring particles has been studied by Bergers (1942) who showed that the velocity was decreased by factor

$$\frac{1}{1 + 6.875\,V} \qquad (13)$$

where V is the volume occupied by the particles in unit volume of aerosol.

The velocity is also modified by the proximity of a surface and at a vertical distance z from a plane horizontal surface, the velocity is decreased by a factor

$$\left(1 + \frac{9}{8}\frac{a}{z}\right) \qquad (14)$$

Happer and Grant(1948) showed that this factor was valid if $\frac{z}{a} > 20$.

Merrington and Richardson (1947) have shown that droplets are no longer spherical if the ratio $\frac{a^2 g}{\gamma}(\rho - \rho_0)$ is greater than 0.39 but this figure is not reached with droplets of the

materials examined until the radius is 200 microns.

A particle may also acquire a determinate velocity under the action of a centrifugal force, sonic vibrations, an electric field, or intense radiation. Only the last effect need be considered here.

The radiation falling normally on a plane surface exerts a pressure

$$p_n = 2 \frac{s}{c}$$

where s is the Poynting vector

c is the velocity of light.

(See Joos 1934)

Hence, when an electromagnetic radiation of intensity I_o is incident on a particle of radius a, the pressure is given approximately by the equation

$$p = \frac{2\pi I_o a^2}{c} \qquad (16)$$

II. 2.3. Phase changes in an aerosol.

Phase changes may occur due to evaporation from the surface of the droplets, to condensation or to spontaneous nucleation.

The rate at which a particle grows or evaporates is dependant

on its radius, on the concentration of the vapour and its physical properties. The relation obtained by Bradley et al (1946) for the evaporation of a particle of radius a is

$$a\frac{dq}{dt} = -\frac{D_i m_i c_o}{\rho}\left[\frac{1}{\frac{a}{a+\Delta} + \frac{D_i}{a\nu\alpha}}\right] \qquad (17)$$

where D_i is the diffusivity of the vapour molecules

m_i is the mass of a single vapour molecule

c_o is the concentration of the vapour molecules

ρ is the density of the liquid

$$\Delta = \frac{kT}{AP}$$

A is the collision area for a gas molecule and an evaporating molecule

P is the gas pressure

$$\nu = \left(\frac{kT}{2\pi m_i}\right)^{\frac{1}{2}}$$

α is the coefficient of accommodation of molecules at the surface of the drop (≤ 1)

This equation applied equally well to condensation if the negative sign is removed.

When the radius of the droplet is very small, the vapour pressure p at the surface exceeds the saturation vapour pressure p_∞ at a plane surface in the ratio given by

$$\ln \frac{p}{p_\infty} = \frac{2\gamma m_1}{\rho k T a} \qquad (18)$$

This equation was derived by Thomson (Lord Kelvin) (1881), and is known as the Kelvin effect. A calculation shows that for D.N.P.* p/p_∞, at room temperature, has a value of 1.11 for a particle of radius 0.1 microns.

The rate of evaporation of such a small particle must be written

$$a\frac{da}{dt} = \frac{D_1 m_1 c_\infty}{\rho}\left[\frac{1}{\frac{a}{a+\Delta} + \frac{D_1}{a+d}}\right]\exp\frac{2m_1\gamma}{\rho k T_a} \qquad (19)$$

If large numbers of particles condense simultaneously, they will compete for the vapour molecules and Reiss (1951) has shown that in a condensing aerosol the rate of growth of a particle is :-

$$a\frac{da}{dt} = \frac{D_1 m_1 c_\infty}{\rho}\left[1 - \exp(-\chi B t)\right] - 2D_1 a^3 n. \qquad (20)$$

* Di-n-nonyl phthalate.

where γ is the rate of cooling ^{o}C/sec.

β is the constant in the vapour concentration relation

$$\ln c = A + BT$$

n is the number of particles per cu.cm.

This equation approximates to the relation for the ratio of growth of a single particle at constant temperature. It may be integrated to give :-

$$a^2 = a_o^2 + F(t) \qquad (21)$$

Consequently, if the original radius a_o was a very small fraction of the final radius a , this would depend almost entirely on a function F(t) of the environment of the particle and if a number of such particles commence growth at the same instant, a monodisperse aerosol results.

The third type of phase change, spontaneous nucleation, occurs when the vapour becomes sufficiently supersaturated, and Becker and Döring (1935) have shown the nuclei to be aggregates of molecules which grow during random collisions in the vapour. These aggregates become stable if they exceed a critical radius a_c and the rate of formation J is given by the relation :-

$$J = \frac{c_o X v}{q_c} \left(\frac{4\pi a_c^2 \gamma}{kT}\right)^{\frac{1}{2}} \exp\left(\frac{-4\pi a_c^2 \gamma}{3kT}\right) \qquad (22)$$

striking the surface

where X is the number of molecules cm^{-2} sec^{-1}

v is the volume occupied by one molecule in the liquid phase.

II. 2.4 The effect of electromagnetic radiation.

An incident beam of light has a negligible effect on the physical properties of an aerosol, but the way in which light is scattered is characteristic of the particle size and concentration. If the radius of a particle is considerably larger than the wavelength then the incident light is refracted according to the laws of geometric optics. However, this is no longer true if the radius is comparable to the wavelength of the incident light, as diffraction occurs and the light is scattered in all directions.

For a single transparent dielectric sphere, the total amount of light scattered was shown by Rayleigh (1903) to be

$$s = 24\pi^3 I_o \left(\frac{m^2 - 1}{m^2 + 2}\right)\left(\frac{4/3\,\pi a^3}{\lambda^4}\right)^2 \qquad (23)$$

m is the refractive index of the material of the sphere

I_o is the incident intensity of illumination

and $\frac{a}{\lambda} < 0.1$

The intensity of the light scattered at an angle θ to the

incident light is given by the relation which was obtained by Mie (1908)

$$I_\theta = \frac{9\pi^2}{2R^2} I_o \left(\frac{m^2 - 1}{m^2 + 2}\right) \frac{\left(4/3\,\pi a^3\right)^2}{\lambda^4} \left(1 + \cos^2\theta\right) \quad (24)$$

R is the distance from the particle to the point of observation, where $R >> a$ and $a/\lambda < 1$

This assumes the incident light to be unpolarised and in the case of a plane polarised wave being incident on the particle the relation becomes

$$I_\theta = \frac{9\pi^2}{R^2} I_o \left(\frac{m^2 - 1}{m^2 + 2}\right) \frac{\left(4/3\,\pi a^3\right)^2}{\lambda^4} \frac{\sin^2\theta}{4} \quad (25)$$

where $R >> r$ and $a/\lambda < 1$

If the radius of the particle is of the same order as the wavelength of light so that $a/\lambda \longrightarrow 1$, then the relations become very complex, The total light scattered by a single particle

$$s = \frac{\lambda^2}{2\pi} I_o \sum_{\nu=1}^{\infty} \frac{a_\nu^2 + p_\nu^2}{2\nu + 1} \quad (26)$$

where a_ν and p_ν are complex functions of $\frac{2\pi a}{\lambda}$ and $\frac{2\pi am}{\lambda}$ Each particle scatters an amount of light KI_o, per unit cross sectional area, so that

$$K = \frac{2}{\alpha^2} \sum_{\nu=1}^{\infty} \frac{a_\nu^2 + p_\nu^2}{2\nu+1} \qquad (27)$$

where $\alpha = \frac{2\pi a}{\lambda}$

and the intensity of the light scattered at an angle γ to the incident direction is

$$I_\theta = \frac{\lambda^2}{8\pi^2 R^2} I_o \ (i_1 + i_2) \qquad (28)$$

where $\gamma = \pi - \theta$

The function i_1 is the component of the scattered light with its electric vector perpendicular to the plane of observation and i_2 has its electric vector perpendicular to i_1.

The functions K_1, i_1, i_2, a_ν and p_ν have been tabulated by Lowan (1949) for several values of refractive index and the parameter α.

The optics of small spherical particles has been discussed by Van der Hulst (1946) who considers the phenomena observed in a range of values of a/λ, and also the effect of absorption by the particles.

The radiation pressure exerted by any electromagnetic radiation has been mentioned in section II. 2.2 of this discussion.

CHAPTER III.

PRELIMINARY EXPERIMENTS

III. 1.

A preliminary investigation was made to determine the important characteristics of the oil aerosols, the relative magnitudes of the changes in concentration and the conditions for more precise experiments.

The observations were made by means of a microscope using samples from a polydisperse aerosol. The samples were collected in a sedimentation cell and the droplets were allowed to settle on to a microscope slide. Samples were taken at two points s_1 and s_2 (figure 3.1) as the aerosol flowed through a vertical tube of 4 cms. diameter.

III. 2. The aerosol generator.

The aerosol was formed by rapid condensation of oil vapour in the apparatus shown in figure 3.2. In the evaporator A, a stream of nitrogen was saturated with oil vapour at 500°C and passed through the jet B, into the mixing chamber C, where it was mixed with a second stream of nitrogen D cooled to -100°C. Consequently the vapour was cooled, became highly supersaturated and condensation occurred . To obtain a steady flow of gas and vapour, the two steams of nitrogen were obtained from a

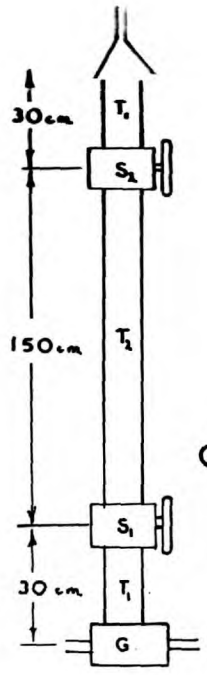


FIGURE 3·1. GENERAL ARRANGEMENT OF APPARATUS.

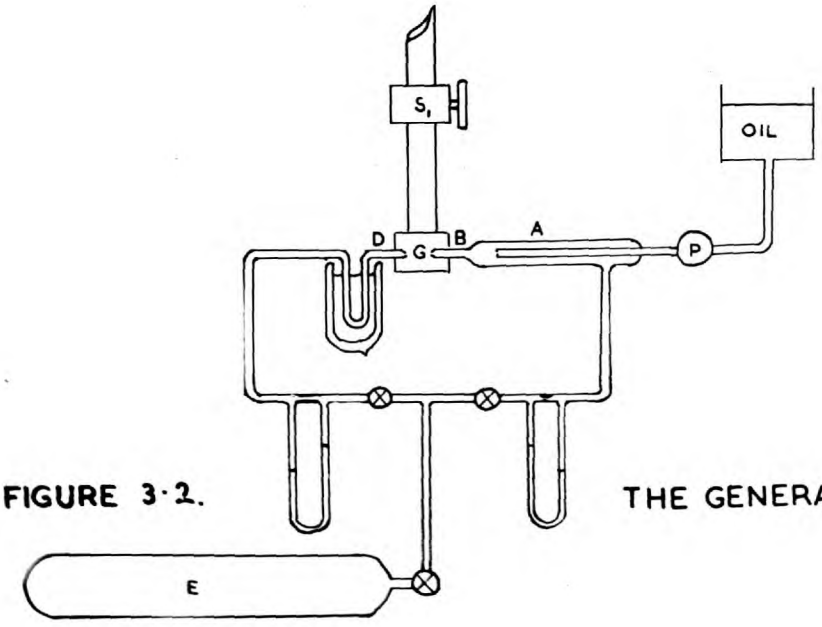


FIGURE 3·2. THE GENERATOR.

100 cu. ft. cylinder E and the oil was fed into the evaporator by means of a pump P driven by a motor with an electronic control. The oil used was 'Telpa 30' having a vapour pressure of less than 10^{-4} cms. mercury at room temperature.

Aerosols of mass concentration up to 10^{-4} gm.cm.$^{-3}$ were obtained with this apparatus but they were lacking in spatial homogeneity and their concentration varied with time.

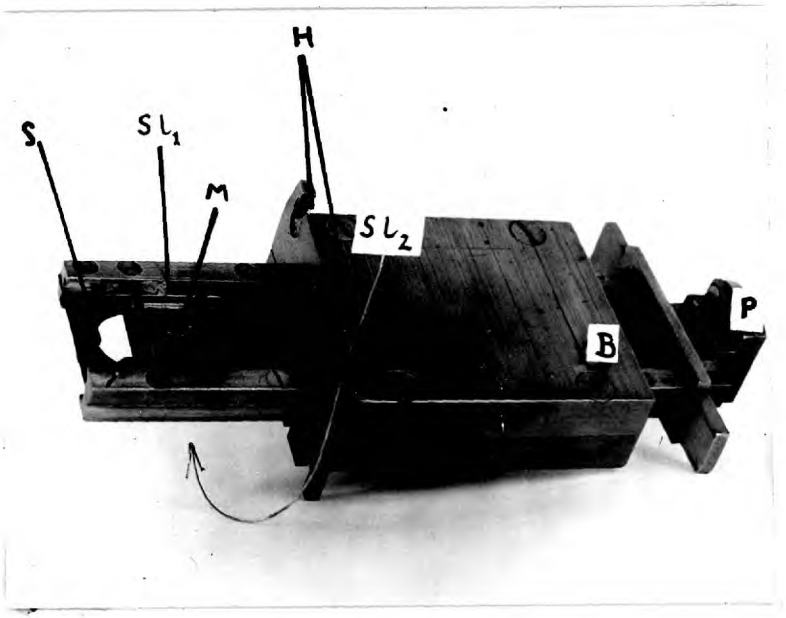
III.3. Analysis of the aerosols.

A microscope and sedimentation cell were used for the examination of the droplets since this method was direct and the apparatus could be assembled quickly.

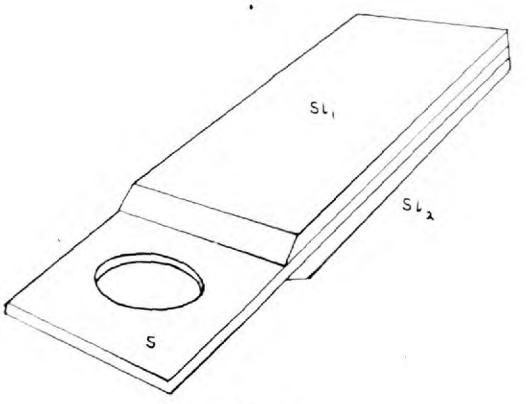
III. 3.1. Sampling the aerosol.

It was necessary to obtain a representative sample of the aerosol and to collect all the particles in it on a slide where they could be measured . The sedimentation cell (figure 3.3) was made sufficiently shallow to limit the number of particles which overlap one another. It consisted of two slides Sl_1 and Sl_2 separated by a spacer S, 0.01 cms. thick and having a circular hole of 1 cm. diameter. A glass plate M, 2 cms. square was fitted into the lower slide. By means of a plate P, the two slides could be moved simultaneously to enclose a known volume of aerosol. The slides and spacer were housed in a metal block B which could be bolted to the apparatus.

The Sedimentation Cell



3.3a



3.3 b.

figure 3.3

Samples of an aerosol which was initially flowing, were isolated by means of a special valve (figure 3.4). When open, this valve presented no obstruction to the aerosol (figure 3,4b) but when closed (figure 3.4c) a stationary volume of aerosol was isolated and a sample could be extracted with the sedimentation cell.

Before using the sedimentation cell, the glass plate was chemically cleaned and passed through a bunsen flame. On such a surface, the droplets spread to a lens shape and the radius of the droplets were calculated from the dimensions of this lens. This calculation was described by May (1945) and is based on two relations obtained by C.N. Davies.

$$\frac{F}{2r} = \frac{1}{2(m-1)\sin\theta} + \frac{1}{2}\tan\frac{\theta}{2} \qquad (1)$$

$$\frac{a}{r} = \frac{1}{2^{1/3}}\left[1 - \left(1 + \frac{r^2}{2R^2}\right)\left(1 - \frac{r^2}{R^2}\right)\right]\cos\theta \qquad (2)$$

a is the true radius of the drop

r is the radius of the lens formed on the glass

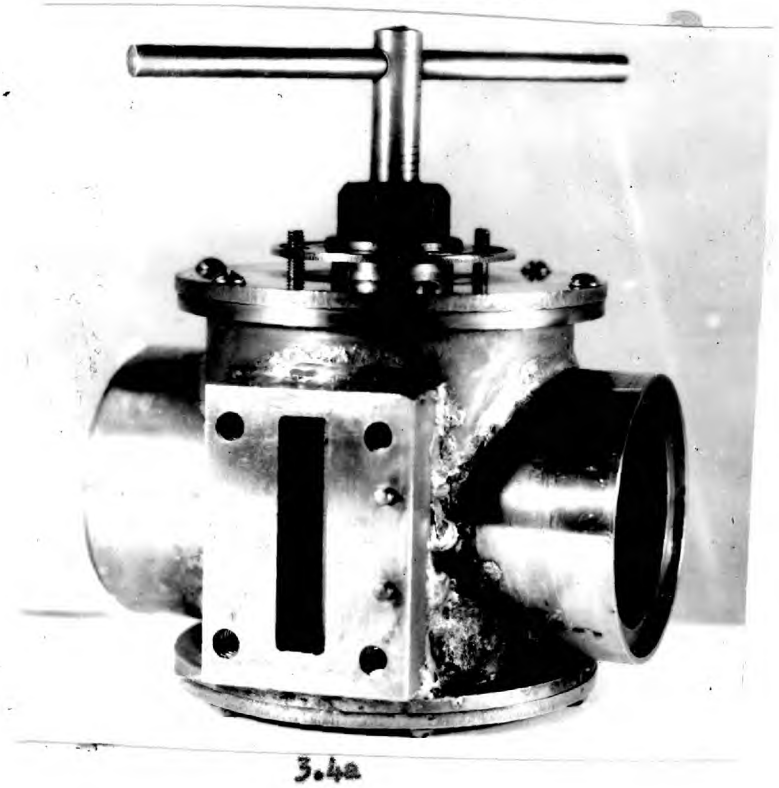
R is the radius of curvature of the convex surface of the lens

θ is the angle of contact of the liquid with the glass

m is the refractive index of the liquid with regard to oil

F is the distance of the focal point of the lens from the glass surface

The Sampling Valve



3.4a

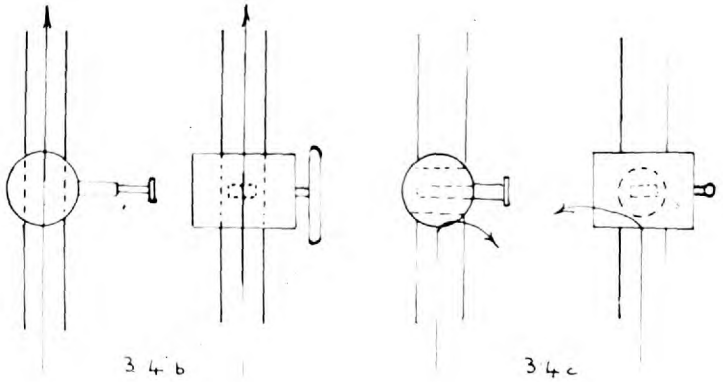


figure 3.4

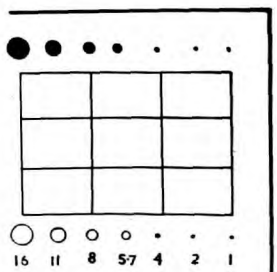
Graphical solutions were obtained by plotting $\frac{r}{2r}$ against θ and $\frac{a}{r}$ against θ. Some values of the 'spread factor' $\frac{a}{r}$ are plotted in figure 3.7

It was found impossible to determine the factor for a lens of radius less than $\frac{1}{2}$ microns and the curve was extrapolated to smaller radii although such a procedure is not strictly justified. The spread factor was found to be critically dependant on the surface of the slide and although the glass surface was carefully treated for each experiment the results were not very reproducible. The surface was coated with several materials, such as aqueous wetting agents, silicones and organic esters without greatly diminishing the spread, and although polytetrafluoethylene gave good results, it could be obtained with neither a sufficiently smooth surface nor in transparent films.

One advantage of the spread was to enable smaller drops to be observed. The limit of resolution of the microscope was 0.5 microns and a liquid lens of this diameter was produced by a droplet of 0.1 microns radius.

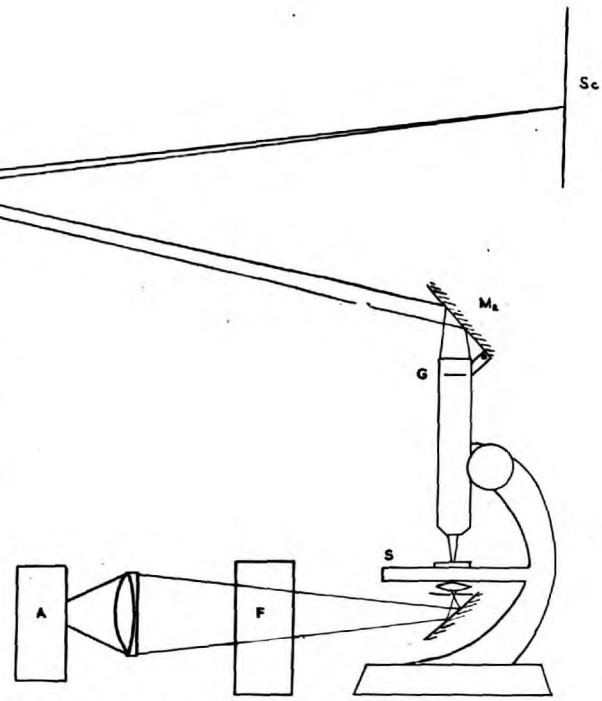
III. 3.2 The microscope

A projection microscope (figure 3.5) was arranged so that an observer could focus the image or move the object while



FAIRS GRATICULE.

FIGURE 3·5a



THE PROJECTION MICROSCOPE.

FIGURE 3·5

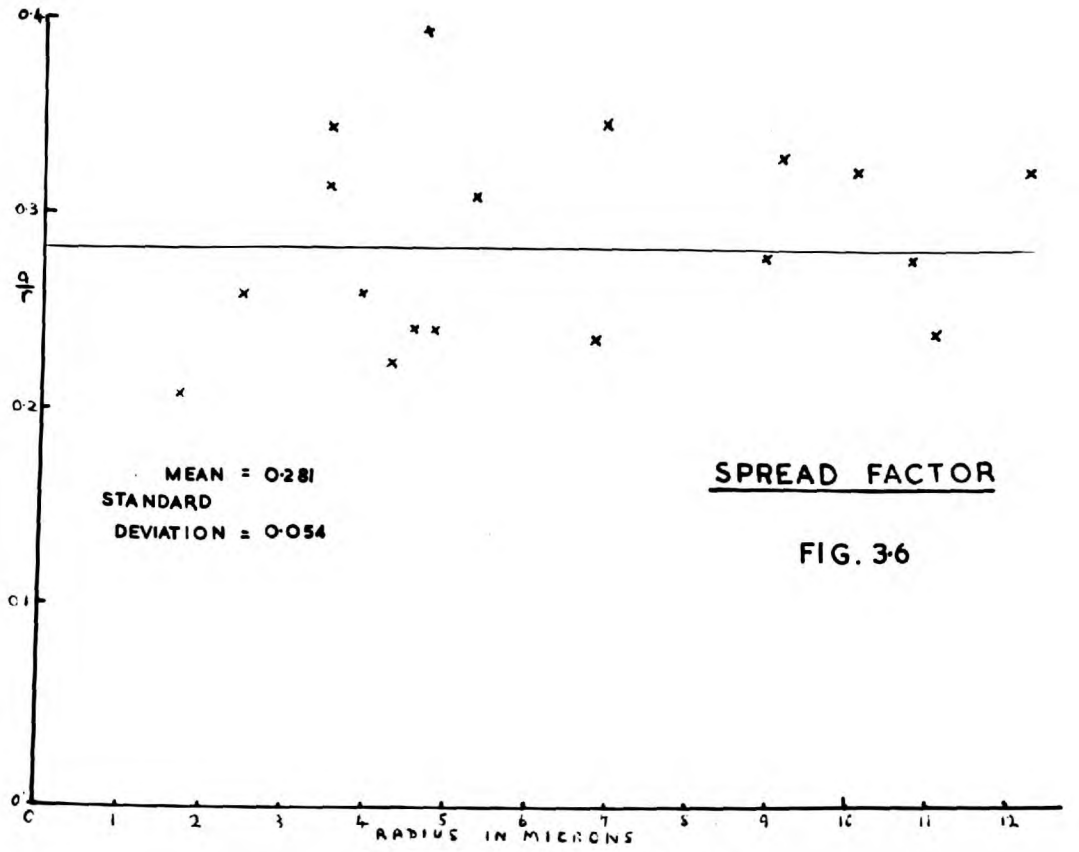
looking at the screen S. Light was supplied by a mercury arc A, heat rays were absorbed in the filter F, lenses were achromatic and mirrors M_2 and M_3 were front-silvered to give optimum definition. Objectives of 4, 16 and 25 mm. focal length were used in conjunction with an eyepiece of power x 10, giving a maximum magnification of 1200 times and a limit of resolution of just under 0.5 microns.

III. 3.3 The analysis

The size distribution was determined by the procedure described by Fairs (1943). The image of a graticule G (figure 3.5) fitted in the eyepiece of the microscope was superimposed on the images of the particles and each particle which occupied part of the ruled area was compared with the black circles and dots and could then be placed in any one of the 6 intervals of radius between 0.5 and 8 microns. The analysis was recorded with the aid of an electromagnetic counter which consisted of two banks of 5 counters. Of these 9 could be operated by micro switches and the tenth counter recorded every time a switch was depressed. With this simple piece of apparatus 9 different groups of droplets could be counted and the total number determined simultaneously.

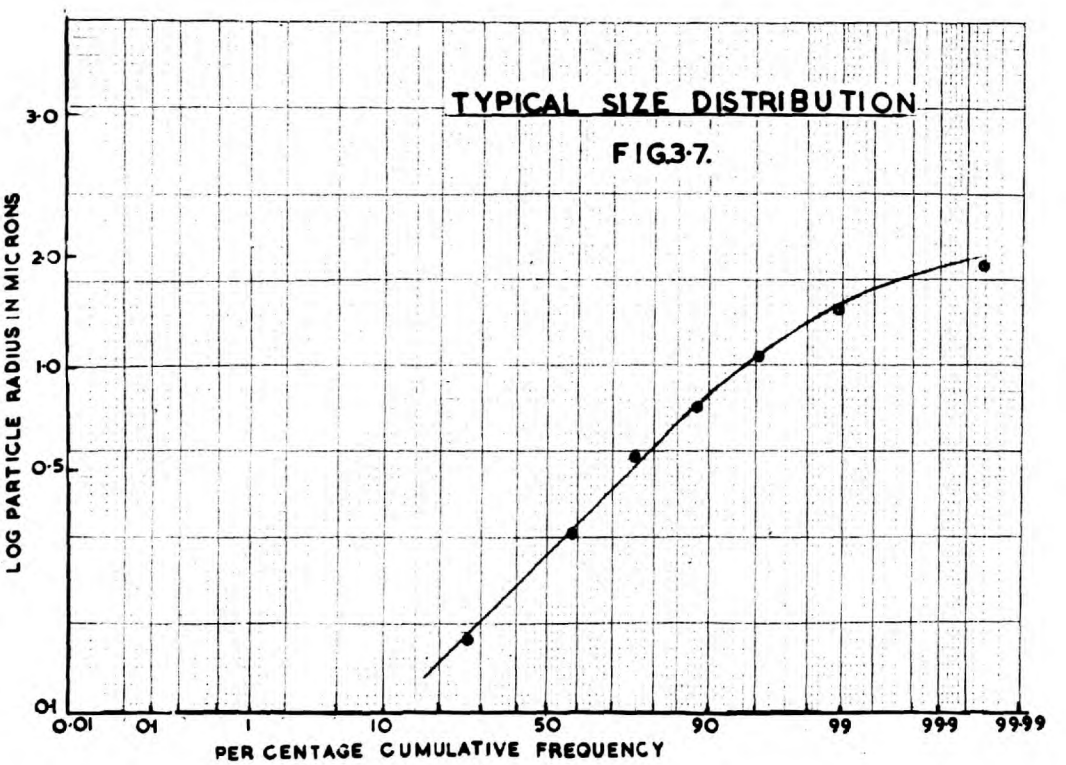
III. 3.4 Criticism of the sedimentation cell.

The sample of droplets collected on the lower slide of the sedimentation cell was found to be unrepresentative for the



SPREAD FACTOR

FIG. 3·6



following reasons :-

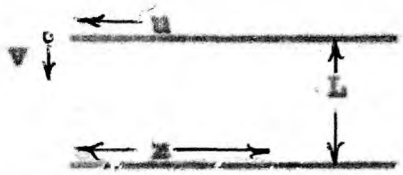
(a) The error due to particles overlapping one another.

To prevent an appreciable proportion of particles overlapping on the slide, the number present should be less than 10^6 cm.$^{-2}$, assuming an average radius of 1 micron (Armitage 1949). To collect such a number from an aerosol of 10^9 particles cm^{-3} required a cell of depth 10^{-3} cms. In the sedimentation cell described, which was 0.013 cms. deep, the error in numerical concentration due to overlap was about 10%.

(b) The selective deposition of larger particles.

A particle of radius a , initially situated at the leading edge of the upper slide, would strike the lower slide at a distance x from its leading edge such that

$$x = \frac{uL}{v} \qquad (3)$$



where u is the velocity at which the slides close, u < 10^{-1} cm.sec.$^{-1}$

v is the sedimentation velocity of a particle of radius a

L is the separation of the slides = 0.013 cms.

The relative distance at which particles settle out are given in Table 3.1

Table 3.1

Radius of particle	Sedimentation velocity	Distance from leading edge
10 microns	1 cm.sec.$^{-1}$	10^{-3} cms.
1	10^{-3}	10^{-1}
0.1	10^{-4}	(10)

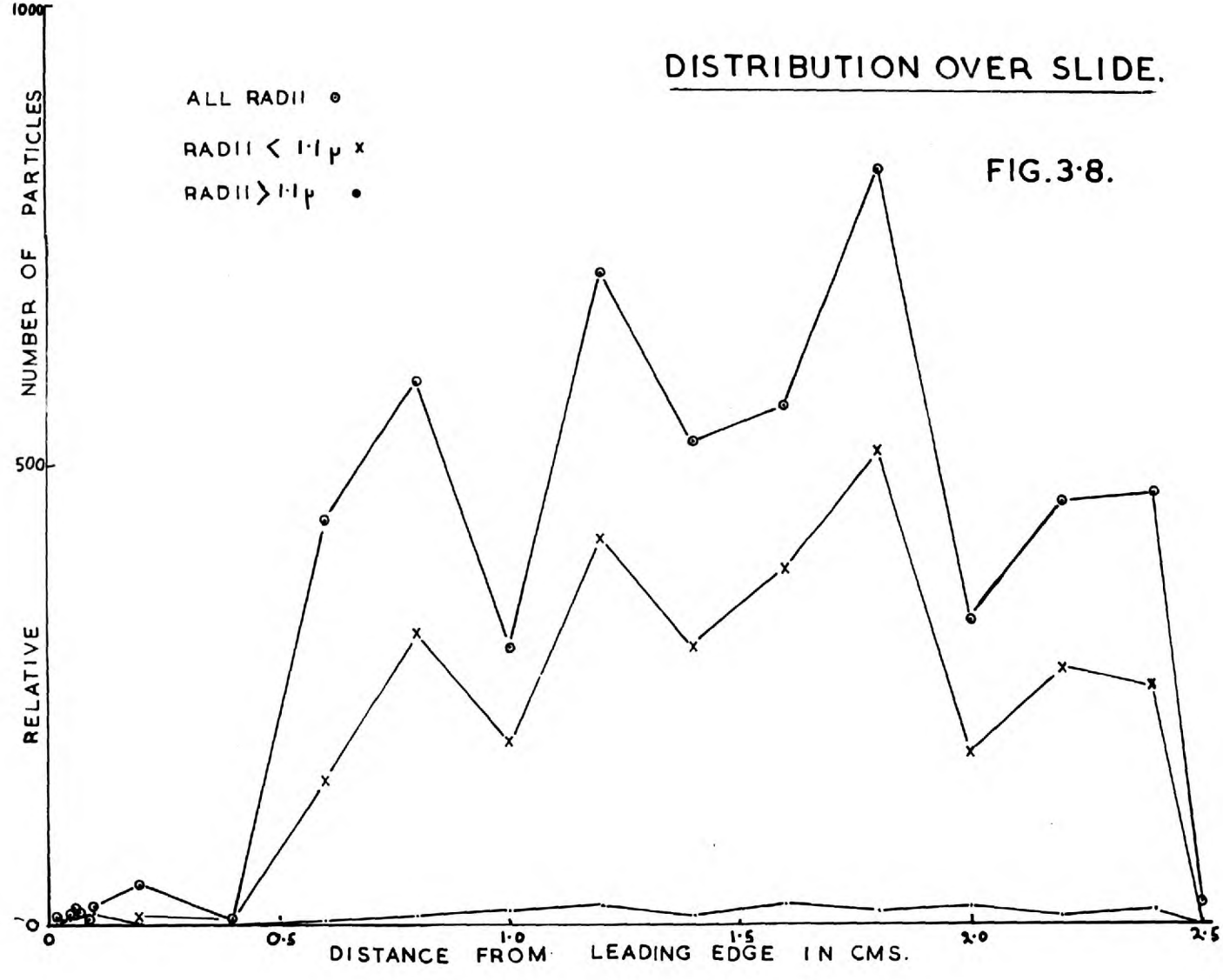
(Assuming the density of the particle is 1gm.cm^{-3} and u = 10^{-1}cm.sec.$^{-1}$)

It can be seen that, particles larger than 1 micron are deposited so near to the leading edge of the lower slide that they cannot be observed but smaller particles had adequate time to settle on the main area of the slide.

A measurement of the size distribution along the lower slide (figure 3.8) showed that particles of radius greater than 0.6 ± .1 microns were more thickly deposited in the first millimetre of the slide than elsewhere.

(c) Preferential deposition of smaller particles.

Particles of radii less than 0.5 microns diffuse appreciably and may strike the upper surface of the cell. An observation of this surface showed that particles of 0.4 microns and less were deposited


DISTRIBUTION OVER SLIDE.
FIG.3·8.
ALL RADII ⊙
RADII < 1·1 μ x
RADII > 1·1 μ •
RELATIVE NUMBER OF PARTICLES
1000
500
0
0
0·5
1·0
1·5
2·0
2·5
DISTANCE FROM LEADING EDGE IN CMS.

(d) The effect of turbulence.

If the slides were closed rapidly, turbulence was set up in the aerosol. In figure 3.8 it is seen that medium size particles were distributed uniformly over the surface of the slide, but the smaller ones appear in regions of high density. This turbulence may well have caused the smaller particles to be carried away from the cell.

(e) Error in the estimation of the radius of a particle.

The ease with which particles could be observed under the microscope depended on their optical properties, size and shape. Weil (1947) showed that the accuracy with which the diameter of opaque discs could be estimated was dependent on the contrast of the background. Consistent over-estimation (or under-estimation) of the particle size may be caused by this physiological effect.

(f) Spreading of the droplets.

The way in which the droplets spread depended on the nature of the glass surface and it was ~~not~~ possible to obtain neither reproducibility nor uniformity of surface. Consequently the spread factor could vary over the surface of the slide and from one slide to the next.

(g) Measurement of mass concentration.

A known volume of aerosol was drawn through a filter packed with slag wool and the increase in weight was determined.

III. 4. Characteristics of the aerosols examined.

From these preliminary experiments it was found that the aerosols were polydisperse and the dispersion had a value of 2 or 3. The particles observed had radii of 0.2 to 5 microns but it was possible that smaller particles were present but not detected. The mass concentration reached a value of 10^{-4} gm.cm^{-3} and consequently the numerical concentration might be as high as 10^{9} particles cm^{-3}.

III. 5 Conclusions.

It was found that consistent, spatially homogeneous aerosols were not produced by the generator and that the observations were made difficult because of the high dispersion. It was concluded therefore that it would be necessary to use monodisperse aerosols in subsequent work.

The method of analysis was unsatisfactory since the samples were unrepresentative, the droplets spread in an irregular manner and the aerosol was disturbed excessively during sampling .
In chapters VII and VIII, two methods of analysis are described which were selected because they were rapid and caused least disturbance in the aerosol.

Because of turbulence in the aerosol flowing through the observation tube, little indication of the magnitudes of sedimentation

evaporation and coagulation was obtained from these experiments. Consequently, in the work described in chapter VII, care is taken to ensure streamline flow from the generator, and complete absence of mass motion of the aerosol during the observations.

CHAPTER IV

REVIEW OF PREVIOUS WORK.

In the first section of this chapter, methods of analysis are discussed which may be utilised in the study of aerosols. The second section is devoted to a discussion of the effects of sedimentation, diffusion and coagulation.

IV. 1. Methods of analysis of aerosols.

In the preliminary experiments, it was demonstrated that the method of analysis should be such as to cause no disturbance in the aerosol and should be rapid and applicable to the measurement of particles of 0.05 to 5 microns. An optical method appeared to be most suitable.

Direct observation by means of a microscope is restricted by the very short working distance (c.a. 1 mm.) of microscope objectives which are capable of resolving the particles. Even so, it is impossible to resolve particles of less than 0.5 microns by this method.

An indirect method can be used depending upon the property of the particles to scatter sufficient light for a diffracted image to be formed by the microscope. This is the basis of a method (the ultramicroscope) first used by Zsigmondy and Siedentopf (1903) to count very small particles. The working distance of such a microscope is of the order of a centimetre and particles as small as

0.01 microns can be observed (Jander and Wygasch 1938). However, it is necessary to find some means of measuring the particles. Schwechendech (1950) determined radii as small as 0.1 microns from measurements of their sedimentation velocity of particles (of density 1 gm.cm.$^{-3}$). The brightness of the diffraction patterns of individual droplets were determined indirectly by Findeisen (1932) and used to measure particles size but the method was very tedious.

Other methods of measuring particle size and concentration utilise the optical properties described in chapter II. Sinclair (1950) has employed the theory of Mie (1908) to determine particle size and numerical concentration in monodisperse aerosols. Particle size was measured from the intensity of the transmitted light and from either the intensity or the degree of polarisation of the scattered light. The concentration was derived from measurements of the light transmitted or scattered.

The most convenient method of measuring mass concentration depends on the filtration of all the suspended material from a measured volume of the aerosol. There are two other methods worthy of brief mention. The first is the measurement of mass concentration by means of a small amount of radioactive material introduced into the droplets (Born and Zimmer 1940). The second is the method used by Jones (1941) to measure particles as small as 0.001 microns from the width of the diffracted lines in an X-ray pattern.

IV. 2. Investigation of the behaviour of aerosols.

It is convenient to discuss earlier work under the headings

1. Sedimentation and Diffusion.
2. Coagulation.
3. Factors which retard coagulation.
4. The combined effects of sedimentation, diffusion and coagulation.

IV. 2.1. Sedimentation and diffusion.

Stoke's expression for the resistive force experienced by a sphere moving through a fluid

$$f = 6\pi\eta a v \qquad (1)$$

was modified by Cunningham (1910) to account for the 'slip' effect (see page 6).

$$f = 6\pi\eta a v F \qquad (2)$$

Knudsen and Weber (1911) evaluated the slip factor and obtained the equation :-

$$F = 1 + \frac{\lambda}{a}\left[0.882 + 0.281 \exp\left(-1.57 \frac{a}{\lambda}\right)\right] \qquad (3)$$

Accurate determinations of the sedimentation velocities of small liquid spheres have been made by Millikan (1913) and Hopper and Laby (1941). Davies (1947) examined the validity of the Stokes - Cunningham law , and showed that the error increases with particle

size and is 1% for a particle of radius 17 microns in air. (Density of particle 1 gm.cm.$^{-3}$ in air at 20°C and 760 mm. Hg). Certain problems of distortion and circulation in liquid droplets were investigated by Merrington and Richardson (1947).

Many of the fundamental laws of diffusion have been examined experimentally and are described by Jost (1952). The study of the diffusion of colloidal particles has centred on an examination of the Brownian motion of single particles in a liquid. Einstein (1905) showed that the diffusivity of a particle of radius r was given by the relation

$$D = \frac{kT}{6\pi\eta a} \qquad (4)$$

This expression should be multiplied by the slip factor F. Westgren (1918) measured the diffusivity of small particles and used the result to calculate Avogadro's number N since

$$N = \frac{R}{k} \qquad (5)$$

where R is the gas constant

The relation expressing concentration changes due to diffusion in a field of force was derived by von Smoluchowski (1915)

$$\frac{dn}{dt} = D\frac{d^2n}{dx^2} - v\frac{dn}{dx} \qquad (6)$$

This equation has been solved for various boundary conditions when D is constant and v is the sedimentation velocity. Five different conditions are indicated in the table below.

Table 4.3

The problem of diffusion in a field of force.

Boundary Conditions		Investigation	
Upper surface	Lower surface	Theoretical	Experimental
Free	Free	von Smoluchowski (1915)	
Free	Reflecting	von Smoluchowski (1915); Fürth (1917)	Perrin (1916); Fürth (1917)
Free	Absorbing	Davies (1949)	
Reflecting	Reflecting	Mason and Weaver (1924)	
Absorbing	Absorbing	Davies (1949)	This Thesis

Perrin (1916) derived and verified the following expression for the density distribution of particles (or molecules) in the atmosphere.

$$n = n_o \exp. \left(\frac{-mgh}{kT} \right) \qquad (7)$$

where n_o is the numerical concentration at an arbitary zero

n is the concentration at a height h above the zero.

The relation was verified by observations on gamboge particles in water.

Fürth (1917) examined the probability distribution of single particles of gamboge and mercury in water when enclosed in a blood count cell and derived a theoretical relation assuming the surfaces to be reflecting.

IV. 2.2 Coagulation.

The following expression for the rate of coagulation was derived by von Smoluchowski (1917)

$$\frac{dn}{dt} = -Kn^2 \qquad (8)$$

where $K = \frac{4}{3}\frac{kT}{\eta}$

Patterson et al (1927) pointed out that the slip factor should be included.

$$K = \frac{4}{3}\frac{kT}{\eta}F \qquad (9)$$

In a later paper by the same authors (1929), the effect of a mixture of two particle sizes is discussed. They made a careful study of coagulation in ammonium chloride aerosols (1932) and obtained experimental values of K 20 to 25 % higher than those given by equation (9). Tikhomirov et al (1942) extended this treatment to a polydisperse aerosol and obtained the following expression for K

$$K = \frac{2}{3}\frac{kT}{\eta}\left[1 + \bar{a}\left(\frac{1}{a}\right) + A\lambda\left(\frac{1}{a}\right) + A\frac{\bar{a}}{\lambda}\left(\frac{1}{a}\right)\right] \qquad (10)$$

where A derives from the slip factor $F = 1 + A\frac{\lambda}{a}$.

$$\bar{a} = \frac{1}{n}\int_0^\infty a\, f(a)\, da \quad \text{etc.}$$

IV.2.3. Factors which retard coagulation.

In addition to deriving equation (10), Tikhomirov et al (1942) showed that intermolecular forces would affect the rate of coagulation by reducing the probablity of coalescence in collision. Using polydisperse aerosols of lubricating oil, experimental values of K were obtained which were 1.2 to 1.3 times those predicted by von Smoluchowski's equation, but in good agreement with their theory.

Tunitsky (1939) derived a modified equation for the coagulation of charged particles.

Direct observation of coalescence between two particles was made by Fuchs (1935) who used an ultramicroscope to observe the impact of dust particles with a wall; he states that 10 to 25% of the particles rebounded. Dady (1947) and Swinbank (1947) used a similar system for the observation of binary collisions, and claimed that no coalescence was seen, but such experiments are inconclusive

unless a stereoscopic image is observed.

IV. 2.4. The combined effects of sedimentation, diffusion and coagulation.

Gillespie et al (1947 and 1953) observed the changes of particle size and of concentration in a stirred ammonium chloride aerosol contained in a cube of volume 0.2 m^3. They showed that the changes in concentration could be represented by equation

$$\frac{dn}{dt} = -k n^2 - \beta n \qquad (11)$$

where k is a parameter of coagulation

β is a parameter for the loss to the surface of the container.

Both these parameters were shown to be affected by electric charges on the particles and k varied by a factor of 10 although the aerosols were of similar size distribution. The charge distribution in aerosols of various materials has been examined (Gillespie (1955))and the variation of k and β with charge determined. A coagulation factor has been calculated for an aerosol consisting of particles of two different radii but an adequate theory has not been derived yet to account fully for the concentration changes observed.

CHAPTER V.

THEORY OF CONCENTRATION CHANGES.

V. 1. Introduction.

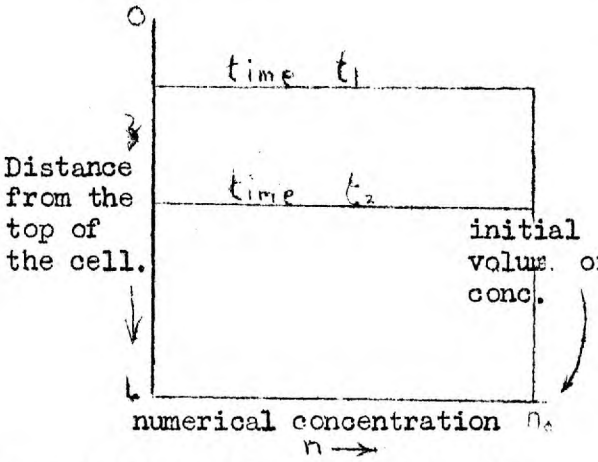
An equation will be derived to account for the concentration changes due to sedimentation, diffusion and coagulation in a monodisperse liquid aerosol which is completely enclosed.

Consider the changes in the vertical direction in such an ensemble of identical particles confined between two horizontal plane and assume that the planes are completely absorbing and that particles always coalesce on collision with one another.

If sedimentation were the only process causing motion of the particles, the surface of the aerosol would be sharply defined and the upper surface would fall at the Stokes velocity (see figure 5.1) If diffusion alone were to occur, equal numbers of particles would reach the upper and lower planes and the concentration gradient would be continuous and symmetrical about the mid-point of the cell (figure 5.2). If the two phenomena occurred simultaneously a continuous concentration gradient would be set up, and the point of maximum concentration would move downwards with time (figure 5.3) Coagulation would cause a decrease in the numerical concentrtaion which was uniform in space and the rate of decrease would fall in time. Combined with sedimentation and diffusion, its maximum effect would occur at the point of maximum concentration (figure 5.4)

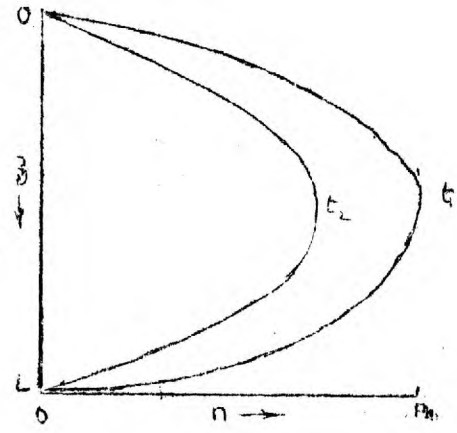
GRAPHS OF THE NUMERICAL CONCENTRATION IN A CLOSED VESSEL.

V.1 Sedimentation



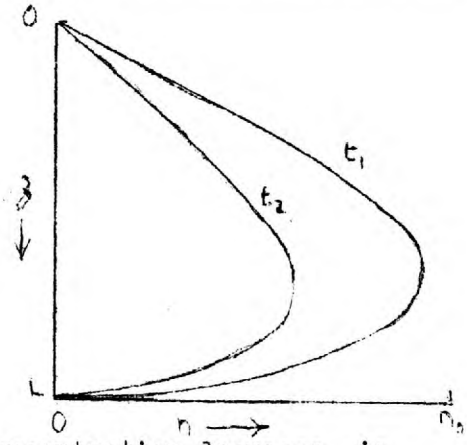
The concentration at any time is zero above a certain value of z and is n_o below.

V.2 Diffusion



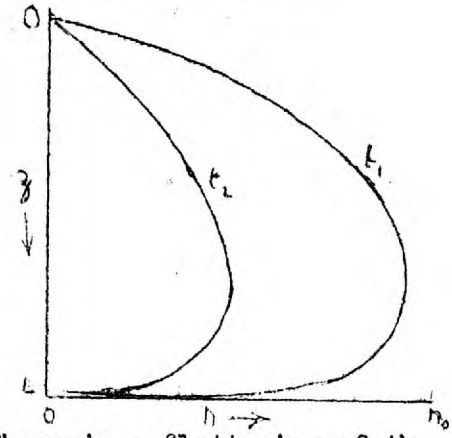
The concentration decreases symmetrically about the mid-point of the vessel.

V.3 Sedimentation and diffusion



The concentration decrease is assymetric and the mode of the distribution moves downwards with time.

V.4 Sedimentation, diffusion and coagulation.



There is a flattening of the region of maximun concentration.

V. 2. Smoluchowski's equation for diffusion in a field of force*

Smoluchowski's equation for the effects of diffusion in a field of force can be used to determine the concentration changes caused by simultaneous sedimentation and diffusion in an aerosol. In chapter X. it will be applied to a problem concerning the coalescence of particles.

If a particle is in Brownian motion in a field of force, its acceleration at any instant consists of a component due to the field and a rapidly fluctuating component which is a characteristic of Brownian motion. From the expression for the acceleration of the particle the probability that it will have certain co-ordinates in phase space at a given time can be derived. By evaluating the first and second moments of the velocity distribution, the following equation is derived for the rate of change of a function $\omega(rt)$, the probability that a particle has the spatial co-ordinate $\underline{r}$ at a time t.

$$\frac{\partial \omega}{\partial t} = \mathrm{div}_r\left[D \,\mathrm{grad}_r\, \omega - \frac{K}{\beta}\omega\right] \qquad (1).$$

(Smoluchowski's equation)

---

* For a general treatment of the theory of Brownian motion see paper by Chandrasekhar (1943) Rev. Mod. Phys. 15, 1. Equation for diffusion in field of force is derived on page 41; that for coagulation on page 60.

where $D = \frac{kT}{m\beta}$; $\beta = \frac{6\pi\eta a}{m}$; K is force exerted on unit mass.

The probability of a single particle having co-ordinates ($\underline{r}t$) is the fraction in which they occur in the total number of observations. Alternatively, it is the fraction, $\frac{n}{\sum n}$ say, which has co-ordinate $\underline{r}$.

$$\omega\ (\underline{r}t) = \frac{n}{\sum n} \qquad (2)$$

where n is the numerical concentration of particles at a point $\underline{r}$

$\sum n$ is the total concentration in the system.

Then equation (1) may be expressed in the form

$$\frac{\partial n}{\partial t} = \mathrm{div}_r\ (D\ \mathrm{grad}_r n - K/\beta\ n) \qquad (3)$$

For a uni-dimensional system in the gravitational field equation (3) becomes

$$\frac{\partial n}{\partial t} = D\frac{\partial^2 n}{\partial z^2} - \frac{v\partial n}{\partial z} \qquad (4)$$

where $D = \frac{kT}{6\pi\eta a}$

$K_\gamma = -\left(\frac{\rho - \rho_0}{\rho}\right) g$

$v = \frac{K_\gamma}{\beta\gamma}$, the Stokes velocity.

V.3. Davies solution of this equation.

Davies (1949) has published a general solution of this equation subject to the following boundary conditions :-

(a) The concentration is initially uniform in the cell

i.e. $n = n_0$ at $t = 0$ $\quad 0 < z < L$

(b) Particles are absorbed at the surface of the two horizontal planes

$$n = 0 \text{ at } z = 0 \quad t > 0$$
$$n = 0 \text{ at } z = L \quad t > 0 \qquad (5)$$

Equation (7) was obtained in a non-dimensional form by the substitutions :-

$$t = T\frac{L}{v}$$
$$n = n_0 c \qquad (6)$$
$$z = ZL$$

where L is the depth of the cell

v is the sedimenation velocity of a particle

n_0 is the initial concentration

Then $$\frac{\partial c}{\partial T} = \alpha \frac{\partial c}{\partial Z^2} - \frac{\partial c}{\partial Z} \qquad (7)$$

where $\alpha = \frac{D}{v L}$

and the boundary conditions are now

$$\left.\begin{array}{ll} \text{(a)} & c = 1 \text{ at } T = 0 \quad 0 < Z < 1 \\ \text{(b)} & c = 0 \text{ at } Z = 0 \text{ and } Z = 1 \quad T > 0 \end{array}\right\} \qquad (8)$$

Davies solved this equation by separation of the variables and obtained

$$c = \tfrac{1}{2}\left[h_1 + h_2 + h_3 + h_4 + h_5 \right] \qquad (9)$$

where

$$h_1 = \exp \frac{1}{\alpha}\left[\operatorname{erf}(2w + v) - \operatorname{erf}(w + v) \right]$$

$$h_2 = -\exp \frac{Z}{\alpha}\left[\operatorname{erf}(w + v) - \operatorname{erf} v \right]$$

$$h_3 = \operatorname{erf}(w - u) + \operatorname{erf} u$$

$$h_4 = -\exp -\frac{(1 - Z)}{\alpha}\left[\operatorname{erf}(2w - v) - \operatorname{erf}(w - v) \right]$$

$$h_5 = \exp \frac{1}{\alpha}\left[\operatorname{erf}(3w - u) - \operatorname{erf}(2w - u) \right]$$

and $u = \frac{Z - T}{2(\alpha T)^{\frac{1}{2}}}$; $v = \frac{Z + T}{2(\alpha T)^{\frac{1}{2}}}$; $= \frac{1}{2(\alpha T)^{\frac{1}{2}}}$

V.4. The effect of coagulation during diffusion in a field of force.

Smoluchowski's equation is applicable to an aerosol of such low concentration that no interference between particles occurs. However, if two particles of radius a approach one another sufficiently closely to coalesce, the number of particles of radius a is reduced by two. The probability of this event is the probability of a particles entering the sphere of influence radius R of another particle. To account for the process of coagulation equation (1) must be modified.

The equation

$$\frac{\partial w}{\partial t} = \mathrm{div}_r \left[\underline{D} \ \mathrm{grad}_r w - \underline{K/\beta} \ w \right]$$

can be considered as the result of a diffusion current j, so that

$$\frac{\partial w}{\partial t} = -\mathrm{div}_r (j) \qquad (10)$$

If a small absorbing element is introduced into the system

$$\int \mathrm{div}_r(j) d\tau = \int \mathrm{div}_r(j_0) d\tau - \mathrm{div}_r(j_R) \delta\tau. \qquad (11)$$

where $\delta\tau$ is the volume of the element

j_0 is the diffusion current at a distance from the absorber

j_R is the diffusion current in the vicinity of the absorber.

If there are n spherical absorbers per unit volume then :-

$$\int \mathrm{div}_r\,(j)\,dr = \int \mathrm{div}_r\,(j_o)\,dr - n \int_{o}^{V} \mathrm{div}_r(j_R)\,d\tau \qquad (12)$$

where $\mathrm{div}_r\,(j_R)$ is integrated over the value V of a single sphere.

Then using Gauss's theorem :-

$$\int \mathrm{div}\ j\,d\tau = \oint j\,ds \qquad (13)$$

where s is the surface of a sphere

hence :-

$$\mathrm{div}_r\,(j) = \mathrm{div}_r\,(j_o) - 4\pi nR^2\,(j_R) \qquad (14)$$

In deriving the rate of coagulation of particles in free Brownian motion, Smoluchowski (1916) showed that the differential equation

$$\frac{\partial \omega}{\partial t} = D\left[\frac{\partial^2 \omega}{\partial r^2} + \frac{2}{r}\frac{\partial \omega}{\partial r}\right] \qquad (15)$$

or

$$\frac{\partial(\omega r)}{\partial t} = D\,\frac{\partial^2(\omega r)}{\partial r^2} \qquad (16)$$

had to be solved with the boundary condition $\omega = 0$ at $r = R$ i.e. complete absorption. occurred at the surface of the sphere.

The solution obtained was

$$\omega_r = \omega_o\left[1 - \frac{R}{r} + \frac{R}{r}\,\mathrm{erf}\,\frac{r-R}{2(Dt)^{\frac{1}{2}}}\right] \qquad (17)$$

where ω_r was the distribution function near the sphere and

ω_o was the distribution function at $r \longrightarrow \infty$.

Fürth (1917) in solving problems dealing with diffusion in a field of force used the transform

$$\omega = \omega' \exp\left[\frac{v}{2D}(r - r_0) - \frac{v^2 t}{4D}\right] \qquad (18)$$

Consequently, equation (16) is to be solved after the transformation represented by (18) has been made. However, it can be seen that in (18), if $r - r_0 \longrightarrow 0$ and a time t is considered, so that $t < \frac{v^2}{4D}$,

then $$\omega \cong \omega' \qquad (19)$$

and ω_r is given by equation (17)

Then $j_R = \left[D \text{ grad}_r - K/\beta\right] \omega_r$

becomes $= \left\{\left[D \text{ grad}_r - K/\beta\right] \omega_\infty \left(1 - \frac{R}{r} + \frac{R}{r}\text{erf}\frac{r - R}{2(Dt)^{\frac{1}{2}}}\right)\right\}_{|r| = R}$

$$= \frac{D\,\omega_\infty}{R} \qquad (20)$$

This assumes that intervals of time of the order of β^{-1} are negligible i.e. $t \gg \beta^{-1}$. If $j(\omega_R)$ were to be observed only during such an interval, fluctuations would be apparent.

Then substituting the result (20) into (14)

$$\text{div}_r(j) = \text{div}_r(j_0) - 4\pi nR^2 \cdot \frac{D \cdot \omega_\infty}{R} \qquad (21)$$

and (10) would be replaced by

$$\frac{\partial \omega}{\partial t} = \mathrm{div}_r \left[D \ \mathrm{grad}_r \omega - \frac{K}{\beta} \omega \right] - 4\pi n R^2 \omega \quad (22)$$

Then using the transformation by which equation (3) was obtained from equation (1) :-

$$\frac{\partial n}{\partial t} = \mathrm{div}_r \left[D \ \mathrm{grad}_r n - \frac{K}{\beta} n \right] - 4\pi D R n^2 \quad (23)$$

Assuming R = 2a and consider all the spheres in diffusion

$$\frac{\partial n}{\partial t} = \mathrm{div}_r \left[D \ \mathrm{grad}_r n - \frac{K}{\beta} n \right] - 8\pi D a n^2 \quad (24)$$

Considering the vertical dimension only :-

$$\frac{\partial n}{\partial t} = D \frac{\partial n}{\partial z^2} - v \frac{\partial n}{\partial z} - 8\pi D a n^2 \quad (25)$$

Equation (25) may be obtained in a non-dimensional form by the substitutions made to derive equation (7).

Then

$$\frac{\partial c}{\partial T} = \alpha \frac{\partial^2 c}{\partial Z^2} - \frac{\partial c}{\partial Z} - \gamma c^2 \quad (26)$$

where $\alpha = \frac{D}{vL}$

and $\gamma = \frac{KLn_0}{v}$

The equation does not account for the particles produced by coagulation. The assumption is made that two particles of radius a collide, coalesce and the concentration is then reduced by 2. It is not proposed to derive an additional term to account for the production during coagulation , of

particles of radius $2^{1/3}a$.

V.5. Discussion of solutions of the equations.

There is no analytical method of obtaining a general solution of a non-linear partial differential equation of the second order such as equation (26). Several attempts were made to fit a possible solution and then test it or to find a transform to make the equation linear; both of these methods were unsuccessful.

A relaxation solution was attempted (see appendix 1) but the solution converged slowly and rounding off errors accrued, so the method was discarded.

The solution of partial differential equations by computing machines is still being investigated and it would appear that this equation can only be solved when such techniques have been developed.

A numerical method was used to obtain values of the parameters α and γ, using the procedure described below.

V. 6. The equations expressed in finite differences.

The equations

$$(7) \quad \frac{\partial c}{\partial T} = \alpha \frac{\partial^2 c}{\partial Z^2} - \frac{\partial c}{\partial Z}$$

and $$(26) \quad \frac{\partial c}{\partial T} = \alpha \frac{\partial^2 c}{\partial Z^2} - \frac{\partial c}{\partial Z} - \gamma c^2$$

can be expressed in finite differences form by making the substitutions :-

$$\left.\frac{\partial c}{\partial T} \triangleq \frac{c_2 - c_4}{2H}\right\} \quad (27)$$

$$\frac{\partial c}{\partial Z} = \frac{c_1 - c_3}{2h}$$

$$\frac{\partial^2 c}{\partial Z^2} = \frac{c_1 + c_3 - 2c_o}{h^2} \qquad (27)$$

where c_1, c_2, c_3, c_4 and c_o represent the concentrations at intervals h and H in the Z T plane as shown in figure 5 and

$h = \Delta Z \; ; \; H = \Delta T = \Delta t \cdot \frac{v}{L}$

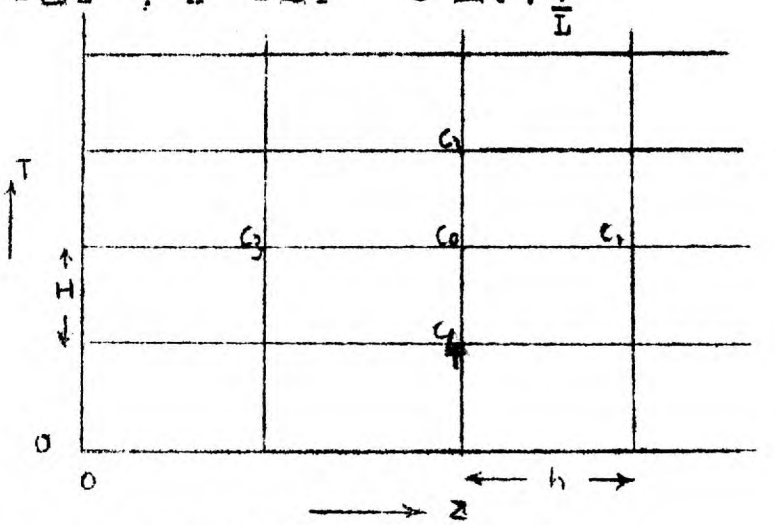


Figure 5.

Hence equation (7) may be written

$$0 = \alpha \frac{(c_1 + c_3 - 2c_o)}{h^2} - \frac{c_1 - c_3}{2h} - \frac{c_2 - c_4}{2H} \qquad (28)$$

and choosing an interval $H = h^2$ this becomes

$$0 = \alpha \frac{(c_1 + c_3 - 2c_o)}{h} - \frac{c_1 - c_3}{2} - \frac{c_2 - c_4}{2h} \qquad (29)$$

Equation (28) becomes

$$0 = \frac{\alpha}{h^2}(c_1 + c_3 - 2c_o) - \frac{(c_1 - c_3)}{2h} - \frac{(c_2 - c_4)}{2H} - \gamma c_o^2 \qquad (30)$$

and assuming $H = h^2$

$$0 = -\gamma c_o^2 - \frac{2\alpha}{h^2} c_o + \left(\frac{\alpha}{h^2} - \frac{1}{2h}\right)c_1 + \left(\frac{\alpha}{h^2} + \frac{1}{2h}\right)c_3 - (c_2 - c_4)\frac{1}{2h^2} \qquad (31)$$

These equations are used below in numerical analysis of the results and in appendix 1 in a relaxation solution.

Equation (28) may be written

$$0 = \alpha x_{11} - x_{12} - \frac{1}{H} x_{13} \qquad (32)$$

and from the experimental results (see chapter VII) x_{11}, x_{12} and x_{13} may be evaluated in terms of the measured values of c and the interval h ($= \Delta z$).

Consequently from two equations such as (32) :-

$$\left.\begin{aligned} 0 &= \alpha x_{11} - x_{12} - \frac{1}{H} x_{13} \\ 0 &= \alpha x_{21} - x_{22} - \frac{1}{H} x_{23} \end{aligned}\right\} \qquad (33)$$

values of α and $\frac{1}{H}$ may be obtained and compared with α and $\frac{1}{H}$ calculated from measurements of the particle radius a . Examples of the uses of these equations is given later.

CHAPTER VI.

THE FORMATION OF A MONODISPERSE AEROSOL.

VI. 1 Introduction.

The necessity of using a monodisperse aerosol in the proposed investigation has already been indicated. Of the methods available for the production of aerosols, that described by La Mer and Sinclair (1949) was chosen since it appeared capable of forming aerosols having the requisite range of size and concentration.

The use of other techniques, the spinning top (May 1949) and the vibrating reed (Dimsock, 1950) were considered and rejected as being incapable of producing particles small enough.

In the La Mer generator, vapour is condensed on suitable nuclei under carefully controlled conditions. The apparatus, described in detail on page 50, comprises a vessel in which liquid is evaporated, a supply of inert gas to carry the vapour, and a source of condensation nuclei. The nuclei, vapour and gas are well mixed before passing through a condensation tube where the aerosol is formed.

VI. 2. Condensation of a cloud of droplets.

The theory of condensation has been discussed in chapter II and it was seen that the growth of one droplet in a cloud could

be represented by the equation :-

$$a^2 = a_0^2 + f(t) \qquad (1)$$

(Reiss 1951)

If the supersaturation ratio f_{ω} and the temperature were functions of the time only, an aerosol of very low dispersion could be obtained. Consequently, the radius of a droplet was not greatly affected by the radius a_0 of the nucleus, provided $a > 10\, a_0$, and depended only on the ambient conditions, represented by the function $f(t)$.

VI. 3. Nucleation.

Condensation can occur on a suitable droplet of liquid, on a solid particle or on a gaseous ion, and spontaneous nucleation, which has already been mentioned, (chapter II, page 13) may be appreciable if the supersaturation ratio is greater than 5.

The effect of various nuclei may be compared by considering the Kelvin effect. At the surface of an uncharged, pure liquid droplet, the vapour pressure f is greater than that at a plane surface f_{ω} at saturation in the ratio

$$\frac{f}{f_{\omega}} = \exp\left[\frac{2\gamma m_1}{\rho kT\, a}\right] \qquad (2)$$

If the liquid contains N moles of a solute of higher molecular weight, Wright (1936) has shown that this relation becomes :-

$$\frac{f}{f_{\omega}} = \exp\left[\frac{2\gamma m_1}{\rho kT\, a}\right] + \frac{750\, CN}{\pi \rho\, a^3} \qquad (3)$$

where ϵ is a factor depending on the properties of the solute. Consequently, a soluble nucleus decreases the evaporation of the drop. For a particle which carries an electric charge e relation (2) must be rewritten (J.J. Thomson 1903)

$$\frac{p}{p_\infty} = \exp\left[\frac{2\gamma m_1}{\rho kT a} - \frac{e^2 m_1}{8\pi kT \rho E a^4}\right] \qquad (4)$$

where E is the dielectric constant of the liquid.

Obviously, if the aerosol is to be monodisperse, the nuclei used must be identical to ensure that the rate of growth of each particle is the same.

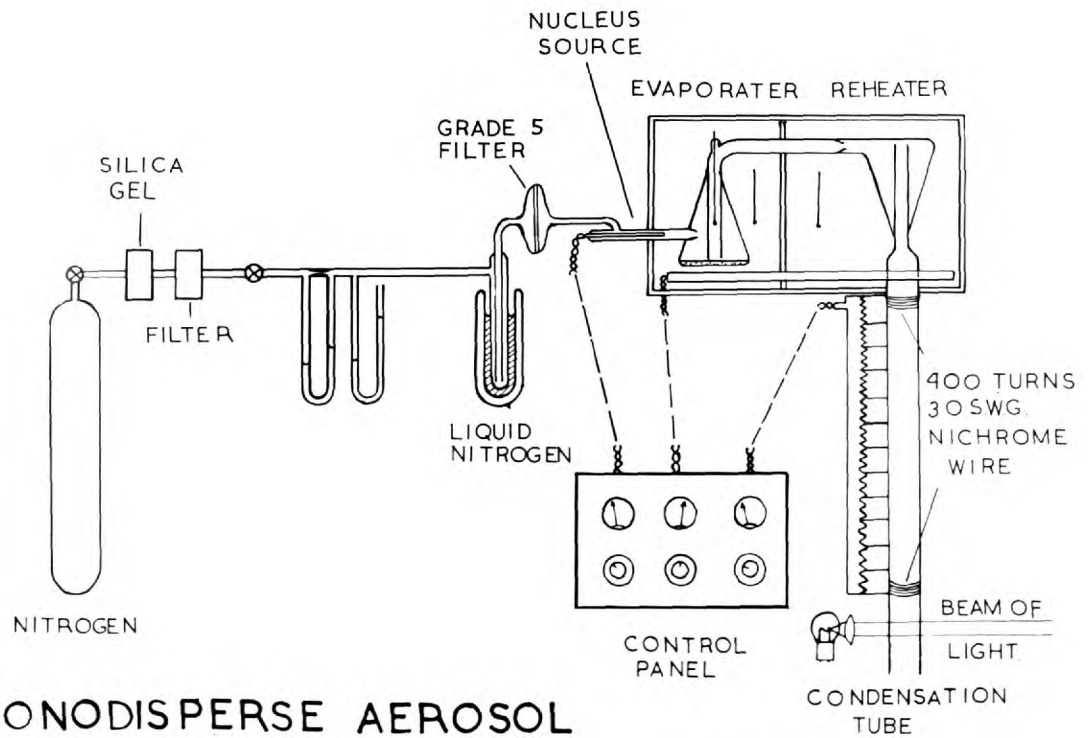
VI. 4. Conditions for formation of a monodisperse aerosol.

The conditions and the apparatus required for producing monodisperse aerosols can now be specified more precisely.

A steady stream of vapour of constant density is supplied by maintaining the liquid at a constant temperature and removing the vapour in a stream of filtered gas. The liquid must be pure so that only one species of vapour molecules is present and it must be thermally stable. Any spray which forms must be removed.

Nuclei are introduced at a constant rate into the gas-vapour stream. Only one type of nucleus must be present and precautions must be taken to prevent spontaneous nucleation.

The gas, vapour and nuclei are well mixed and then allowed



MONODISPERSE AEROSOL GENERATOR

FIGURE 6·1

to cool uniformly in such a way that the aerosol which is formed cannot return to mix with the partially condensed vapour.

VI. 5. Description of the apparatus.

The apparatus used was a modification of that described by La Mer (1949), and the main components shown in figure 6.1, are an evaporator, a cylinder of nitrogen, a source of nuclei, a combined reheater and a mixing chamber and a condensation tube.

The nitrogen * was obtained from a cylinder, was partially dried over silica gel, roughly filtered and passed through a liquid nitrogen trap to remove moisture, oxygen and carbon dioxide. Just before entering the evaporator it was passed through a grade 5 sintered filter and into the nuclei source. The components were connected with copper tubing from the cylinder to the needle valve and with glass and polythene tubing from the needle valve to the evaporator. All connections were washed free from dust and grease before use.

The nucleus source, shown in figure 6.2 consists of an alumina tube coated with sodium chloride §, which could be heated up to 1000°C by a nichrome coil. The purified nitrogen entered

---

* The composition of the nitrogen was
Nitrogen 99.5% by volume
Oxygen 10 parts per million
Carbon dioxide 20 " "
Water vapour indefinite
Helium, Hydrogen and Argon up to 100%

§ The sodium chloride used was analytical quality containing 99.8% NaCl.

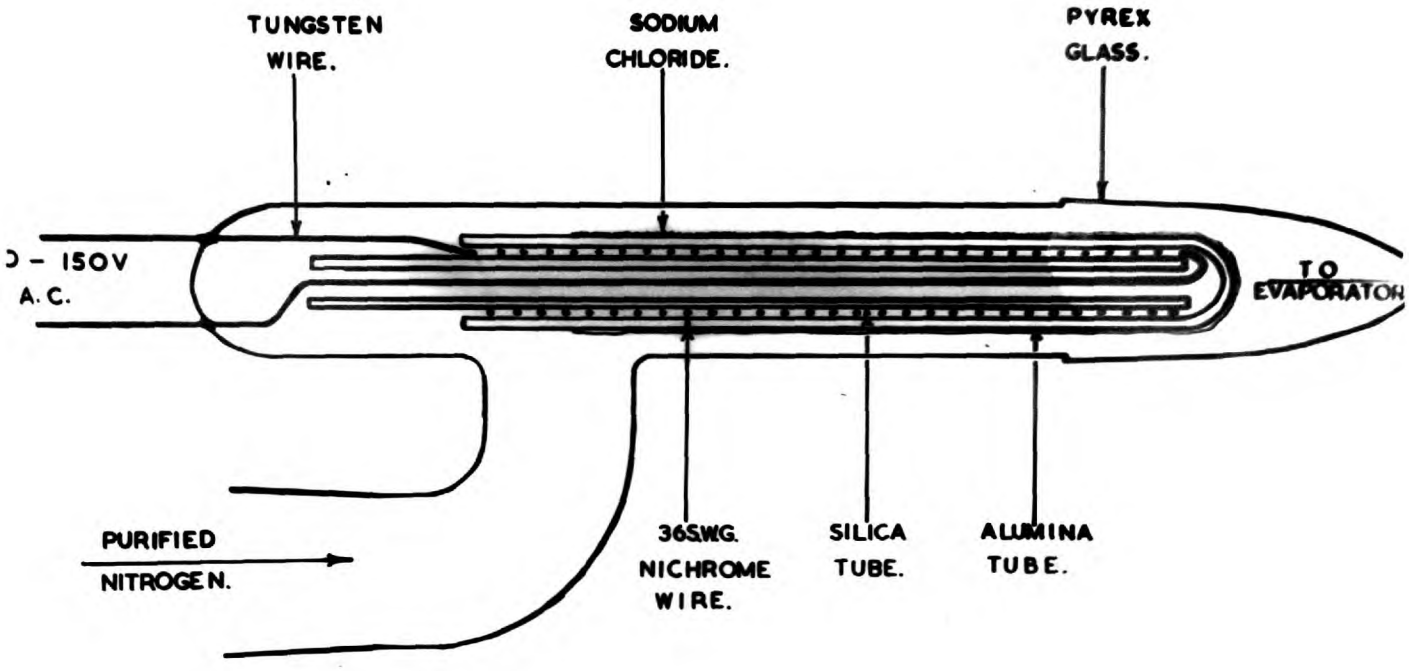


FIG. 6·2

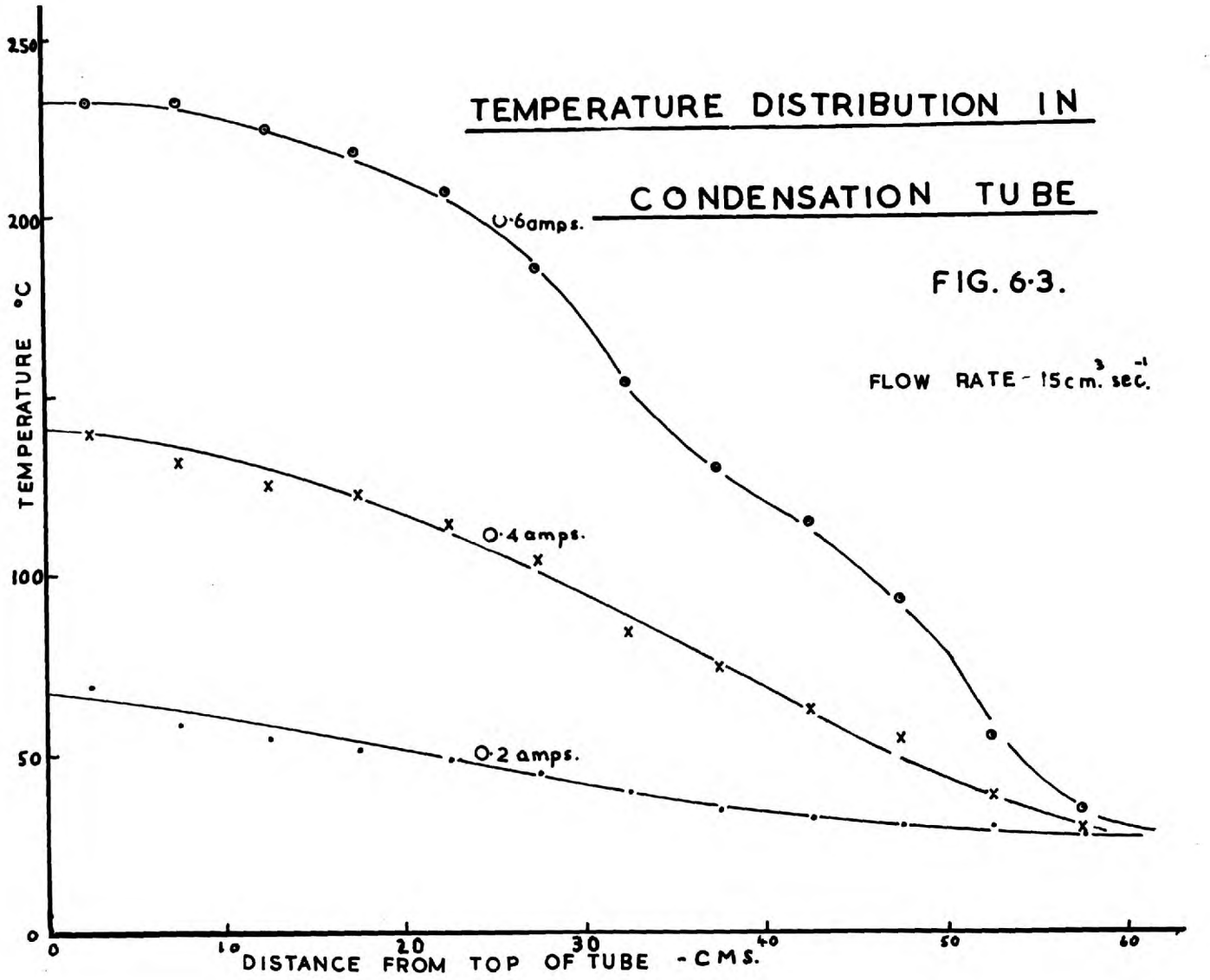
THE NUCLEUS SOURCE.

the side arm, and was saturated with sodium chloride vapour which subsequently condensed forming a very fine dust which passed into the evaporator.

The entry to the evaporator, was tangential to facilitate mixing and to separate larger nuclei by centrifugal action. The body of the evaporator was a half litre conical flask holding about 100 cm^3 of liquid. The reheater was a similar flask but inverted and the two were connected by a tube terminating in a fine nozzle. The rotational motion of the gas in the reheater precipitated larger drops of spray and the smaller ones were evaporated. (In both flasks internal tubes lead the gas away and encouraged a rapid rotational motion of the entering gas).

The evaporator and reheater were enclosed in a thermally insulated box with a partition and were heated by two 1 K.watt heater elements. The evaporator compartment could be heated to 250°C and the reheater about 20°C higher by adjusting the proportion of the heater exposed in the compartment. All temperatures were measured by thermocouples.

The stream of nitrogen, vapour and nuclei, thoroughly mixed, was passed down the condensation tube where a suitable temperature gradient was maintained by means of a coil of nichrome wire arranged in 10 equal sections (figure 6.1). Resistances connected in parallel enabled the current in each section to be adjusted initially and figure 6.3 shows the gradients obtained for three values of the


TEMPERATURE DISTRIBUTION IN
CONDENSATION TUBE
FIG. 6·3.
FLOW RATE - 15 cm.³ sec.⁻¹
0·6 amps.
0·4 amps.
0·2 amps.
TEMPERATURE °C
250
200
100
50
0
0
10
20
30
40
50
60
DISTANCE FROM TOP OF TUBE - CMS.

total current through the coil.

It was essential to obtain streamline flow in the condensation tube since turbulence or convection would cause mixing of the aerosol with undondensed vapour.

It was found that the radial temperature gradient was large enough to cause slightly larger particles to form near the axis of the tube. Consequently, the inlet to the observation cell was arranged to accept only the aerosol formed in a small zone near to the axis.

Since the nucleus source was heated to 800 or 900°C, it was possible that ions or thermoelectrons might be produced but as the sodium chloride was evaporating at the same time recombinations of ions and electrons could occur. The use of a pure salt and an alumina sheath round the heater to prevent the production of nuclei other than sodium chloride particles was adequate but some nuclei however might carry an electric charge.

The only other nuclei which might be present in the apparatus were those due to stray radioactivity and cosmic rays and the average rate of production of ions by these effects is 2 per $cm.^3$ per second. With the usual flow of 20 $cm.^3$ of gas per second, the time of residence of the aerosol in the condensation tube (50 cms. long and 2.2 cms. diameter) was about 12 seconds and in this time 24 ions per $cm.^3$ would be formed; this was negligible in an aerosol



ELECTRON MICROGRAPH
OF NUCLEI. FIGURE 6·4.

of concentration greater than 10^3 particles per cm^3

Spontaneous nucleation could be prevented by adjusting the rate of cooling of the aerosol.

Examination of the nuclei under an electron microscope and a diffraction camera showed that the crystals were cubic as would be expected (figure 6.4) for sodium chloride. The majority of the particles were about 0.01 microns in diameter.

VI. 6. Operation of the generator.

So that the apparatus could be set to produce an aerosol having approximately known characteristics, it was roughly calibrated. Measurements were made of mass concentration, numerical concentration and particle size for various settings of the controls.

The mass concentration of dinonyl phthalate in an aerosol was measured by the method described in chapter IX and is plotted against the evaporator temperature in figure 6.5.

The numerical concentration was determined by the photographic method described in the next chapter and is plotted against the current in the nucleus source in figure 6.6.

An indication of the dispersion was obtained from the Tyndall spectrum exhibited in the light scattered from a parallel beam (indicated in figure 6.1). This spectrum is displayed by monodisperse aerosols of transparent dielectric spheres of radii 0.2 to 1.5 microns (depending on their refractive index), and

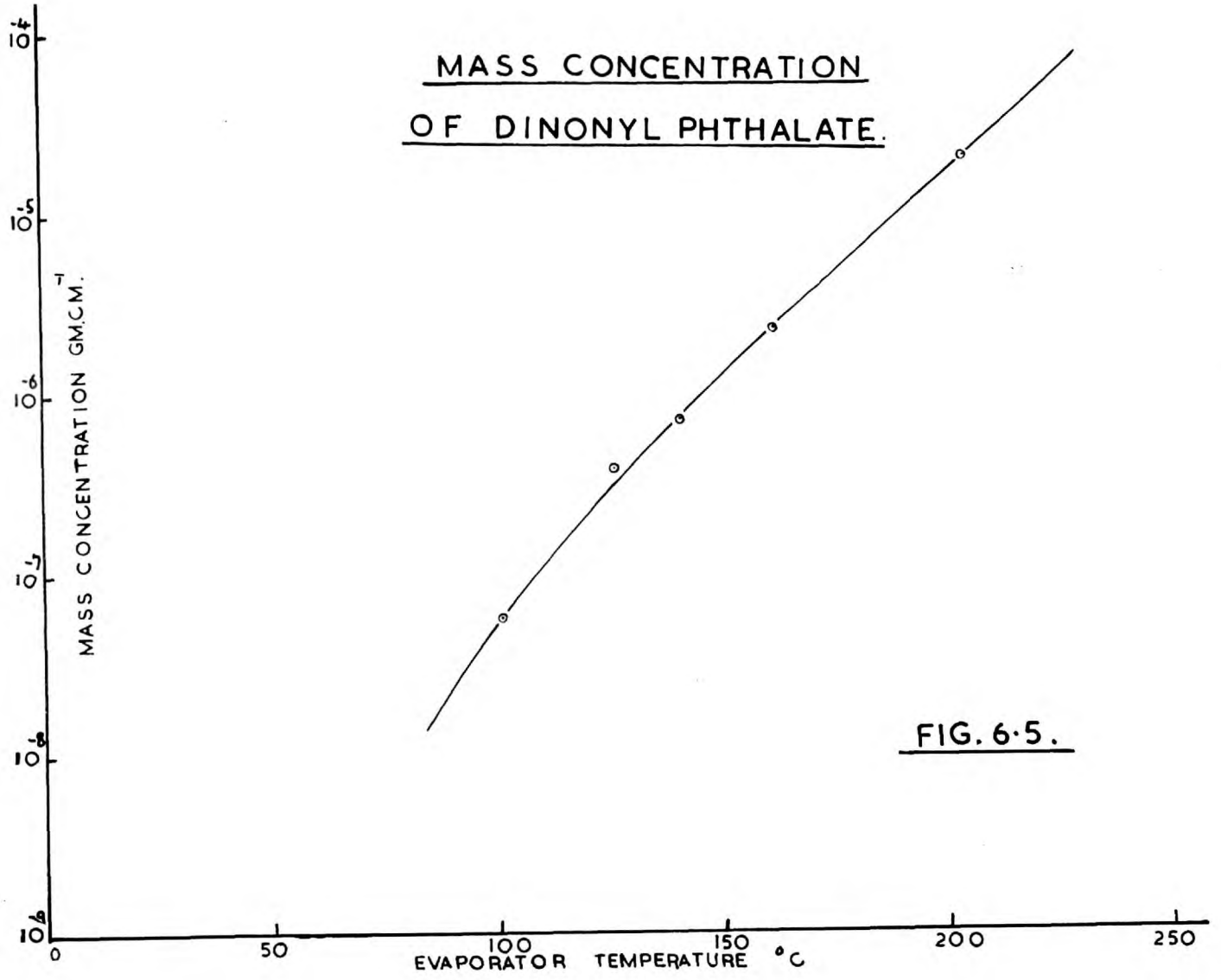

MASS CONCENTRATION
OF DINONYL PHTHALATE.
MASS CONCENTRATION GM.C.M.$^{-1}$
10^{-4}
10^{-5}
10^{-6}
10^{-7}
10^{-8}
10^{-9}
0
50
100
150
200
250
EVAPORATOR TEMPERATURE °C

FIG. 6·5.

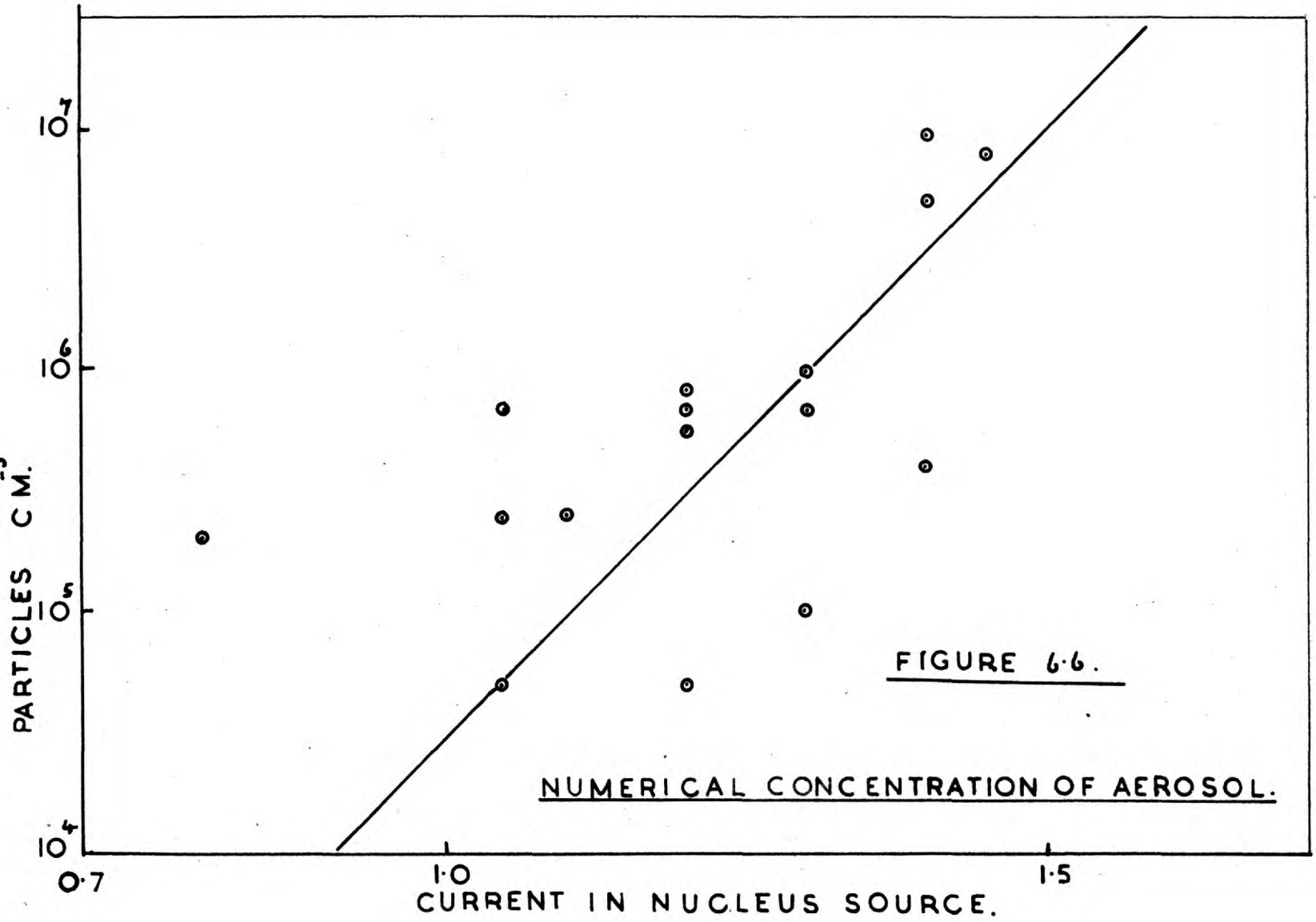


FIGURE 6·6.

NUMERICAL CONCENTRATION OF AEROSOL.

consists of a number of pure colours. The colours become diffuse with increasing dispersion until the scattered light appears orange or even white.

The droplet radius may be calculated from the numerical concentration and the mass concentration, and typical values are shown in figure 6.7

The procedure adopted for producing an aerosol of the required (approximate) characteristics was to set the nucleus-source current to give the requisite number of nuclei, then to set the evaporator temperature to give the desired mass concentration. Adjustments were made to the current in the winding or the condensation tube to reduce the dispersion.

Since the controls were not completely independent repeated fine adjustments were necessary to obtain the required aerosol.

VI. 7. Behaviour of the generator.

The apparatus was found capable of producing aerosols with the properties required for this investigation. The particle radii were between 0.08 and 2 microns, the mass concentration was from 10^{-8} to 10^{-4} gm.cm.$^{-3}$ and the numerical concentration extended from 10^{3} to 10^{9} particles per cm.^{3}

It might have been possible to obtain smaller particles but they could not be measured with sufficient accuracy.

Table 6.1 Physical characteristics of materials used in production of aerosols.

Material	Density gm/cc	Melting Point °C	Boiling Point	Refractive Index	Diffusivity	Vapour Pressure cms. Hg 20 °C	100 °C	200 °C	300 °C	400 °C	Molecular Weight	Surface Tension
Lubricating oil Telpa 30	0.9009 15/15	0	Initial 210 Final 400	1.496		10^{-4}	1.7. 10^{-4}			2		32.6 dynes/cm 21°C
Cetane ‡ n. Hexadecane	0.7711 20/4	18.1	287.5	1.4360 19°C 1.4347 20°C	x 0.0380 14.97°C 0.0385 16.97 0.0393 20.01	7.9. 10^{-5}	8.10^{-2}	8.1			226.44	
Dibutyl Phthalate $C_6H_4(CO_2C_4H_9)_2$ Mono.n.D.b.P.	1.0619	ca -35 75	338	1.4929 20	x 0.034 15.0 0.0386 19.90 0.0415 25.00 0.0426 30.00	1.3 10^{-6}	2.5. 10^{-3}	6.5. 10^{-1}	7.1		278.34	
Dioctyl Phthalate $C_6H_4(CO_2C_8H_{17})_2$ ‡ di-2-Ethylhexyl Phthalate.	0.990 15.5°	-50	386	1.485 20 D		6.5. 10^{-8}	1.8. 10^{-4}	1.1. 10^{-1}	8.1		390.5	
Tricresyl Phthalate (Tritolyl Phosphate) ‡ para.	1.17	ca. -30 77	410	Hg.yellow 1.5565 19°C Green 1.5551		10^{-5}	10^{-3}	1	56		368.36	
Dimonyl Phthalate $C_6H_4(CO_2C_9H_{19})_2$ di(3:5.5 - trimethyl hexyl phthalate) ‡	0.97088 20/		340	Hg.yellow 1.4838 19°C Green 1.4815		2. 10^{-9}	6.5. 10^{-5}	2.10^{-1}	39		418.34	
Sodium chloride ‡		800	1465							10^{-7}		

≠ Bradley and Shellard 194

x Birks and Bradley 1949

‡ Stull (1947)

≠ Small et al (1948)

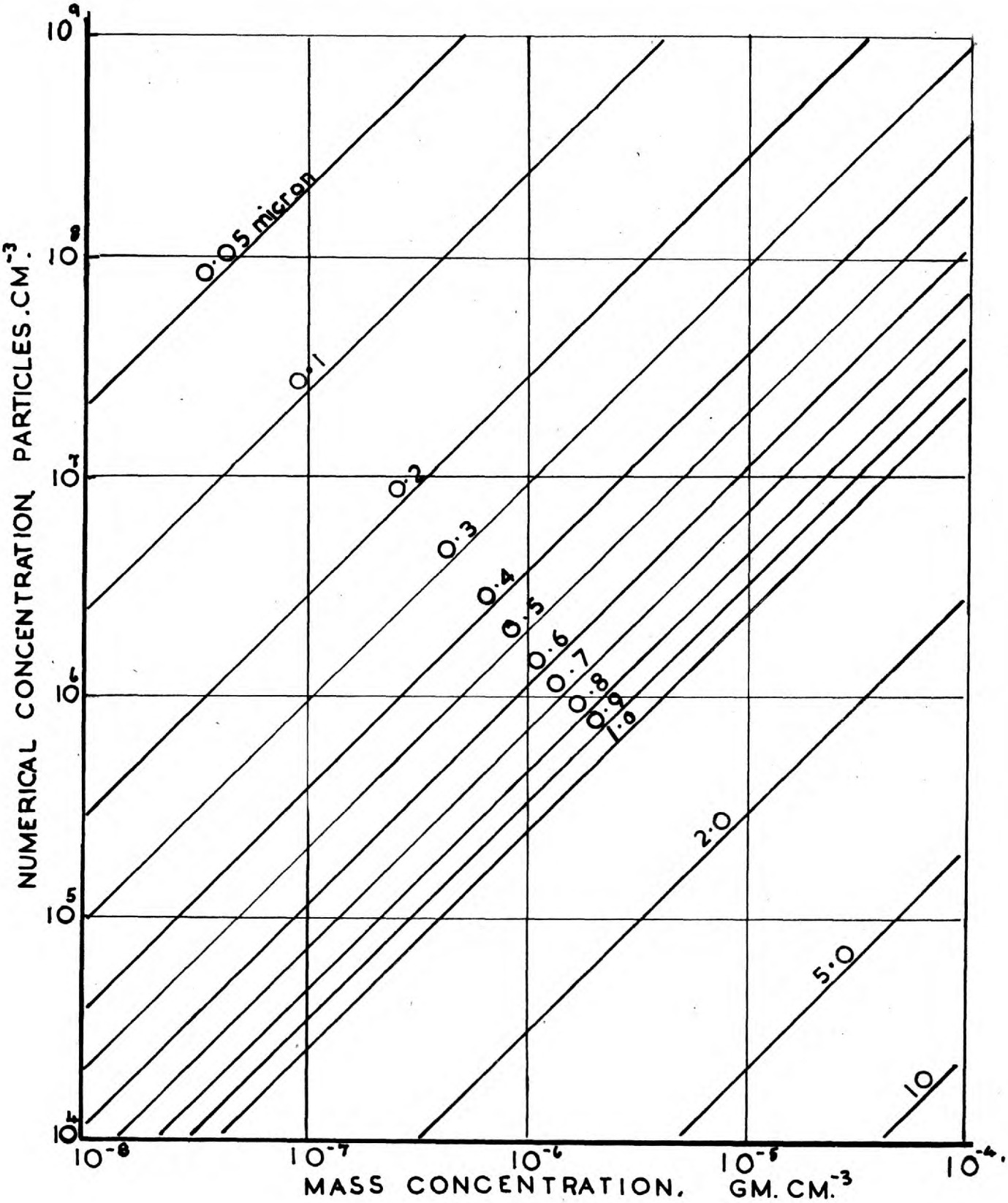

NUMERICAL CONCENTRATION, PARTICLES.CM.-3
10^9
10^8
10^7
10^6
10^5
10^4
0·05 micron
0·1
0·2
0·3
0·4
0·5
0·6
0·7
0·8
0·9
1·0
2·0
5·0
10
10^-8
10^-7
10^-6
10^-5
10^-4
MASS CONCENTRATION, GM. CM.-3

FIGURE 6·7.

CHAPTER VII.

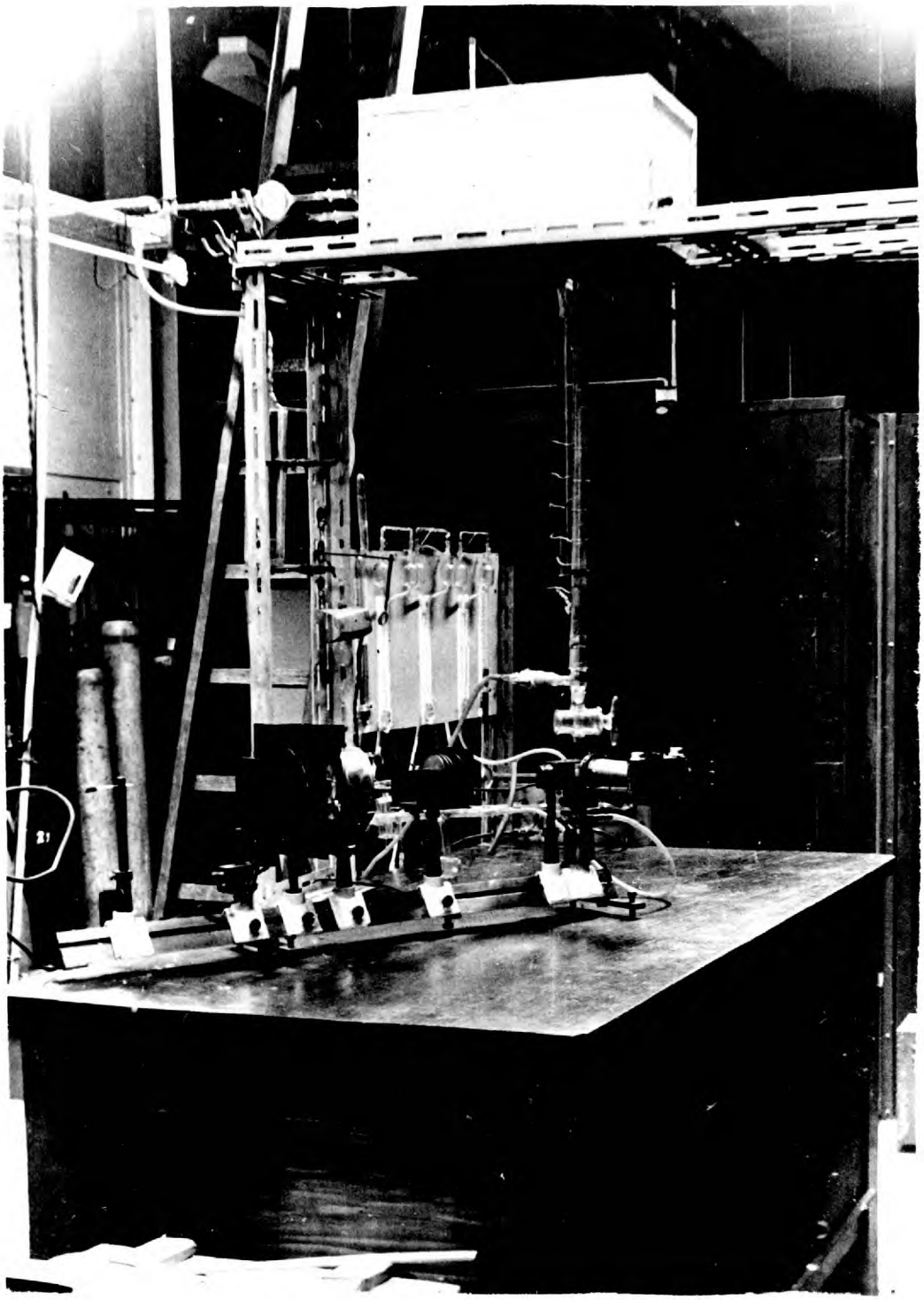
THE PHOTOGRAPHIC OBSERVATIONS.

VII.1. Introduction.

To test the theories discussed in chapter V experiments were designed to enable the changes in concentration in a monodisperse aerosol enclosed between two horizontal plane surfaces to be measured. From the measurements, values of the parameters of the differential equations could be calculated and compared with those predicted by the theory. This appeared to be the simplest test of the validity of the equations.

For each value of the parameter, a family of surfaces in c.Z.T. space should exist.

An ultramicroscope was used to observe the aerosol, the concentration being determined by a direct count of the number of particles in a known volume and particle size being calculated from measurements of the Stoke's velocity. The changes in concentration were recorded by a series of photomicrographs obtained when the aerosol was enclosed in a specially designed cell through which passed a narrow beam of light. The cell, the illumination system and the camera were mounted on an optical bench with the aerosol generator immediately above it (figure 7.1)



GENERAL ARRANGEMENT OF APPARATUS

FIG. 9-1

VII. 2. Design of experiments and apparatus.

Measurements of the concentration and particle size in a monodisperse aerosol were required for comparison with theoretical values predicted by equations (7) and (26) which were derived in chapter V.

$$\frac{\partial c}{\partial T} = \alpha \frac{\partial^2 c}{\partial Z^2} - \frac{\partial c}{\partial Z} \qquad (1)$$

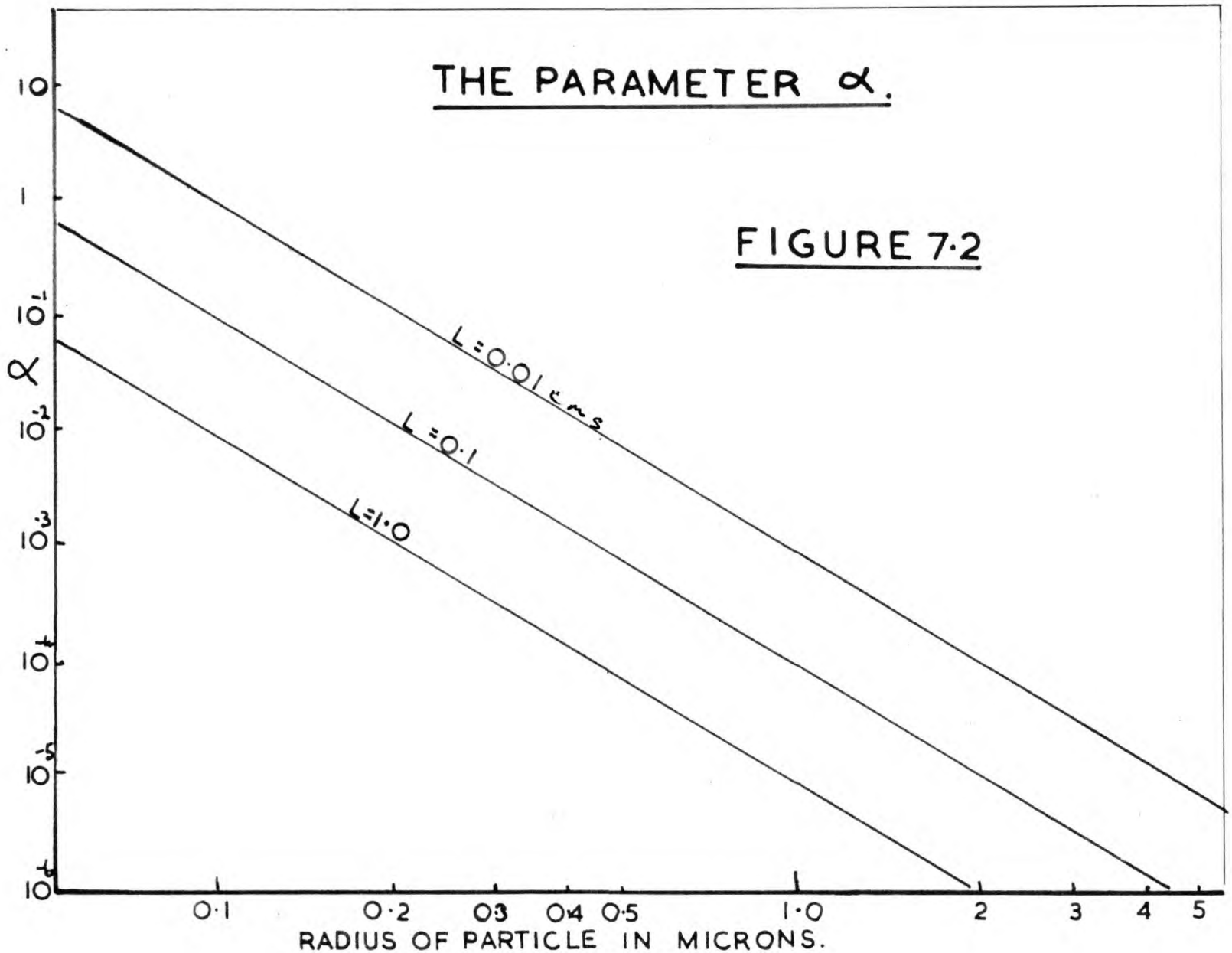
and $$\frac{\partial c}{\partial T} = \alpha \frac{\partial^2 c}{\partial Z^2} - \frac{\partial c}{\partial Z} - \gamma c^2 \qquad (2)$$

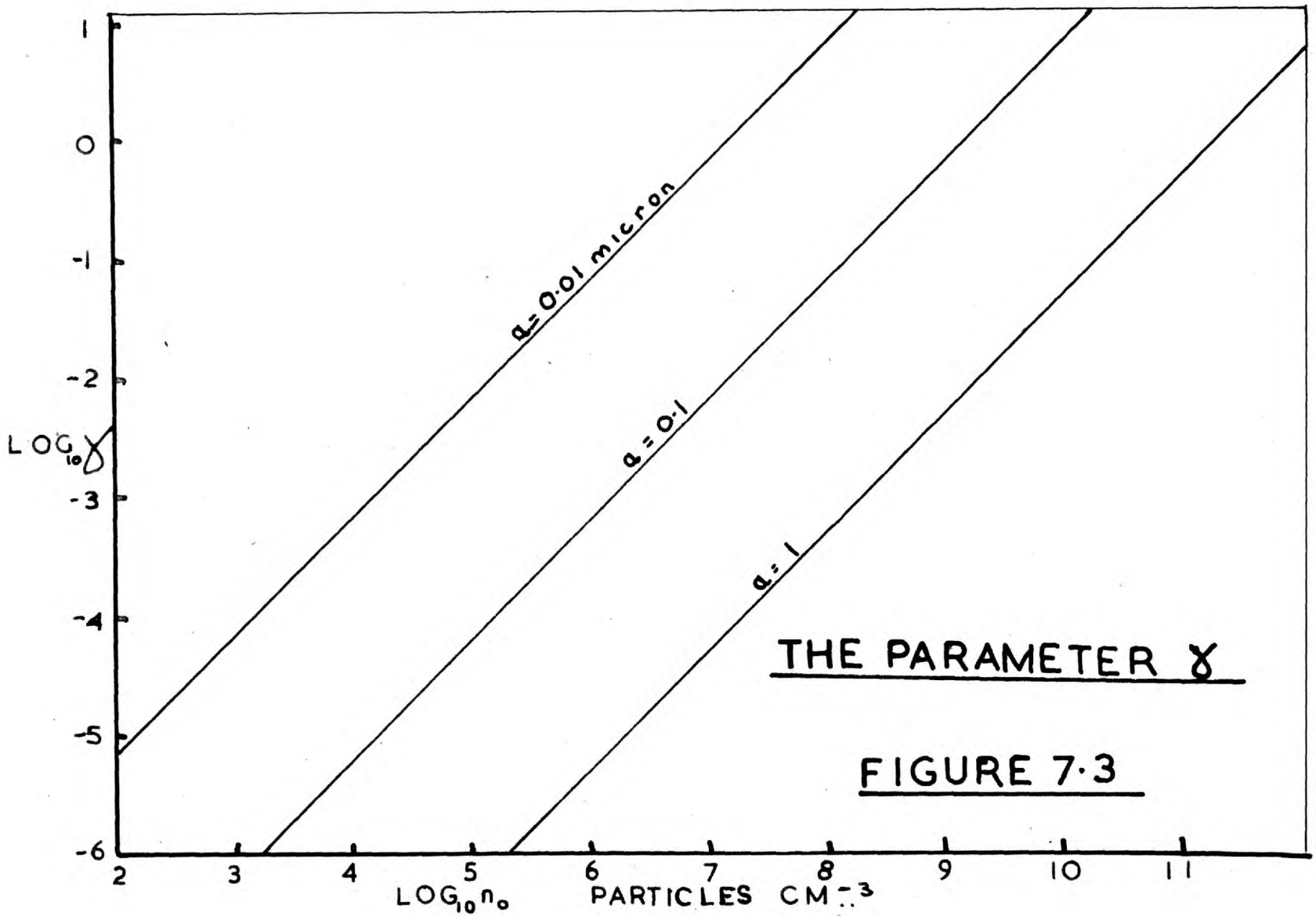
where $$\alpha = \frac{D}{v L}$$

and $$\gamma = \frac{K n_0 L}{v}$$

For a given aerosol, it is seen that α is a function of the depth of the cell which should be designed to permit observations of a convenient range of values of the parameter.

From the solution of equation (1) obtained by Davies (1949) it is seen that if α is greater than unity diffusion is more important than sedimentation in causing concentration changes whereas the converse is true when α tends to 10^{-4}. Values of α are plotted for different particle sizes and cell-depths in figure 7.2 from which it is seen that the required range of α is obtained in aerosols of the particle size to be investigated


THE PARAMETER α.
FIGURE 7·2
α
10
1
10⁻¹
10⁻²
10⁻³
10⁻⁴
10⁻⁵
10⁻⁶
L=0·01 cms
L=0·1
L=1·0
0·1
0·2
0·3
0·4
0·5
1·0
2
3
4
5
RADIUS OF PARTICLE IN MICRONS.



THE PARAMETER χ

FIGURE 7·3

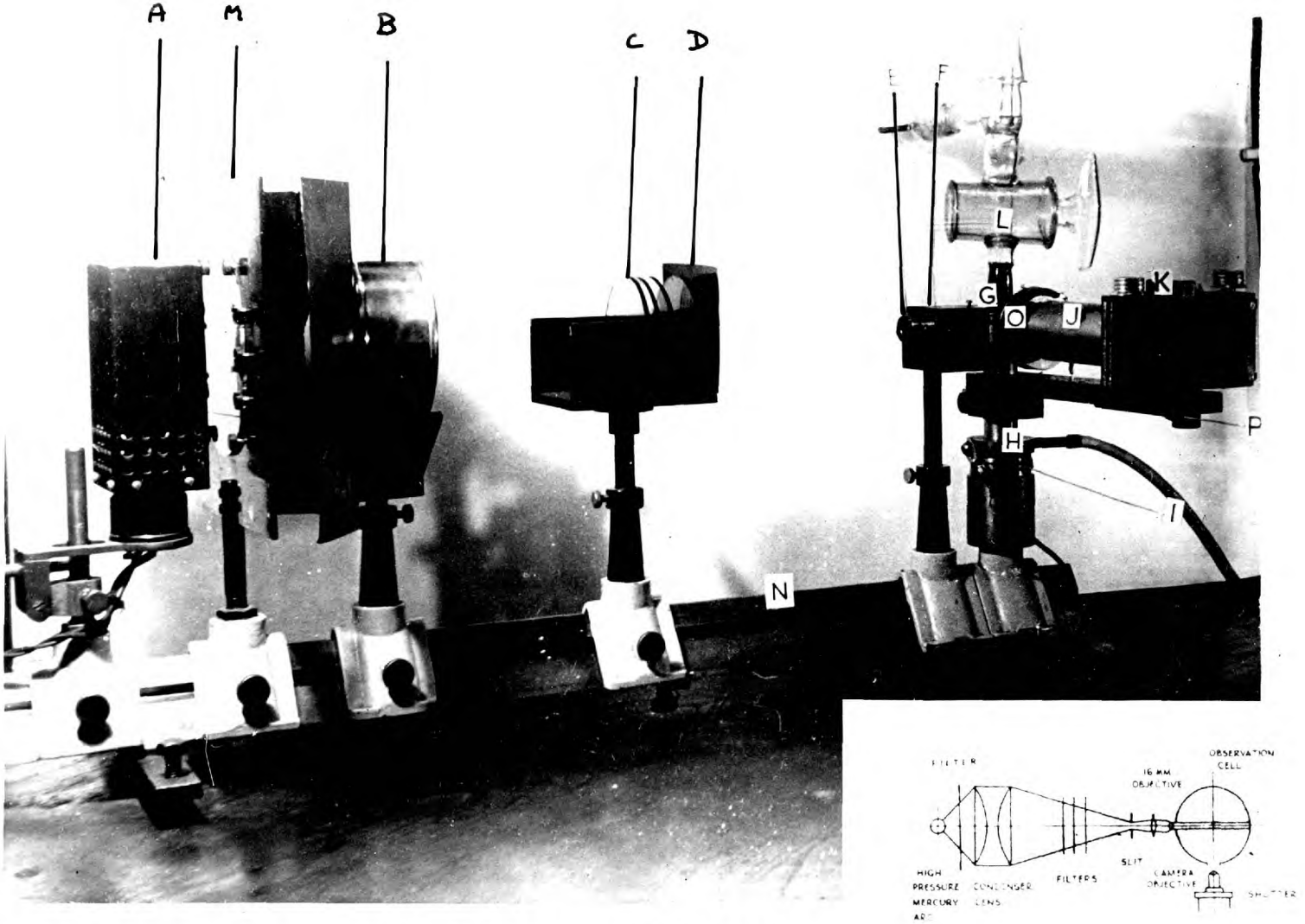
(0.05 to 1 microns) in a cell 0.1 cms. deep. A calculation from Stoke's law shows that a particle of 1 micron radius would fall this distance in about 10 seconds and one of 0.05 microns in about 1000 seconds thus allowing adequate time for observation. In the construction of the cell it was found more practical to make the depth 0.2 cms. Values of the coagulation parameter between 10^{-4} and 1 would be obtainable in such a cell if the initial concentration was 10^{7} particle $cm.^{-3}$ (figure 7.3).

The aerosol should enter the cell without encountering any obstruction and should then be completely enclosed at a constant temperature.

VII. 3. The apparatus.

VII.3.1. General arrangement.

The essential components of the apparatus mounted on an optical bench are shown in figure 7.4. The observation cell was situated immediately below the stopcock through which the aerosol was admitted. The cell was mounted on a pillar H and a thrust bearing I permitted partial rotation in a horizontal plane. An arc A was used as a source of illumination and observations were made using the ultramicroscope J and the camera K both mounted on a rigid arm P.



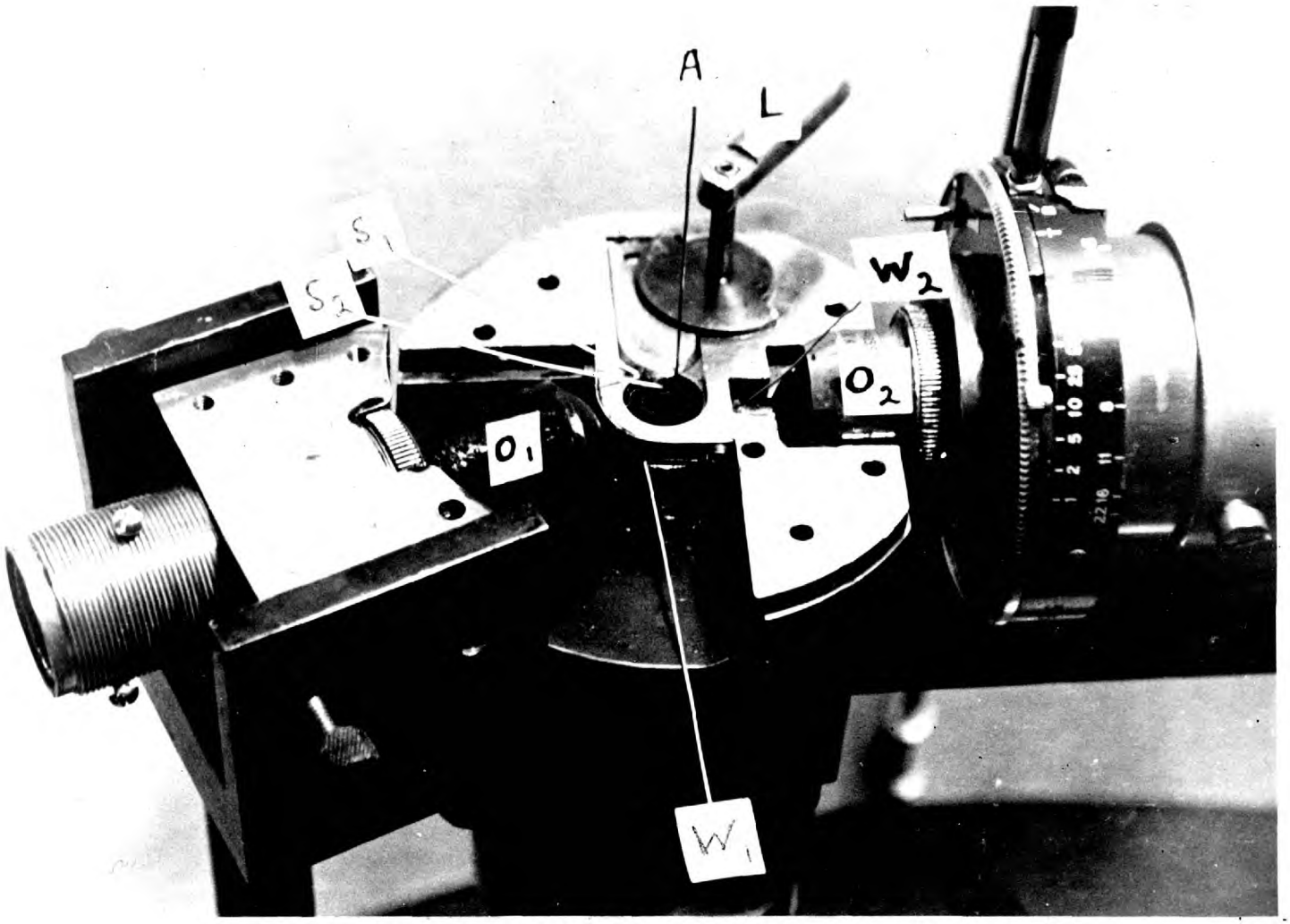
GENERAL VIEW OF APPARATUS FIGURE 7·4.

VII. 3.2 The observation cell.

Details of the cell in which the aerosol was observed appear in figures 7.5 to 7.9. It was constructed in three sections from a block of brass 7 cms. in diameter and 2 cms. high (figures 7.5 and 7.6). Two slides S_1 and S_2 were used to isolate a volume of aerosol which was then illuminated through window W_1 and observed through a second window W_2. The illuminating objective O_1 and the microscope objective O_2 can be seen in figure 7.5 The upper and lower sections of the cell gave it rigidity, increased the thermal capacity and supported parts of the optical system.

The mode of operation of the slides is indicated in figure 7.8. Motion of a lever caused a cam to rotate and a pin fixed to it exerted a translational force on the slide.

The window W_1 figure 7.6 was made from a thin film of mica which was held in place by a brass plate and two screws and cemented at the edges. The thin mica films were obtained from a selected sheet by splitting the edge with a razor blade, inserting a drop of water and easing a thin card along the cleaving plane to obtain complete separation. The process was repeated until the film was sufficiently thin. It was then sealed into place with acetone collodion and trimmed when dry. 'Cellophane', Perspex', very thin glass and cellulose nitrate films were examined but failed to meet many of the requirements.



DETAILS OF OBSERVATION CELL FIGURE 7·5.

The smaller window W_2 (figure 7.5) was made from a piece of micro cover glass sealed in position with 'Picein'.

Since the windows were rather fragile a pressure release (figure 7.9) was used to prevent the application of a pressure greater than 1 cm. of water.

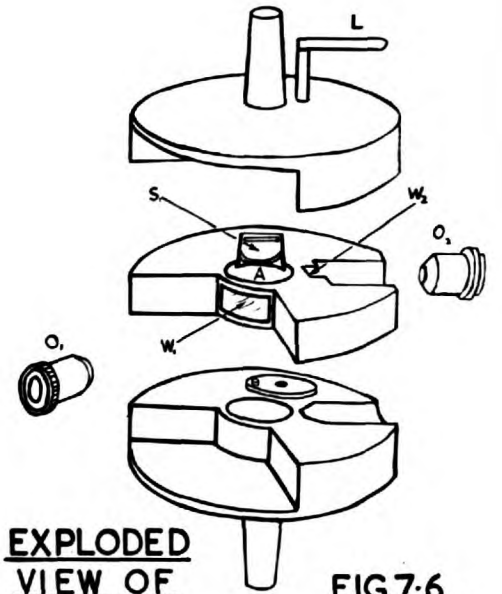
In assembling the cell, metal surfaces in contact were coated with 'Vaseline' to prevent leaks and all internal surfaces were painted dead black to diminish ~~strong~~ stray reflections.

The cell was designed so that observations could be made between 0 and 90^0 to the incident beam. The photographs were all taken at right angles but the photometric measurements described in chapter VIII were made at various angles between 0 and 90^0.

VII. 3.3 Illumination.

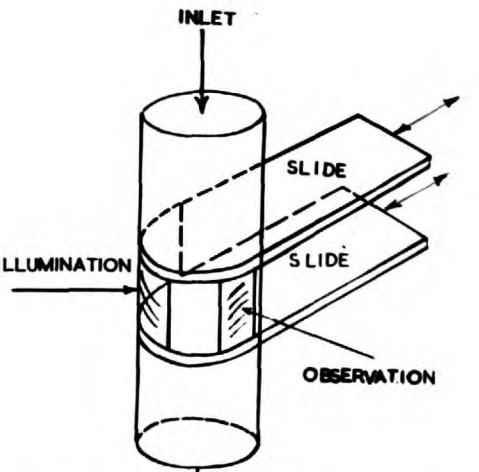
A narrow beam of light passing diametrically through the cell was obtained from a mercury arc. The lens B (figure 7.4) focussed thr light in the plane of the vertical slit E (figure 7.10), an image of which was formed at the centre of the cell by objective O_2 in the block F. The optics of the system are shown in figure 7.4 a.

The initial brightness of the arc was 20,000 candles cm^{-3}, and since an appreciable ~~function~~ fraction of energy was emitted in the infra red region of the spectrum, five thicknesses M and C of heat



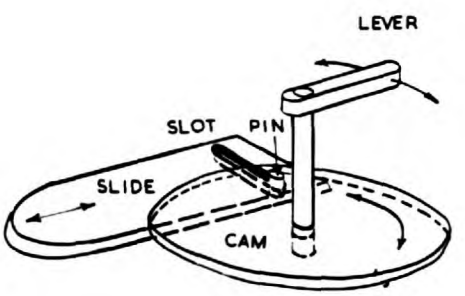
EXPLODED VIEW OF CELL.

FIG.7·6.



PRINCIPLE OF THE OBSERVATION CELL.

FIG.7·7



OPERATION OF THE SLIDES.

FIG.7·8.

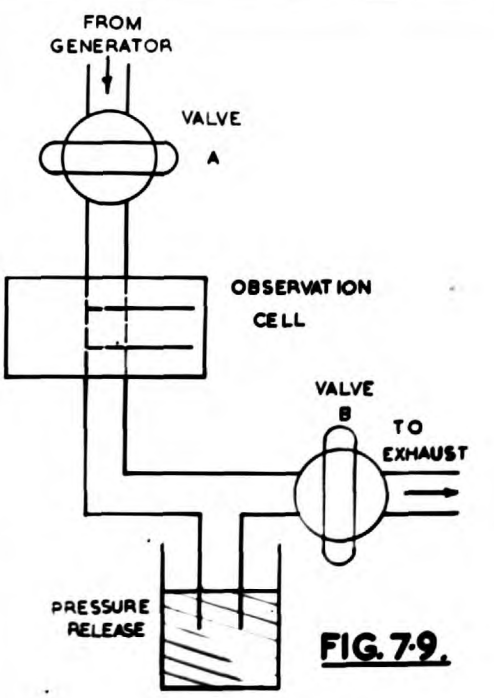


FIG.7·9.

absorbing glass (ON20) each 1 mm. thick were interposed between the arc and cell. These transmitted 59% of the visible energy and 10^{-5}% of the infra red.

A shutter D was opened only during observations. The beam through the cell is shown in section in figure 7.11 and in profile 7.12. Its breadth was of the order of 0.01 cms.

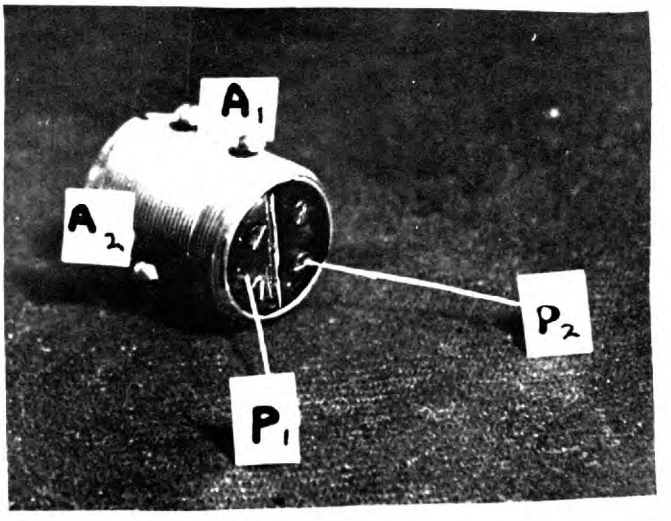
VII. 3.4 The ultramicroscope and camera.

An objective O_2 (figure 7.5) was fitted behind the observation window W_2 and formed a real, inverted image of the contents of the cell in the plane of the film in the camera.

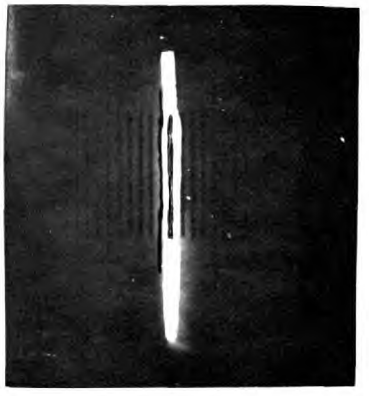
The objective had a numerical aperture of 0.15, a focal length of 2.5 cms. and a working distance of 1.7 cms. The camera body was obtained from a 'Nea Fotos' 35 mm. camera and was fitted with an adjustable extension tube J so that the distance between the lens and the film was 17 cms. The shutter O was an Ensign 'Epsilon' having exposure times of 1/150 to 1 second. The camera was mounted on a rigid steel arm P, 1 cm. thick and 5 cms. wide.

VII. 3.5 Alignment of the apparatus.

The cell was fixed with its optical axis 17.5 cms. above the top of the optical bench and this axis used as a datum line. The other components were adjusted until the beam passed diametrically through the cell, each being adjustable as follows.

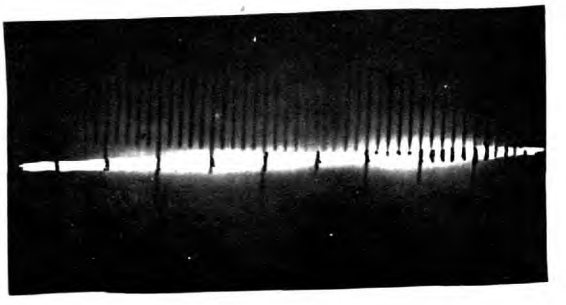


DETAILS OF THE SLIT FIG.7·10



SECTION OF BEAM.

FIGURE 7·11.



PROFILE OF BEAM.

FIGURE 7·12.

(a) The arc A (figure 7.4) had lateral and vertical adjustments.

(b) The condenser B (figure 7.4) had lateral and vertical adjustments and could be rotated slightly about lateral and vertical axes.

(c) The slit E (figure 7.4) could be adjusted in a longitudinal direction by screws A_1 A_2 (figure 7.10) and could be tilted slightly by screws A_1 . The tube in which the slit was mounted allowed some longitudinal motion and enabled it to be rotated about the optical axis.

(d) The block F (figure 7.4) carrying the slit and the objective could be moved a few degrees in either direction about the vertical axis of the cell.

(e) The objective O_2 (figure 7.5) could be moved to focus the camera.

Alignment of the optical system was obtained by the following procedure.

With the aid of a pointer fixed at a height of 17.5 cms. above the optical bench, all components were made to lie on the optical axis and the centre portion of the arc was then focussed onto the slit. By making a direct observation through the ultramicroscope, which was set in line with the optical axis of the system, the slit was adjusted until no apparent sideways motion occurred when it was rotated through 180°.

Focussing of the camera was carried out in two stages. The cell was filled with aerosol and a microscope eyepiece was held in the plane of the film; the objective was then adjusted until individual particles could be seen. Accurate focussing was obtained with a piece of clear film having several fine scratches on the emulsion side. The microscope was carefully adjusted until the images of the scratches coincided with these scratches.

VII.4.The experimental procedure.

The photomicrographs used to record the changes in the aerosol were obtained by the technique described below. The measurements which were then made on the photomicrographs are described in the subsequent sections.

VII. 4.1 The photomicrographs.

The generator was set to give the desired aerosol and was allowed to reach steady conditions. A visual observation was made using the ultramicroscope to estimate the total time of settling and the photographic exposures were then made at intervals corresponding to a tenth of this time. In each experiment, the procedure described below was followed.

To fill the cell, valves A and B shown in figure 7.9 were opened and the aerosol allowed to flow freely through the apparatus. The flow was stopped by closing valve B and a few

PHOTOGRAPHS USED IN TYPICAL EXPERIMENT



FIG.7·13. INITIAL CONCENTRATION.

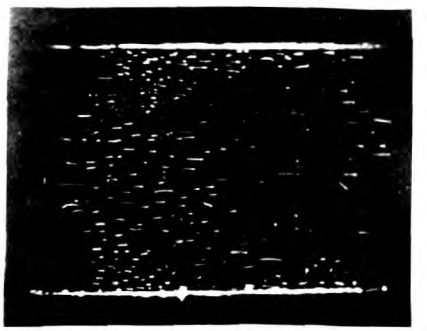


FIG.7·14. ZERO OF EXPERIMENT



FIG.7·15 PARTICLE SIZE.



FIG.7·16. CONCENTRATION CHANGES

PHOTOGRAPHS USED IN TYPICAL EXPERIMENT. CONTD.

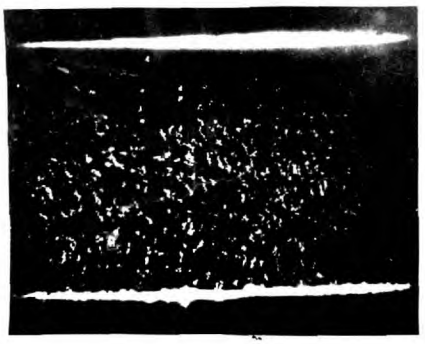


FIG.7·17. PARTICLE SIZE.



FIG.7·18. CONCENTRATION.



FIG.7·19. CONCENTRATION.

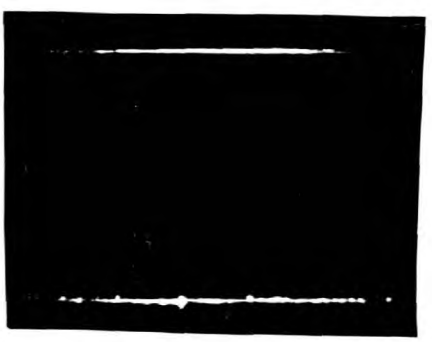


FIG.7·20. CONCENTRATION.

seconds later, valve A. Then the initial concentration was recorded by an exposure of 0.1 to 1 second as soon as the aerosol had become stationary (figure 7.13). Repeated observations of concentration changes were made at intervals of 10 to 60 seconds after the slides (figures 7.14 to 7.20) had been closed and the changes were recorded by photographic exposures of 0.1 to 1 second.

Particle size was recorded by a larger exposure of 1 to 10 seconds (figure 7.15).

The volume of aerosol observed in the cell was determined from measuremanst of the breadth of the beam and from the area observed on a photographic negative. The breadth of the beam was recorded in each experiment when the slit (figure 7.4) had been rotated through 90° and the cell refilled.

The photographs taken in a typical experiment are tabulated (Table 7.1) . Blemishes in the negative were reduced in number by preparing the photographic solutions with distilled water and filtering them before use.

Table 7.1 The photographs used in a typical observation.

Experiment number A 126.

Exposure Number	Description	Time Seconds	Exposure Time Seconds	Figure Number
1	Initial concentration		0.5	7.13
2	Zero of experiment	0	0.5	.14
3	Particle size	5.25	0.5	.15
4	Concentration as a function of time.	32.5	0.5	.16
5	Particle size	60.25	0.5	.17
6	Concentration	77.5	0.5	.18
7	Concentration	90.25	0.5	.19
8	Concentration	120.25	0.5	.20
9	Width of beam		0.5	.21

VII. 4.2. Determination of the initial concentration.

The initial concentration was determined from the exposure made just before the slides were closed. The photograph obtained as the slides closed showed the particles in lateral motion and could not be used for measurements though it could be used to verify that the aerosol was spatially homogeneous.

The particles in a known area were counted when the photographic negative was projected onto a screen. A graticule with a vertical dimension equal to the magnified image of the depth of the cell and divided into ten equal horizontal elements ~~(figure 7.13)~~ was superimposed on the screen. Its width was about a third of the height (29.6 cms. x 11 cms. with magnification of 132.3 times).

By counting the number of particles in each element and dividing by the volume, the initial concentration was determined as a function of position in the cell. Particles, lying on a boundary were included in the element in which their mid-points lay.

A typical result appears in Table 7.2.

The intensity of the beam was a maximum at the centre of the cell due to the effect of the small apertures in the system. Consequently, more particles were observed at the centre of the cell than near the top or bottom. This distribution was

determined in each experiment and was used in section V.1 to calculate the relative concentration c.

VII. 4.3. Determination of the changing concentration.

The concentration at successive intervals was determined, as previously described (see figures 7.15 to 7.20). The results of a typical experiment are shown in Table 7.2

VII. 4.4. Determination of particle size.

The radius of a particle was determined by means of the Stokes - Cunningham relation given in chapter II.

$$v = \frac{2}{9} \cdot \frac{a^2 g}{\eta} (\rho - \rho_0) F \qquad (3)$$

The vertical distance d, which a particle fell in an exposure time e was determined by measuring the distance s'on a photomicrograph with a travelling microscope; then

$$d = \frac{s'}{M} \qquad (4)$$

where M is the magnification of the photographic image.
The velocity, v, is given by

$$v = \frac{s'}{eM} \qquad (5)$$

Hence the radius of the particle could be determined graphically from (3).

Since the photographic image spread so that a point object

Table 7.2

Frame Number	Number of particles observed in each element of the cell										Figure.
	Z = 0.05	0.15	0.25	0.35	0.45	0.55	0.65	0.75	0.85	0.95	
1	9	11	13	13	12	11	18	11	7	6	7.13
3	2	6	11	11	12	12	14	12	14	6	7.15
4	0	0	3	10	11	10	10	10	13	5	7.16
5	0	2	4	10	11	10	11	12	11	8	7.17
6	0	0	0	6	14	11	11	8	9	4	7.18
7	0	0	0	0	3	7	9	13	8	5	7.19
8	0	0	0	0	1	4	9	9	7	3	7.20

Volume of single element = 1.59×10^{-5} cubic centimetres.

Initial concentration = 7.00×10^{5} particles per cubic centimetre.

appeared as a circle of 0.005 cms. radius, the width m of a particle track on the negative was deducted from the length s' so that the corrected form of equation (4) is

$$d = \frac{s' - m}{M} \qquad (6)$$

In each experiment, the length and width of ten tracks were measured. The sample was obtained with a graticule of such spacing that two or three tracks were observed in each area; particles in three or four areas were at different depths in the cell were measured. The arithmetic mean radius $\bar{a}$ for the particles observed was calculated, a typical result being shown in Table 7.3

VII.4.5. Determination of dispersion of the particle radius.

The standard deviation $\sigma(a)$ of the particle radii was calculated and the dispersion $\vartheta(a)$ was obtained from the relation,

$$\vartheta(a) = \frac{\sigma(a)}{\bar{a}} \qquad (7)$$

where $\sigma(a) = \left[\overline{a^2} - \bar{a}^2\right]^{\frac{1}{2}}$

The necessary measurements are shown in Table 7.3

VII. 4.6. The volume of an element of the observation cell.

The volume of a single element (figure 7.22) was determined

Table 7.3 Determination of particle size.

Experiment number A 126 Frame number 3 Figure number 7.15

Length of track of film cms.	Breadth of track of film cms.	Distance fallen by particle $\times 10^{+4}$ cms.	Velocity of particle $\times 10^{+4}$ cms.sec.$^{-1}$	Radius of particle Microns.
0.0269	0.0028	7.43	1.49	0.205
0.0232	0.0018	6.60	1.32	0.190
0.0304	0.0031	8.42	1.68	0.220
0.0358	0.0043	9.71	1.94	0.240
0.0386	0.0046	10.48	2.10	0.250
0.0189	0.0046	4.41	0.88	0.148
0.0274	0.0040	7.22	1.64	0.202
0.0380	0.0045	10.33	2.07	0.248
0.0446	0.0046	12.33	2.47	0.275
0.0310	0.0041	8.29	1.66	0.216

Magnification M = 6.485
Exposure time $\underline{e}$ = 5.00 seconds
Mean radius $\bar{a}$ = 0.219 microns
R.M.S. radius $(\bar{a^2})^{\frac{1}{2}}$ = 0.222 microns
Standard deviation of radius $\sigma(a)$ = 0.0344 microns
Dispersion of radius $\vartheta(a)$ = 0.157

by measuring the depth of the cell L, the effective breadth b of the beam and the width w which was observed when the negative was projected.

The depth was measured with a travelling microscope and gave

$$L = 0.2237 \pm 0.0003 \text{ cms.}$$

Hence $\frac{L}{10} = 0.0224$ cms.

The breadth b of the beam was determined in each experiment using a photograph (such as figure 7.21) of given magnification taken with the cell filled and the slit horizontal. The breadth was of the order of 0.01 cms.

The width w of the element was determined during projection of a negative to determine numerical concentration and was equal to the width of the graticule divided by the magnification. The width of the element was of the order of 0.1 cms.

Consequently the volume of a single element is given by the relation

$$V = \frac{bwL}{10} \text{ cms.}^3 \qquad (8)$$

is of the order of 10^{-5} cm.^{3}.

VII. 4.7. Determination of the magnification.

The apparent depth of the cell was measured in a photograph and since the true depth was known the magnification M of the

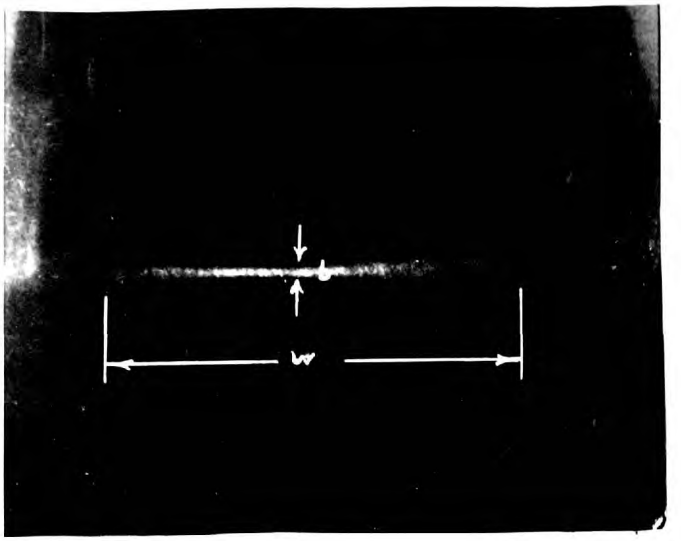


FIG. 7·21

DIMENSIONS OF BEAM.

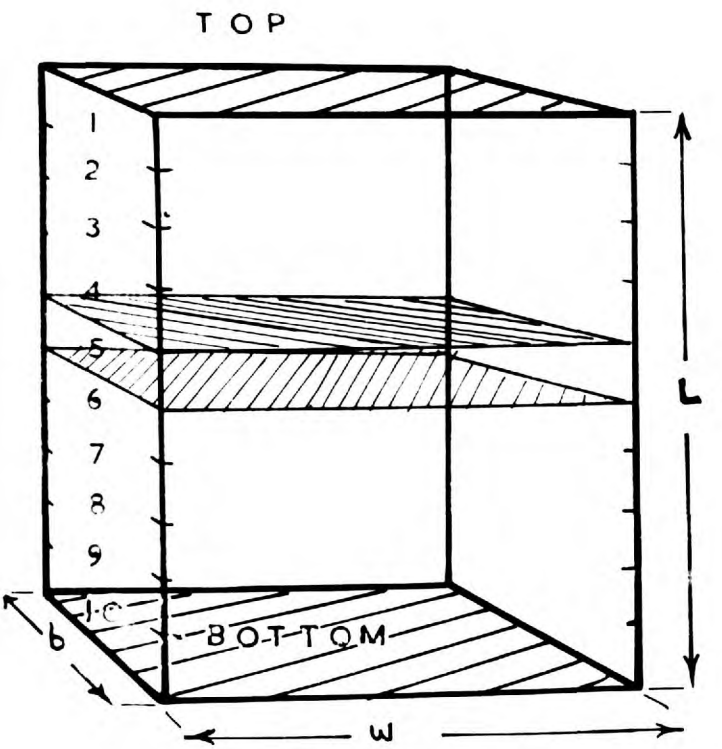


FIG. 7·22

ELEMENTS OF VOLUME
OF OBSERVATION CELL

photograph could be calculated. It was determined in each experiment since it changed when the ultramicroscope was refocussed.

The values of M were approximately x 6.5 in a negative and x 130 under the projector.

VII. 5. The experimental results.

VII. 5. 1. To illustrate the treatment of the results, the calculations made in a typical experiment are presented. The parameter in equations (1) and (2) were calculated from measurements of the numerical concentration and were compared with values calculated from the particle size which was measured.

The photographs obtained in a typical experiment appear in figures 7.13 to 7.21 and are described in table 7.1.

The measurements made in the determination of particle size from figures 7.16 appear in table 7.2. The concentration at various times and positions in the cell were measured from figures 7.13 and 7.15 to 7.20 and the results are shown in table 7.2.

Since the measurements of concentration were subject to random variations with time and position, they were smoothed before making any calculations. The relative concentration $c = \frac{n}{n_o}$ was calculated and was again smoothed (n_o is the initial concentration). From the set of values of c two or three equations were obtained and solved simultaneously for α and H (or α, H and γ). To

avoid assumptions regarding the radius, the interval of true time ΔT was used in the calculations, not the reduced time ΔT. Each step of the process will now be described in detail.

The values of the concentration were smoothed by the following procedure;-

Represent the unsmoothed values by n_{jk} as in the table below :-

Table 7.4

	Z 1	Z 2	Z 3	Z 4	Z 5
t 1	n_{11}	n_{12}	n_{13}	n_{14}	n_{15}
t 2	n_{21}	n_{22}	n_{23}	n_{24}	n_{25}
t 3	n_{31}	n_{32}	n_{33}	n_{34}	n_{35}

Then the smoothed values of n are obtained as follows :

First smoothing in the Z direction

$$(n_{jk}) = \frac{1}{3}\left[n_{j,k-1} + n_{jk} + n_{j,k+1} \right] \qquad (9)$$

e.g.

$$(n_{13}) = \frac{1}{3}\left[n_{12} + n_{13} + n_{14} \right]$$

These values were then smoothed in the t direction, by using the following equations :-

$$(n_{jk}) = \tfrac{1}{3}\left[n_{j-1.k} + n_{jk} + n_{j+1.k} \right] \qquad (10)$$

e.g. $(n_{34}) = \tfrac{1}{3}\left[n_{24} + n_{34} + n_{44} \right]$

In table 7.5, horizontal and vertical arrows indicate smoothing in the Z direction (constant t) and the t direction (constant Z). Values of n obtained by smoothing table 7.3 appear in table 7.5.

The relative concentration c was calculated ($0 < c < 1$) for each position in the cell and the values were further smoothed by plotting the first differences Δc against t for a constant value of Z (table 7.6) drawing the graph which best fitted the points and reading smoothed values of Δc from the graph. (N.B. Since there was an apparent variation of initial concentration with depth the values of n_o at the appropriate position in the cell were used to calculate c). These differences were used to obtain a new set of values of c at intervals of 10 seconds (table 7.7)

Using the finite difference equation (28) chapter IV values of α and H were calculated

$$0 = \alpha \frac{(c_1 + c_3 - 2c_o)}{h^2} - \frac{c_1 - c_3}{2h} - \frac{c_2 - c_4}{2H} \qquad (11)$$

Table 7.5

Frame Number	Smoothed values of numerical concentration n Z =	0.05	0.15	0.25	0.35	0.45	0.55	0.65	0.75	0.85	0.95
1	→	10.11	10.99	12.22	12.33	12.74	12.99	12.99	11.33	8.78	7.00
	↓	8.18	9.36	11.07	11.73	12.45	12.77	12.98	11.66	10.03	6.81
3	→	4.33	6.11	8.77	10.55	11.88	12.33	12.88	12.33	10.88	6.44
	↓	4.92	6.28	8.44	10.14	11.36	11.85	12.10	11.18	9.59	6.29
4	→	0.33	1.74	4.44	7.55	9.55	10.22	10.44	9.89	9.11	5.44
	↓	1.77	3.17	6.14	8.68	10.36	11.70	11.40	11.04	9.44	5.81
5	→	0.66	2.66	5.22	7.93	9.66	10.55	10.89	10.89	9.33	5.55
	↓	0.33	1.69	4.15	7.27	9.52	10.50	10.59	9.85	8.59	5.07
6	→	0	0.66	2.78	6.33	9.55	10.74	10.44	8.78	7.33	4.22
	↓	0.22	1.11	1.78	5.01	7.55	8.91	10.00	9.73	8.11	4.70
7	→	0	0	0.33	1.44	3.44	5.44	8.66	9.44	7.66	4.33
	↓	0	0.22	1.07	2.81	4.29	8.80	8.51	8.52	7.22	3.92
8	→	0	0	0.11	0.66	1.88	4.22	6.44	7.33	6.66	3.22
	↓	0	0	0.39	0.70	1.77	3.22	5.03	5.59	4.74	2.52

Table 7.6 First differences of c

t	c(Σt)	Δ c
t_1	c_1	
		$c_1 - c_2$
t_2	c_2	
		$c_2 - c_3$
t_3	c_3	
		$c_3 - c_4$
t_4	c_4	
		$c_4 - c_5$
t_5	c_5	
		$c_5 - c_0$

Table 7.7 Final values of relative concentration

Time Seconds	Z = 0.05	0.15	0.25	0.35	0.45	0.55	0.65	0.75	0.85	0.95
0	1.000	1.000	1.000	1.000	1.000	1.000	1.000	1.000	1.000	1.000
10	0.520	0.690	0.720	0.904	0.930	0.935	0.949	0.986	0.998	0.940
20	0.340	0.526	0.618	0.816	0.869	0.934	0.933	0.966	0.988	0.928
30	0.238	0.416	0.478	0.734	0.818	0.930	0.920	0.943	0.973	0.912
40	0.173	0.336	0.444	0.655	0.771	0.916	0.904	0.919	0.953	0.888
50	0.127	0.276	0.384	0.579	0.725	0.888	0.883	0.893	0.929	0.857
60	0.097	0.229	0,332	0.505	0.676	0.847	0.855	0.863	0.897	0.819
70	0.077	0.193	0.284	0.433	0.621	0.793	0.818	0.828	0.860	0.793
80	0.062	0.165	0.241	0.363	0.558	0.727	0.769	0.785	0.813	0.719
90	0.054	0.140	0.201	0.294	0.483	0.646	0.706	0.731	0.757	0.656
100	0.050	0.115	0.163	0.227	0.388	0.544	0.626	0.656	0.690	0.587

Similarly values of α, γ and H may be obtained from equation (30) chapter V.

$$0 = \alpha\left(\frac{c_1 + c_3 - 2c_0}{h^2}\right) - \frac{(c_1 - c_3)}{2h} - \frac{1}{2H}(c_2 - c_4) - \gamma c_0^2 \qquad (12)$$

From the values of c in table 7.7, values of α and H were calculated and the result is shown in Figure 7.25. (The method of calculating α γ and H is similar). Before discussing calculations it is advisable to observe the form of the intervals h and H which occur in the difference equations since the reduced co-ordinates Z and T were used, where

$$\left.\begin{aligned} Z &= \frac{z}{L} \\ \text{and} \quad T &= t.\frac{v}{L} \end{aligned}\right\} \qquad (13)$$

The interval in Z is h and is equal to 0.1, which is the distance between the mid-points of adjacent horizontal elements of the cell. The interval in T is H and since $T = t.\frac{v}{L}$

$$H = \Delta t \frac{v}{L} \qquad (14)$$

In reading the values of the first differences from the graphs used for smoothing, new intervals in t of 10 seconds have been taken. Consequently

$$H = 10 \frac{v}{L} \qquad (15)$$

where v is unknown

Equation (13) may be rewritten

$$a_{11}x_1 + a_{12}x_2 = b_i \qquad (16)$$

where
$$\left.\begin{aligned} a_{11} &= (c_1 + c_3 - 2c_o) \\ a_{12} &= \frac{-h^2}{2}(c_2 - c_4) \\ b_i &= \frac{h}{2}(c_1 - c_3) \\ x_1 &= \alpha \\ x_2 &= \frac{1}{H} \end{aligned}\right\} \qquad (17)$$

It is seen that 110 values of c occur in table 7.7, permitting 72 equations suchas (16) to be obtained whereas only two were required. Owing to the length of the calculation required, a fractional analysis of all the possible values of α was not attempted. If intervals of h = 0.2 and $\triangle$ t = 20 seconds were taken, values of c could be obtained at points having co-ordinates in the ranges of Z between 0.25 and 0.75 and t 20 seconds to 80 seconds.

Two equations free from bias were obtained from the sums of the values of c obtained at the points indicated in table 7.7 by a dot for the first equation and a cross for the second.

$$\left.\begin{aligned} a_{11}x_1 + a_{12}x_2 &= b_1 \\ a_{21}x_1 + a_{22}x_2 &= b_2 \end{aligned}\right\} \qquad (18)$$

Table 7.8 Results of Experiment A 126

Radius $\bar{a}$	=	0.219 ± 0.0001 microns
Dispersion	=	0.157
Volume of single element	=	$1.59.\ 10^{-5}$ cm^3
Initial concentration	=	$7.00.\ 10^{5}$ particles cm^3
Mass concentration	=	$1.0.\ 10^{-7}$ $gm.cm^3$ - ~~from $\bar{a}$~~
Theoretical value of α	=	0.0041 from $\bar{a}$
Experimental value of α	=	0.0054
Theoretical value of γ	=	0.0004 (from $\bar{a}$ and n_o)
Experimental value of γ	-	not calculated

VII. 6.1 Discussion of the accuracy of the measurements

VII. 6.1(Measurements made on the photographic image.

In making the measurements on the negatives, it was assumed that they contained a representative sample of the contents of the observation cell. The limit of resolution of the lens was 0.00024 cms. and the radius of the Airey disc produced in the image space was 0.0016 cms. Light was scattered in the photographic emulsion and caused some diffuseness in the image. Although the grain size was only 0.0002 cms., the limit of resolution of the medium was 0.0020 cms.

As a result of these factors the image of a point object was a diffuse circle whose radius was a function of the brightness of the object and the method of processing the negative. Although the negative may have shrunk during the processing, shrinking was automatically accounted for in the measurement of the magnification.

The error in a measurement made on the negatives is due to the travelling microscope and the difficulty of setting the cross-wires on a diffuse edge. In setting the microscope to observe a sharply defined line, the standard deviation of 10 consecutive readings was 0.00027 cms. but for the comparatively diffuse image of a particle it was increased to 0.00039 cms.

In the determination of particle size a correction was made to the track length for the spread of the photographic image by

deducting the width of a track from its length. The error in measuring the length of the track on the negative was taken to be 0.0004 cms.; the standard deviation of 10 repeated settings.

All the measurements depend on the accuracy with which the magnification M is determined.

$$M = \frac{L'}{L} \qquad (19)$$

where L is the depth of the cell

L' is the apparent depth in a magnified image

The separation L of the two slides was measured with a travelling microscope and was 0.2237 $\pm$ 0.0003 cms.

The separation L' in a typical photograph was 1.4541 $\pm$ 0.0004 cms.

The error in M may be estimated as follows :-

$$M = \frac{L'}{L}$$

Hence $$dM = \frac{\partial M}{\partial L'} . dL' + \frac{\partial M}{\partial L} dL \qquad (20)$$

Now the variance V(x) of a variate x is given by the relation

$$V(x) = \overline{(x - \bar{x})^2} \qquad (21)$$

Consequently $$V(M) = \overline{dM^2}$$

$$= M^2 \left[\frac{dL'}{L'} - \frac{dL}{L} \right] \qquad (22)$$

Hence the standard deviation of M is given by

$$\sigma(M) = M\left[\frac{V(L')}{L'^2} + \frac{V(L)}{L^2}\right]^{\frac{1}{2}} \quad (23)$$

Since the values of L L' and their variances were known σ (M) could be determined

$$\sigma(M) = 0.0089$$

Now that the errors of the basic measurements have been assessed, the errors of the determination of particle size and concentration may be evaluated.

VII. 6.2 Accuracy of determination of particle size.

In the measurement of particle size, the length of a track on a photographic negative was measured, the corresponding length in the cell was calculated and the sedimentation velocity determined.

In addition to the errors in the determination of the track length and the magnification, those in timing the exposure and reading the graph of Stokes Law must be considered.

The camera shutter was calibrated by Wallace Heaton Ltd. and the error was stated to be 2%. For exposure times up to 1 second, exposures of 5 to 20 seconds were timed with a stop-watch where the error was ±0.1 or 2 to 0.5 % .

From equations (3) and (5) the radius is given by

$$a = \left[\frac{s}{bMe} \right]^{\frac{1}{2}} \qquad (24)$$

where $b = \frac{2}{9} \frac{g}{\eta} (\rho - \rho_0) F.$

The standard deviation of the radius may be determined by an argument similar to that used to obtain equation (23).

$$\sigma(a) = \frac{\bar{a}}{2} \left[\frac{V(s')}{s'^2} + \frac{V(b)}{b^2} + \frac{V(M)}{M^2} + \frac{V(e)}{e^2} \right]^{\frac{1}{2}}$$

In the equation, s' is the track length corrected for spread (see equation (6), s' = s-m), and V(b) is taken as the error in reading the graph. If this error were negligible

$\sigma(a)$ = 0.002 microns for a = 0.1 micron

= 2%

and $\sigma(a)$ = 0.003 microns for a = 1 micron

0.3%

It was decided that an error of 2 to 5% was tolerable and the graph of Stoke's Law was plotted on the appropriate scale.

The Brownian motion superimposed on the sedimentation velocity v of a particle during an interval of time t results in a vertical displacement $z - z_0$ which is given by

$$z - z_0 = vt + r_z \qquad (26)$$

In this relation, r_z represents the integral

$$\int_0^t B(t)_z \, dt \qquad (27)$$

where $B(t)$ is a fluctuating velocity component, characteristic of the Brownian motion and the $B(t)_z$ is the component in the z direction. $B(t)$ follows a Maxwellian distribution.

In the determination of particle size, an observation was made of the apparent vertical displacement of a particle in a given time, and from this a velocity was calculated. If the observation had recorded the co-ordinate z_o at time $t = 0$ and z at $t = e$ the mean value of $z - z_o$ calculated for several particles would enable the sedimentation velocity to be determined

$$\frac{\overline{z - z_o}}{e} = \bar{v} \qquad (28)$$

since $\bar{r}_z = 0$

From this, the root mean square radius could be calculated. Alternatively, a value of v could be determined for each particle track and used to calculate an arithmetic mean radius.

With the photographic method the displacements of the particle was continuously recorded during an interval of time e. Consequently, the displacement observed was not the mean value

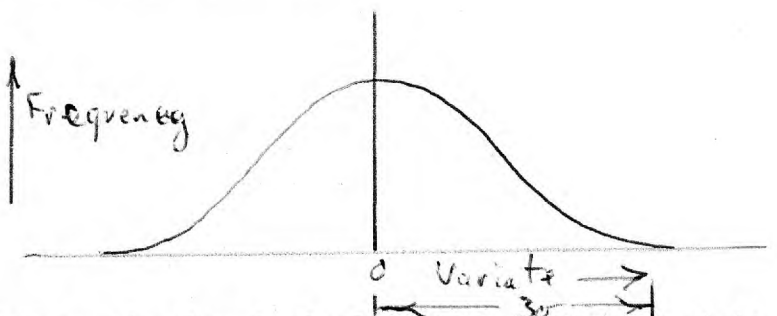
$\overline{z - z_0}$ but the maximum value of the modulus of $z - z_0$

Because $\left| r_{\frac{3}{5}} \right|_{max} \neq 0$ it follows that

$$\left| z - z_0 \right|_{max} \quad \overline{z - z_0} \qquad (29)$$

and the particle size determined was slightly too large, but there is no single way of calculating the requisite correction.

An approximate correction may be made as follows. Since the 'relaxation time' β^{-1} is of the order of 10^{-7} seconds (for a radius of 0.1 micron), a representative sample of the individual displacements of the Brownian particle should be observed. An approximation to the positive half range in any normal distribution is 3σ.



where σ is the standard deviation of the variate. This assumes that the displacement for 3σ or less has a probability of 99.73%.

In the Brownian motion

$$(\overline{z^2}) = (2Dt) \qquad (30)$$

and $\sigma = (\overline{z^2})^{\frac{1}{2}}$

Consequently, if 10 particles were observed the mean value of σ was

$$\frac{\sigma}{\sqrt{10}} = \frac{(\bar{z}^2)^{\frac{1}{2}}}{3.3} \qquad (31)$$

Hence $$|z-z_o|_{max} \qquad \frac{3(2Dt)^{\frac{1}{2}}}{3.3} \qquad (32)$$

This correction was applied in several determinations of particle size and then the order was correct but the magnitude too high. In the graph of values of the parameter α, the theoretical value of α was determined for a radius which had not been corrected by this method.

VII. 6.3 Accuracy of the measurements of the initial concentration.

In the determination of the initial concentration, the number of particles in a certain area of the photographic negative was counted and divided by the corresponding volume.

The errors of counting the particles are due to the personal error and obscuration of one particles by another. Since the volume observed is a small part of the total, statistical fluctations in concentration are appreciable. The motion of particles may cause an apparent increase in the concentration and variations in intensity of the beam which affected the counting of particles.

The personal error was expressed as the standard deviation

of ten repeated counts of one area and was found to be 6% of the total number of particles.

Since the beam had an appreciable thickness it was possible for a particle nearer the camera to obscure a more distant particle. The error introduced can be estimated from the probability of overlap of circles falling at random into a plane area. This problem was investigated by Armitage (1949) who showed that the percentage error ε is given by

$$\varepsilon = \frac{2 \pi n_1 a^2}{A} \cdot 100 \% \qquad (33)$$

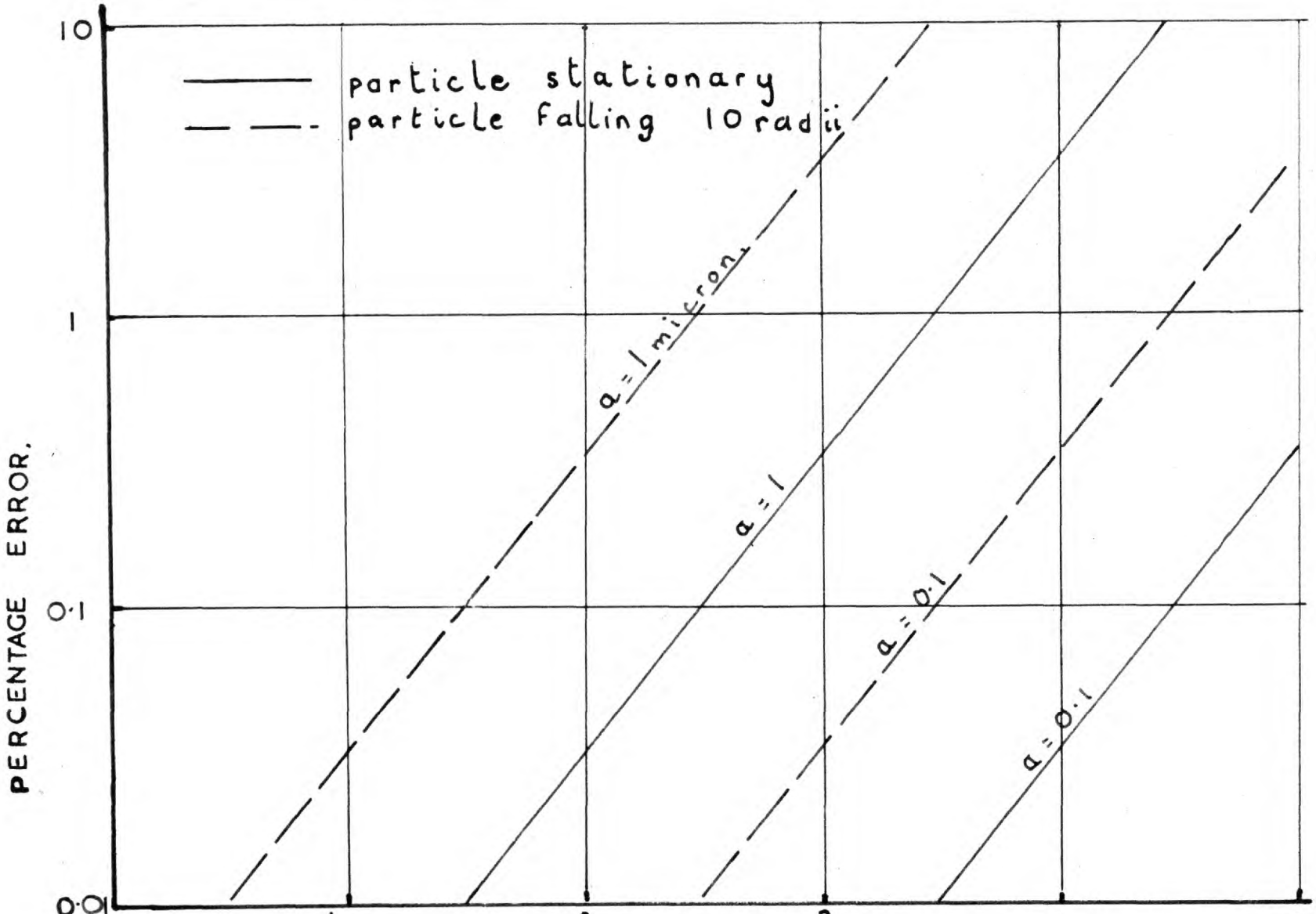
where n_1 is the number of particles of radius a observed in an area A

Then the true number n is given by

$$n = n_1 \frac{100 + \varepsilon}{100} \qquad (34)$$

Equation (33) applies to the overlapping of identical circular discs; ε is plotted against n in figure 7.23 for two different radii.

In drawing the graph, the effect of spreading of the photographic image has been neglected but sedimentation is accounted for by taking the area of the track made by a falling particle.



ERROR DUE TO OVERLAP

FIGURE 7·23

It may be seen that for particles of 1 micron radius the effect is of the order of 3% when 10^3 particles are observed in the field. Taking into account the irradiation of the photographic image, the number of particles which can be observed is 10^2, corresponding to the maximum concentration observable of 10^7 particles cm^{-3}.

Since the number of particles n_1 observed in each element was but a small fraction of the total number in the cell, statistical variations were observed from one element to the next. Assuming these variations to follow a Poisson distribution, the standard deviation is

$$\sigma(n) = \left(\frac{\bar{n}_1}{10}\right)^{\frac{1}{2}} \qquad (35)$$

In a typical experiment $\bar{n}_1 = 170.8$, the average number of particles in one element.

and $\sigma(n) = 4.1$

The standard deviation of the particles in 10 elements was calculated and found to be 6.6, which is rather more than expected from equation (35) and includes the personal error.

Since the particles were in motion, migration occurred in and out of the volume if the observations were carried out for an appreciable time. Then the number of particles recorded in

in a photomicrograph would be larger than the number present at any instant. When the motion was due to sedimentation, no error was introduced if only those particles were counted which had their mid-points in the element. In Brownian motion, the mean square path (in one dimension) is given by equation (30). Consequently, if a particle of 0.1 microns was observed for 10 seconds $(\overline{x^2})^{\frac{1}{2}} = 1.5 \cdot 10^{-2}$ cms. about the width of the beam consequently such a particle might be lost *. If so, the average concentration ~~details~~ determined should still be the true value, since it is expected that as many particles diffuse in as out during an interval as long as 10 seconnds. The particle size determined would be in error as the track would be cut short.

---

* This result is only an approximation. The probability P that a particle somewhere inside a volume τ will have emerged after a time t , is called the probability after-effect factor. (Chandrasekhar (1943) p.45).

When the motions of the individual particles are governed by the laws of Brownian motion

$$P = 1 - \frac{1}{(4\pi D t)^{3/2}} \int_{\tau} \int_{\tau} \exp - \frac{(r_1 - r_2)}{4Dt} \, dr_1 \, dr_2$$

where r_1 is the position of a particle at $t = 0$

r_2 is its position after a time t extended

and the integration is extended over all points inside τ .

If the particles follows linear trajectories but have a Maxwellian distribution of velocities then the probability after-effect is given by the relation

$$P_0 = \frac{s}{\tau} \left(\frac{kT}{2\pi m} \right)^{\frac{1}{2}}$$

where s is the surface area of the volume element τ .

A few imperfections were observed in the photographic negative, but the majority of them were easily distinguished from particle tracks and as the total number of imperfections in the area of negative observed were of the order of 10, the error introduced would be negligible.

The errors in the measurement of volume of an element were :-

Error in measurement of depth of element $\frac{L}{10}$ = 0.0003 cms.

Error in measurement of breadth of element b = 0.004 cms.

Error in measurement of width of element w = 0.00038 cms.

The standard deviation σ (V) of the volume may be obtained from an equation similar to (23) giving

$$\sigma (V) = 6.8. 10^{-8} \text{ cm}^3$$

The standard deviation of the initial concentration is

$$\sigma (n) = n \left[\frac{V(n_1)}{n_1^2} - \frac{V(V)}{V^2} \right]^{\frac{1}{2}} \qquad (36)$$

where n_1 is the number of particles in one element of volume.

In the experiment which has been discussed

$$\bar{n}_1 = 11.1 \text{ particles /element}$$

$$V(n_1) = \frac{\bar{n}_1}{10} = \frac{11.1}{10}$$

$$V = 1.59. 10^{-5} \text{ cm}^3$$

$V(V) = 4.65 \cdot 10^{-15}$

$n = 6.98 \cdot 10^{5}$ particles $cm.^{-3}$

Hence $\sigma(n) = 6.62 \cdot 10^{4}$

The error of the average of the initial concentration in the experiment described was 9.5% but is of the order of 1% when the concentration is as high as 10^{7} particles $cm.^{3}$

VII. 64 Errors in determination of the changing concentration.

The concentration determined during the experiments was subject to the errors which affect the initial concentration. However, the values obtained were carefully smoothed and it was not possible to determine the random errors to which the individual values of n(Zt) were subjected. Consequently it was impossible to attach an error to the relative concentration.

There are certain other errors which are not random. The distribution of intensity in the beam caused an apparent variation in concentration with depth but this was corrected by calculating the relative concentration in each element of volume as a fraction of the initial concentration in that element.

Some consistent errors may have been introduced by the smoothing process which would tend to reduce high values,

increase lower values and reduce the curvature of the graph.

VII. 6.5 Errors in determination of dispersion.

The determination of the dispersion was affected by errors of measurement of particle size which have been described above.

A further error is introduced due to the Brownian motion. The root mean square value of the vertical displacement of a particle during a time t is given by equation (30)

$$(\overline{z^2})^{\frac{1}{2}} = (2Dt)^{\frac{1}{2}}$$

Consequently the dispersion of the aerosol cannot be determined by this method if it is less than a value given by the ratio

$$\frac{\sigma\ (d)}{\overline{d}} \qquad (37)$$

where σ (d) is the standard deviation of the track length and $\overline{d}$ is the mean value.

VII. 6.6 Estimation of the accuracy of the parameters.

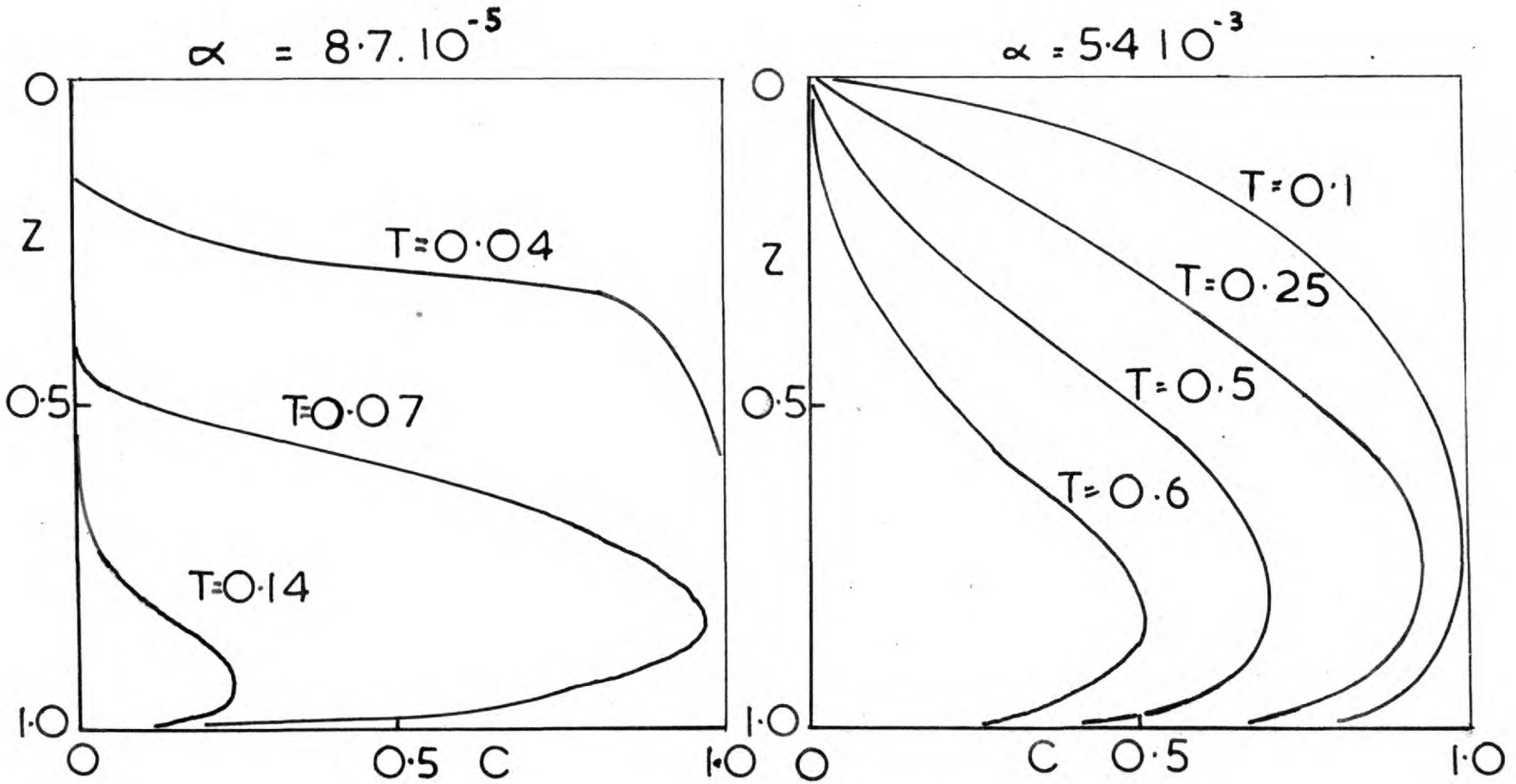
Since no estimate could be made of the error in the relative concentration, it was not possible to assess the accuracy of the experimental determination of the parameters α and γ. Consequently the results obtained by numerical analysis of the concentration measurements were compared with those calculated from measurements of the radius. In figure

Table 7.9 Typical vaules of the measurements and their accuracy.

Particle size	0.1	± 0.001	microns
	1.0	± 0.02	microns

(An error of 5% was tolerable and the graph of Stoke's Law which was used in the determination was plotted on a scale which would permit such an accuracy).

Numerical concentration	10^3	± 10^2	particles cm^{-3}
	10^7	± $7.4.10^4$	" "
Numer of particles per element	10	± 1	
	200	± 4.5	
Volume of an element	(1.5	± 0.007) 10^{-5}	cm^3
Magnification of the negatives	6.5	± 0.009	



VALUES OF C(Z T) OBSERVED.

FIG. 7·24.

7.25 several values of the parameter α are shown.

VII. 6.2 Discussion of the validity of the experiments.

In order to ensure complete freedom from secondary effects the experiments were carried out under carefully controlled conditions. The factors which might invalidate a result are discussed below and their magnitudes are assessed.

1. Mass motion of the aerosol.
2. Motion of the particles under the influence of the incident radiation.
3. Interference with the motion of the particles by the walls of the observation cell.
4. Evaporation of the particles.
5. The effect of dispersion of particle size.
6. Fluctuations in initial concentration.

VII. 6.2.1 Mass motion of the aerosol.

Mass motion could be caused by convection in the aerosol or by air leaking into the cell. In either instance, this would result in motion in a vertical direction near the centre of the cell and radial near the upper and lower surfaces.

In each experiment, one exposure of between 5 and 20 seconds was used in the determination of the particle size. If the particles have moved at an angle greater than 10° from the vertical, it was assumed that mass motion had occurred and the experiment was

rejected. This effect was usually found to be due to leakage and it was necessary to replace the windows in the cell from time to time as dinonyl phthalate removed the adhesive.

VII. 6.2.2 Motion due to radiation.

In chapter II it was shown that radiation of intensity I on a particle would exert a pressure P given by :-

$$P = \frac{2I}{C} \qquad (38)$$

where C is the velocity of light

Hence the force F on a particle of radius a is given by

$$F = \frac{2\pi a^2 I}{C} \qquad (39)$$

This force would produce a terminal velocity v_r given by

$$v_r = \frac{1}{3} \frac{aI}{\eta C} \qquad (40)$$

The initial brightness of the arc was 2.10^4 candles. cm^2 and, from the dimensions of the optical system, the intensity of the beam in the cell was calculated to be of the order of 0.1 erg.cm^{-2}

Hence for a particle of 1 micron radius :-

$$v_r = 1.9.\ 10^{-12}\ cm.sec^{-1}$$

Since the sedimentation velocity was c.a. 10^{-2} cm.sec^{-1} this

was negligible.

The phenomenon of photophoresis has not yet been completely explained. Particles have been observed to move in complex orbits and the motion is probably due to a radiometer effect but there was no evidence of such motion in any of the photomicrogaphs observed.

VII. 6.2.3. Interference of the walls of the observation cell with the motion of the particles.

The effect of the walls of a cylinder through which a sphere was falling was determined by Ladenburg (1907) who showed that the velocity decreased by a factor

$$\frac{1}{1 + 2.4 \frac{a}{R}} \qquad (41)$$

where R is the radius of the cylinder.

In the observation cell $a = 10^{-4}$ cms.

$R = 1$ cm.

Hence the correction is $(1.00024)^{-1}$ which is not appreciably different from unity.

The effect of a horizontal surface was studied by Hopper and Grant (1948) who showed that the decrease in the velocity at a distance z from a horizontal plane was

$$\frac{1}{1 + 1.125 \frac{a}{z}} \qquad (42)$$

This factor is appreciable at a distance of 10^{-3}cms. from the bottom of the cell and therefore, particle size determination should not be made in this region.

VII. 6.2.4 Evaporation of the particles.

In chapter II it was shown that the rate of evaporation of a single droplet surrounded by vapour of concentration c_o was given approximately by the equation

$$a \frac{da}{dt} = \frac{D_1 m_1 c_o}{\rho} \qquad (43)$$

As an example, the rate of evaporation is calculated when droplets of 1 and 0.1 microns are surrounded by saturated vapour.

For dinonyl phthalate :-

D_1 0.03 cm^2 $sec.^{-1}$

$m_1 = 6.98.10^{-22}$ gm.

$c_o = 1.25.10^6$ molecules cm^{-3} at 20°C

$\rho = 0.971$ $gm.cm.^{-3}$

Then $a \frac{da}{dt} = 2.7.10^{-17}$ cm^2 $sec.^{-1}$

and the time taken for the radius to decrease by 10% is :-

$$t = 1.84\ a^2.10^{16} \text{ secs.} \qquad (44)$$

Hence for an initial radius of 1 micron $t = 1.8.10^8$ secs. and for 0.1 micron $t = 1.85.10^6$ secs. For a decrease of 1%

the times are $1.85.\ 10^{8}$ and $1.85.\ 10^{6}$ respectively.

The Kelvin effect becomes appreciable when the radius of a particle is 0.1 microns or less but it can be seen that the effect of evaporation is negligible during an experiment which lasts 10^{3} seconds or less.

VII. 6.2.5 The effect of dispersion of particle size.

If the aerosol were polydisperse, the parameters α and γ being functions of the particle radius may vary with time and position in the cell.

As an example of the effect of dispersion, the distribution of particles in the cell is calculated in appendix 2 assuming sedimentation to be the only process causing concentration changes. If the initial concentration is uniform through the cell, the relative concentration is given in terms of time and position by the relation

$$c(ZT) = \operatorname{erf}\left[\left(\frac{Z}{T}\right)^{\frac{1}{2}} \left(\frac{\bar{r}^{2}}{\sigma}\right)^{2} - \frac{1}{\vartheta} \right] \qquad (45)$$

It can be seen that since α and γ are not directly proportional to the radius, the values determined from concentration measurements in a polydisperse aerosol differ from those calculated from the average radius.

The parameter α is proportional to $\frac{1}{a^{3}}$; γ to $\frac{1}{a^{2}}$

$$\text{Say } \alpha = \frac{\alpha'}{a^3} \tag{46}$$

$$\gamma = \frac{\Delta'}{a^2} \tag{47}$$

Then $d\alpha = \frac{-3}{a}\alpha\, da$

and $\sigma(\alpha) = 3\alpha\gamma(a)$

Calculating the dispersion γ of α,

$$\gamma(\alpha) = \frac{\sigma(\alpha)}{\alpha} = 3\gamma(a) \tag{48}$$

Similarly

$$\gamma(\beta) = 2\gamma(a) \tag{49}$$

Consequently it can be seen that the parameters are very sensitive to the dispersion of the aerosol.

VII. 6.2.6 Fluctuations in concentration.

Occasionally, the initial sample of aerosol contained a small volume of higher concentration and diffusion from this region occurred during the experiments.

If the concentration in the region was not more than 10% greater than that in the remainder of the sample the effect was completely eliminated by smoothing the results. If the

concentration fluctuations were seen to be very high the experiment was rejected.

Table 7.10 Characteristics of typical aerosols.

Radius (Microns)	Numerical Concentration	Dispersion
0.079	$1.34 \cdot 10^{6}$	
0.112	$1.2 \cdot 10^{6}$	0.428
0.220	$7.0 \cdot 10^{5}$	0.157
0.299	$3.13 \cdot 10^{5}$	0.148
0.398	$6.0 \cdot 10^{6}$	
0.529	$9.9 \cdot 10^{6}$	0.344
0.810	$2.18 \cdot 10^{5}$	0.165
0.828	$7.0 \cdot 10^{5}$	0.301
2.6	$1.76 \cdot 10^{4}$	0.100

VII. 7. Conclusions.

A considerable number of aerosols have been examined with the apparatus described in this chapter. It was found that particle sizes in the range 0.08 to 2.6 microns could be measured at concentrations below 10^7 particles $cm.^{-3}$. The errors of the measurements have been assessed.

It was not possible to study aerosols of higher concentrations due to adjacent particles obscuring one another under the microscope. In the next chapter a method which can be used at higher concentrations is discussed although the method is applicable to certain particle sizes only.

The Brownian motion introduces an error into the measurement of particle size in the photomicrograph. An uncertainty of the order of $(2Dt)^{\frac{1}{2}}$ is attached to the determination of the position of a particle. The position could be determined more accurately during a short observation but this would introduce a larger error into the determination of the time of observation and vice versa.

Values of the parameter in equation (1) have been obtained by two distinct methods and are plotted in Figure 7.26. In one, concentration was determined as a function of time and position in the cell, and values of the parameter were calculated on the assumption that the theory given in chapter V. was valid. For

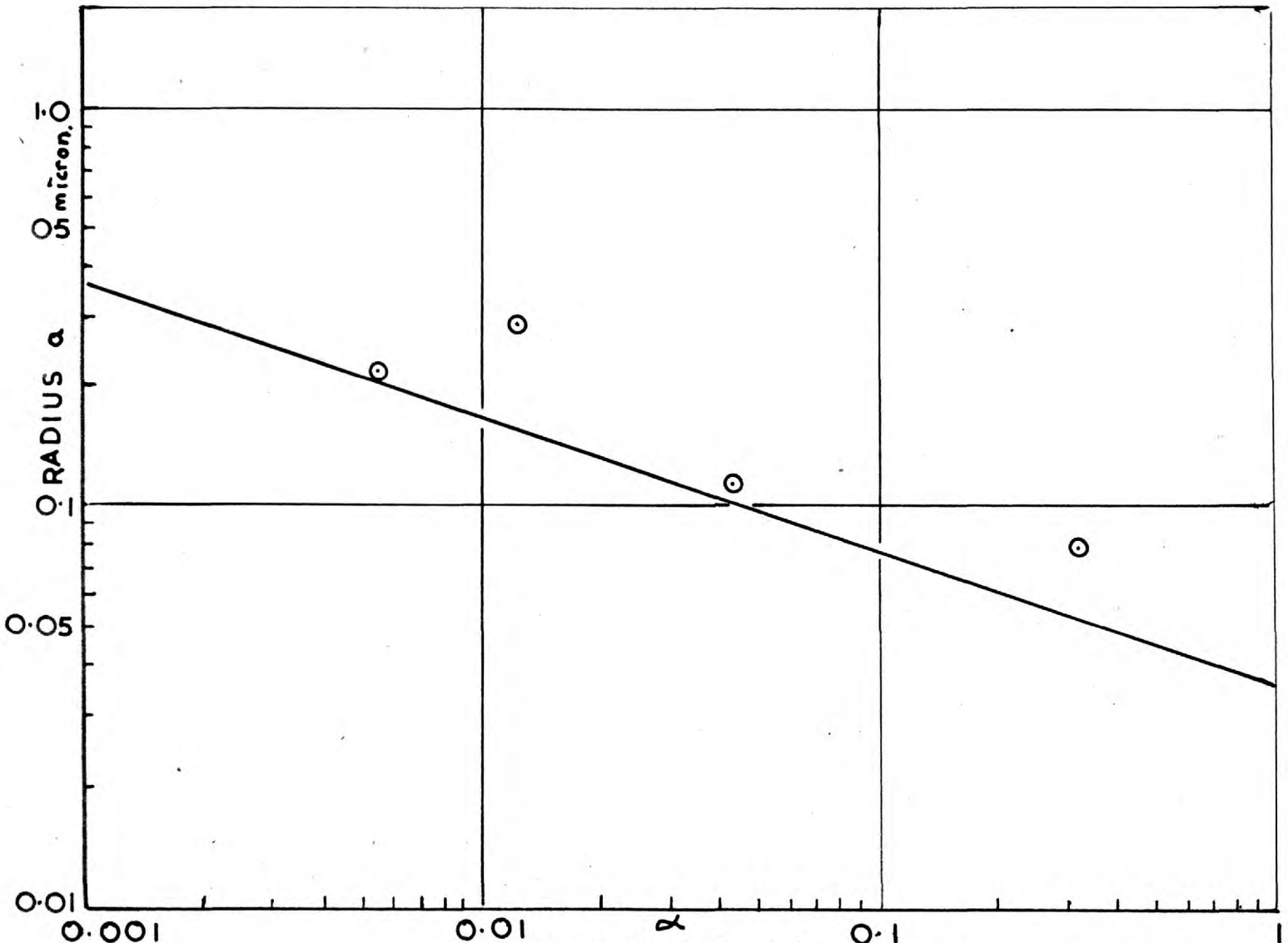


FIGURE 7·25.

the same aerosol, measured radii were used to calculate values of α. They are represented by the line in the graph and it is seen that good agreement was obtained. The discrepancy is always in the same direction and can be attributed partly to the error in the measurement of particle size, due to the effect of the Brownian motion.

This would suggest that it is more accurate to determine the concentration changes in an aerosol and hence calculate the particle size than to determine particle size from measurement of sedimentation velocities. The error $(2Dt)^{\frac{1}{2}}$ can be made negligibly small by short observations since no information is required concerning the velocity of the particle.

Due to the difficulty in measuring higher concentrations, the value of the coagulation parameter γ in equation (2) was always less than $0.01\ \alpha$ and the measurements of the concentration were not sufficiently accurate to allow γ to be determined.

CHAPTER VIII.

THE PHOTOMETRIC TECHNIQUE.

VIII.1. Introduction.

When a small particle of isotropic dielectric material is illuminated by a parallel beam of light, whose wavelength is comparable with the radius of the particle, light is scattered in a regular and known manner. The theory of scattering derived by Lie was discussed in section II.4. where reference was made also to tables of relevant functions.

Particle size and concentration in an aerosol may be determined by means of this theory since the scattered intensities are additive under certain conditions and the characteristics of the material of the aerosol are measurable. Several methods of analysis of aerosols by measurementof scattered light have been described by Sinclair (1950).

VIII. 2. Outline of the method used.

The determination of particle size and concentration require measurements of the intensity and angular distribution of the scattered light. The aerosol is enclosed in the observation cell described in the previous chapter, and the intensity of the scattered light is measured with a photoelectric photometer.

Particle size is determined from measurements of the

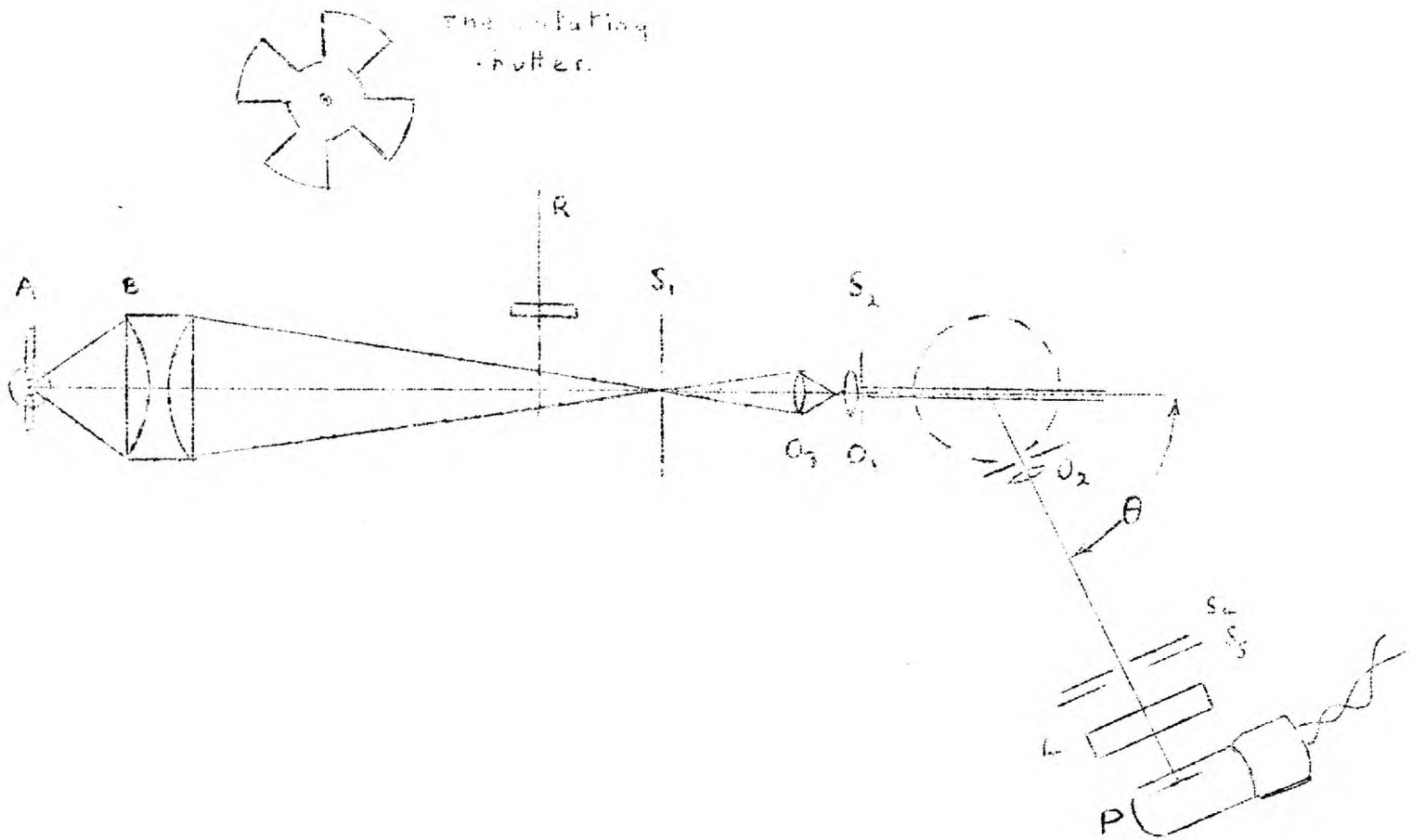


Diagram of the Photometric Apparatus. Figure 8.1

variation with the angle of scattering of the intensity of monochromatic might. The initial numerical concentration is determined from the light transmitted by the aerosol and changes in concentration are determined from the variation with time of the intensity of the light scattered at a given angle. The apparatus is arranged so that light can be accepted from any one of the ten elements into which the depth of the cell is divided.

VIII.3. Apparatus.

VIII.3.1. General arrangement.

The apparatus shown in figure 8.1 utilized the observation cell described in the previous chapter. An intense, parallel beam of light illuminated the aerosol and a photometer was used to measure the intensity of the scattered light.

VIII.3.2 The illumination.

Light from the arc A figure 8.1 was focussed onto an adjustable slit S_1 by means of a condenser C. An image of the slit was formed in the focal plane of a 16 mm. objective O_1 by means of a lens O_3. This second lens was necessary since the construction of the objective made it impossible to place the slit at its focus. This arrangement produced divergent pencils of parallel light since the arc was not a point source of light, so that the divergence was limited by a 1 mm. slit S_2. Heat absorbing filters M and C and the shutter D in figure 7.4

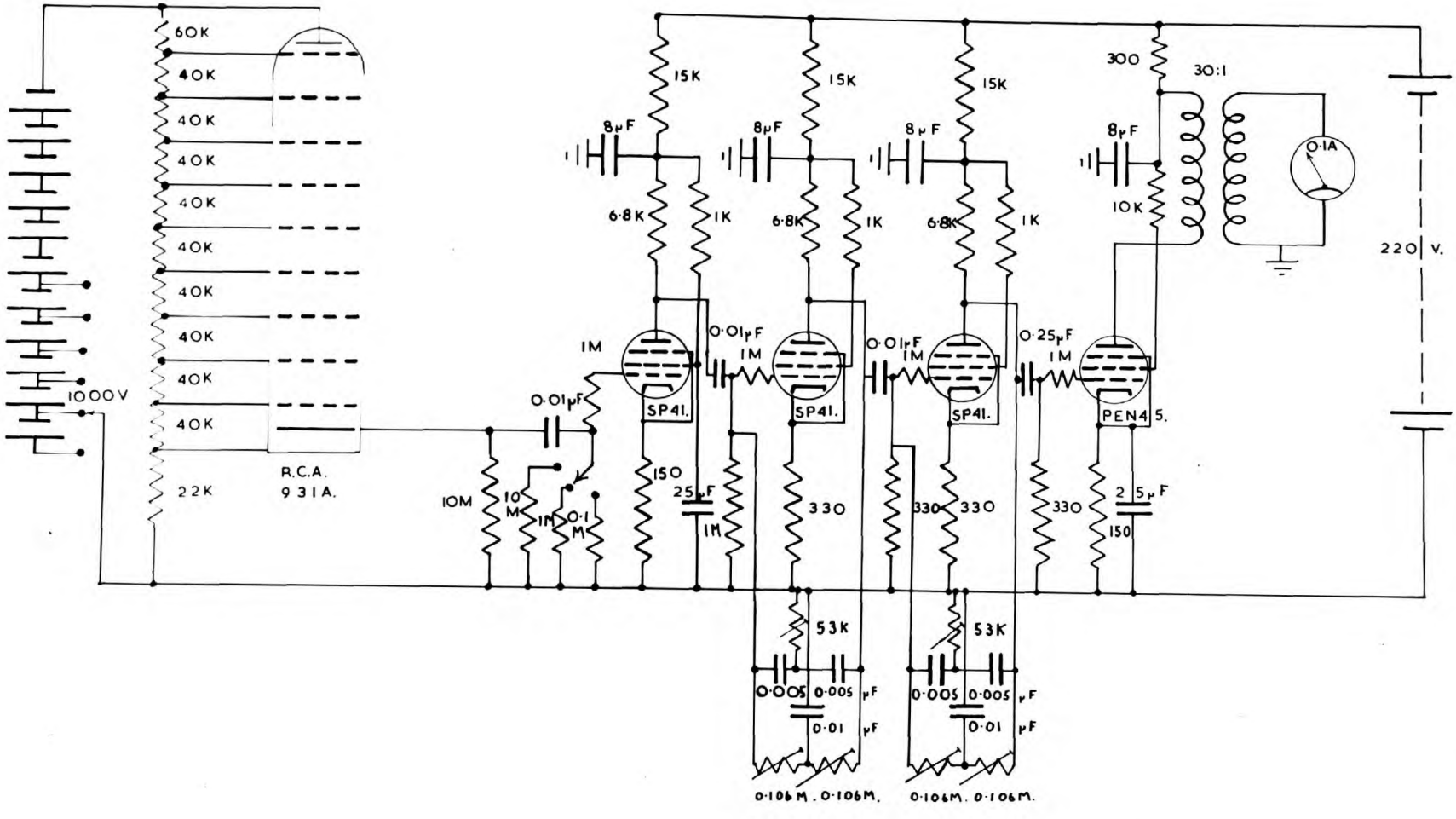


DIAGRAM OF PHOTOMETER.

FIGURE 8·2.

were also included to limit the heat entering the cell.

The light beam was interrupted 600 times /sec. by a rotating shutter R, since the photometer utilized an A.C. amplifier.

VIII.3.3 The photometer.

The photometer used to measure the intensity of the scattered light comprised a photomultiplier, an A.C. amplifier and an ammeter (figure 8.2). It was arranged so that light could be accepted from different positions in the cell and at various angles to the incident beam.

VIII.3.3.1 The optical system of the photometer.

The optical system transmitted light scattered by the aerosol to the cathode of the photomultiplier (figure 8.1 and 8.3), suitable precautions being taken to reduce stray light in the system.

A real image of the aerosol in the cell was formed in the plane of the horizontal slit S_5 by means of a 25 mm. objective O_2 and the light transmitted by the slit was focussed on the cathode C of the photomultiplier by a cylindrical lens L_4. Light from each of the 10 regions of the cell, could be received by the photomultiplier since the horizontal slit S_5 which could be moved in a vertical direction by means of the micrometer screw M.S (0.1317 cms.

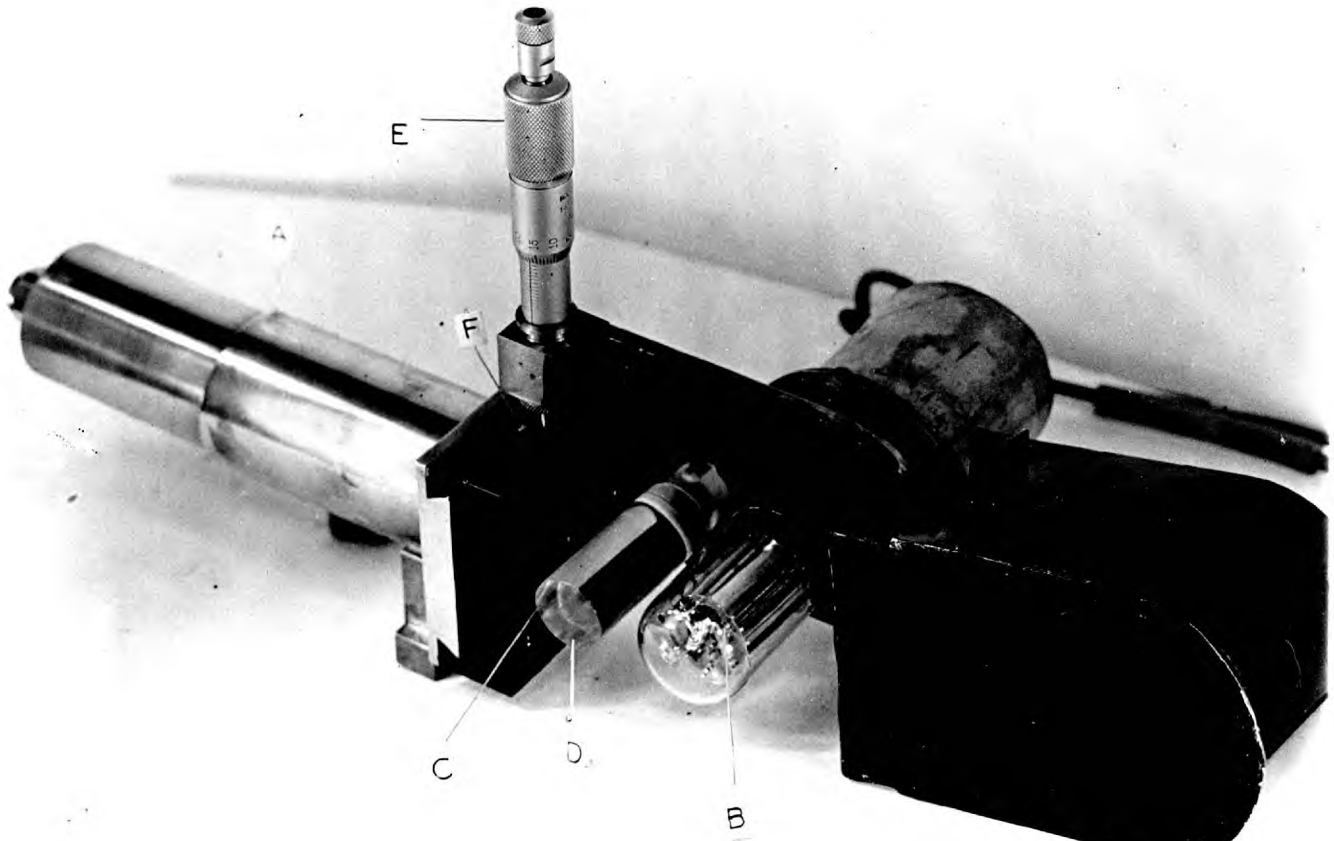


Fig. 8.3 The Photometer

gap) limited the depth from which light was accepted to less than a tenth of the vertical dimension (0.22 cms.) of the cell. By adjustment of the micrometer, the slit S_5 the lens L_4 and the photomultiplier were moved simultaneously so that light (figure 8.3) always fell on the same region of the cathode. This was important as the sensitivity of the cathode was not constant over its whole surface.

The vertical slits S_3 and S_4 limited the angle from which light was accpeted in a horizontal plane. The angle of acceptance 2u, was calculated from the relation

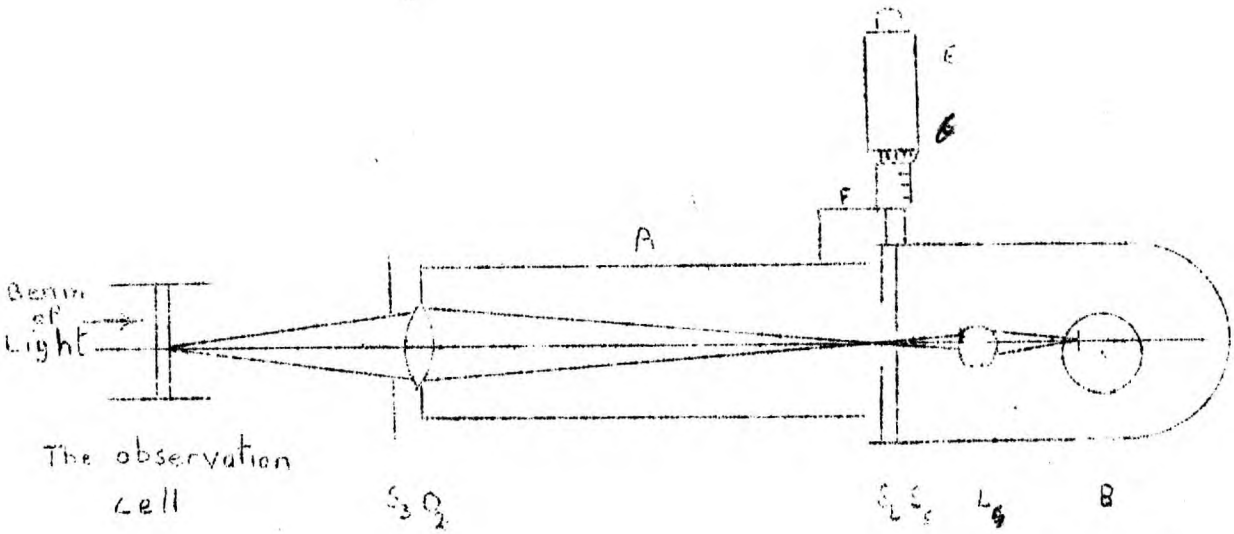
$$2u = \tan^{-1} \frac{x}{y} \qquad (1)$$

is indicated in figure 8.4

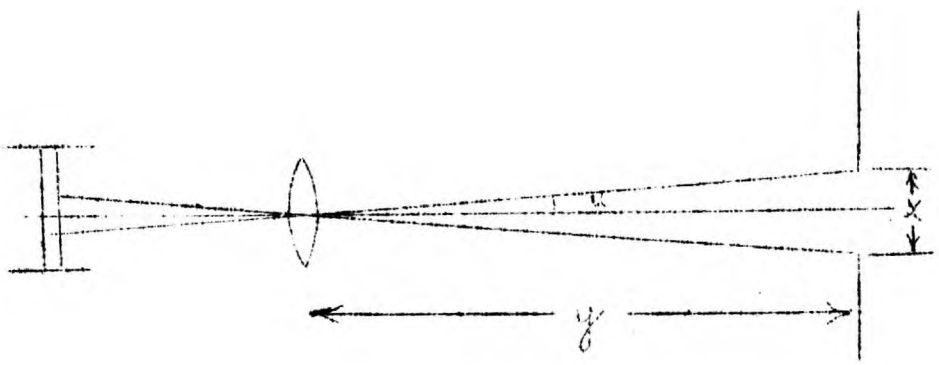
The angle of acceptance of the vertical slit S_3 was 19 minutes of arc; and of the horizontal slit S_5 , 26 minutes of arc. So that light could be accepted at various angles to the incident direction, the photometer was mounted on a rigid steel arm 1 cm. thick and 7 cms. wide which could be rotated between 0 and 90° to the direction of incident beam.

VIII. 3.3.2. The photomultiplier.

The photomultiplier used was an R.C.A. 931 A. whose characteristics are described by Engström (1947). A potential difference of 50 to 100 volts was applied between adjacent secondary electrodes and



OPTICAL SYSTEM OF THE PHOTOMETER FIGURE 8·4



ANGLE OF ACCEPTANCE OF PHOTOMETER FIGURE 8·5

was obtained from a potentiometer network connected in series with 10 high tension batteries. With such an arrangement a maximum sensitivity of 1200 amps. watt^{-1} was obtained at the wavelength of 5500 angstrom when the potential difference between adjacent electrodes was 100 volts. The random emission of electrons in the photomultiplier was reduced by using only 90 volts and the sensitivity was consequently reduced to 2000 amps. watt^{-1}. The sensitivity of the photomultiplier was not appreciably reduced by using an intermittent beam of light provided the frequency was less than a megacycle per second.

The current from the anode of the photomultiplier passed through a megohm resistor and the voltage thereby produced was applied to an amplifier (figure 8.2).

VIII. 3.3.3 The amplifier.

An A.C. amplifier was designed to have a high amplification factor and a narrow bandwidth. It was used because it was more stable than a D.C. one and a high gain was necessary to enable aerosols of low concentration to be investigated using the photometer. To increase the signal noise ratio of the photometer, the frequency response was limited to a narrow band on either side of 600 c.p.s., the frequency at which the light was interrupted.

In the circuit diagram (figure 8.2) the four stages of the amplifier are indicated. The valves used were pentodes; S.P. 41.s

for voltage amplification and a Pen 45 in the output stage. The grid circuit of the first valve which received signals from the photomultiplier included a gain control consisting of 6 resistors of 20 M to 1 K. (Only three are shown in figure 8.2). The second and third stages incorporated parallel-tee filters tuned to 600 c.p.s. (Sturtevant. J.M. 1947). The output stage utilized a Pen 45 valve and in the anode circuit was a transformer having a voltage ratio of 30:1. The output of the amplifier was indicated by an ammeter in the secondary circuit of the transformer.

Unwanted oscillations were minimised by using decoupling condensers in all ~~made~~ anode circuits, and a cathode condenser in the last stage only, and precision components were used in the filters. All connections to batteries, and the photomultiplier and grid leads were screened and the anode circuits and cathode circuits were shielded from one another. High tension batteries were used to obtain 220 volts for the amplifier and the valves were indirectly heated by current from accumulators. A constant voltage was maintained by this arrangement for a period of one or two hours.

VIII.3.3.4. Alignment of the apparatus.

First, a beam of light was made to pass diametrically through the observation cell, using the method described in chapter VII.,

Then parallel light was obtained by adjusting the position of slit S_1 until a sharp image was seen by a telescope focussed to receive light from an infinite distance and when placed to receive the illuminating beam. A ~~vertical~~ neutral filter was necessary to protect the observer's eyes.

The light was then focussed onto the photomultiplier when the photometer was in line with the incident beam. The objective O_2 was adjusted until a sharp image of the upper and lower surfaces of the cell was formed in the plane of slit S_5. To achieve this, the photomultiplier and the cylindrical lens were removed, a piece of ground glass placed in the plane of the slit so as to receive the image which was observed with a lens. (Although it was convenient to determine the magnification at this stage, the procedure is described below). A white card was fitted in place of the cathode of the photomultiplier and the lens L_4 was replaced and adjusted until a sharp image of slit S_5 was formed in the centre of the card. Finally the photomultiplier was replaced.

To determine the magnification of the optical system, slit S_5 was adjusted by means of the micrometer until its upper edge coincided in turn with the mid-point of the upper and lower surfaces of the cell. The size of the image was obtained from the difference in the two readings of the micrometer and, since the

depth L of the cell was known, the magnification M could be calculated.

So that the concentration could be measured at 10 different heights in the cell, the width of slit S_4 was adjusted to 0.08 of the vertical dimension of the image of the cell.

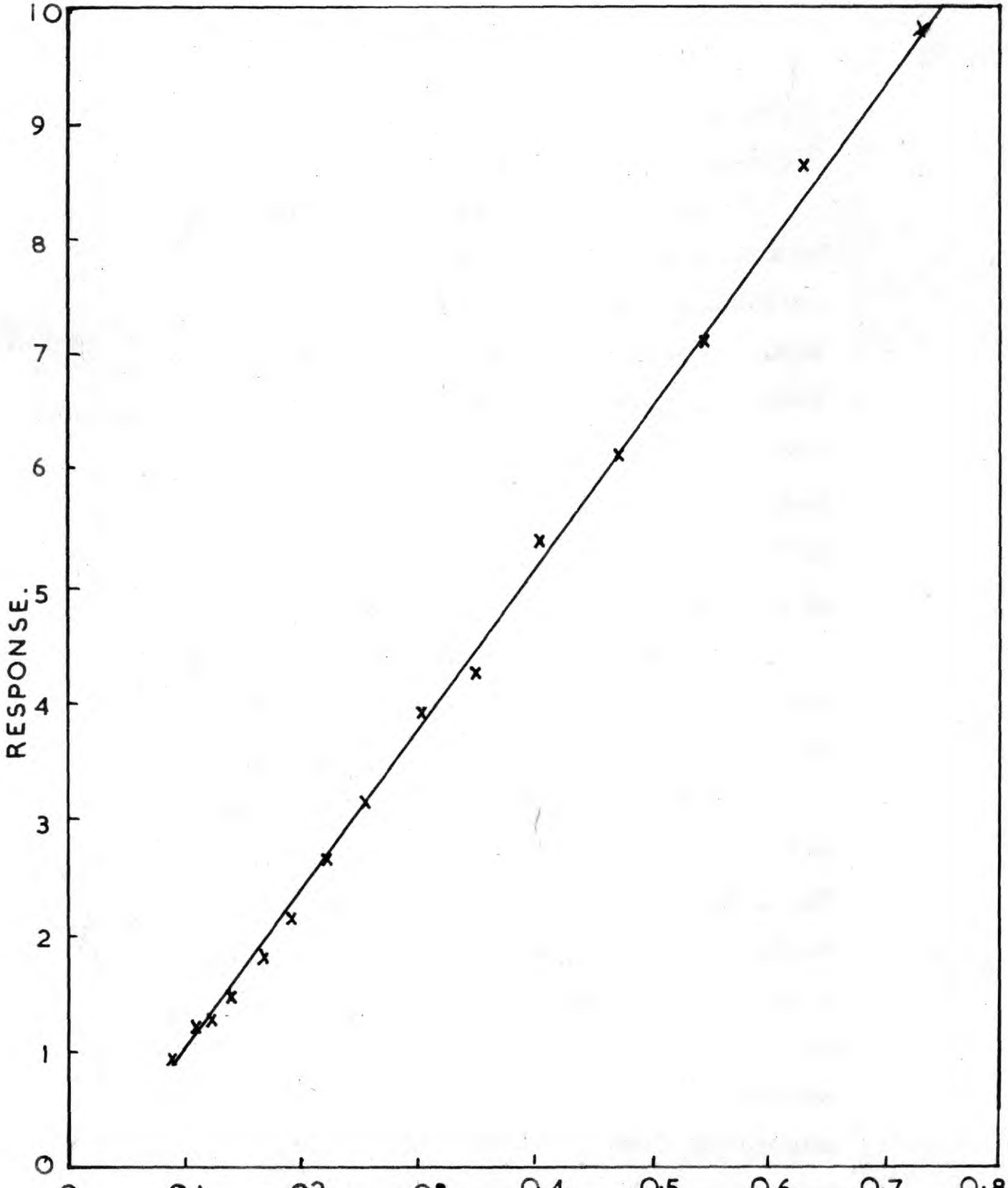
This separation was made slightly less than one tenth of the depth of the magnified image to avoid measuring light reflected from the surfaces of the cell when the concentration was determined in the top and the bottom regions.

VIII.4. Behaviour of the apparatus.

The apparatus was required to have a linear response, an adequate range of sensitivity and to be stable; and the light received by the photometer should not include light reflected from the walls of the cell.

VIII.4.1. Linearity of the photometer.

To determine the response of the photometer to various intensities, a neutral wedge of density range 0 to 2 was placed in the incident beam. Only 0.5 cms. out of a total of 15 cms. of the wedge were operative at any one time. Light was allowed to fall on the photometer directly and the reading of the ammeter was taken for various settings of the neutral wedge. In figure 8.6, the meter readings are plotted against the transmission which was directly proportional to the intensity



LINEARITY OF PHOTOMETER. FIG. 8·6.

of the light falling on the photometer.

VIII.4.2. The sensitivity of the photometer.

The luminous energy scattered at 90° to the incident light by a single particle varied from 10^{-12} to 10^{-10} watts. steradian^{-1} per watt. cm^{-2} of incident light as the radius increased from 0.1 to 0.6 microns. An the assumption that the incident beam had an intensity of the order of 10^{-1} watts. cm^{-2}., the energy scattered was 10^{-13} to 10^{-11} watts. steradian^{-1}. Consequently, the luminous energy received by the photometer was of the order of 10^{-13} to 10^{-11} watts. (The solid angle subtended by the lens of the photometer was of the order of 1 steradian).

The sensitivity of the photometer was 10^{3} amps. watts^{-1} and when the currents produced were applied to a 1 megohm resistance, the voltages sensitivity was 10^{9} volts. watt^{-1}.

The voltage across the resistance produced by single particles in the cell would therefore be between 10^{-4} and 10^{-2} volts. Since a full scale deflection of the meter (100 divisions) was obtained when a signal of 0.1 volts at 600 c.p.s. was applied to the amplifier, at maximum gain, a single particle would produce a deflection of between 10^{-1} and 10 divisions. The sensitivity could be reduced by adjusting the gain control, by reducing the potential applied to the secondary electrodes of the photomultiplier or by reducing the width of the slit S_1.

The signal to raise the ratio is proportional to the square root of the bandwidth (Δf) of the amplifier and is a function of $i_t^{\frac{1}{2}}$, where i_t is the thermonic emission from the cathode. The amplifier was designed to make $\Delta f^{\frac{1}{2}}$ about 40. $(c.p.s.)^{\frac{1}{2}}$

The dark current produced by the photomultiplier due to thermionic emission and leakage across its base produced a deflection of 2 divisions which could be regarded as equivalent to a zero error. Daylight of low intensity was not recorded since the amplifier did not respond to a direct current but appeared to increase the random emission of electrons in the photomultiplier.

It can now be seen that the range of sensitivity has a lower limit of between 10^{-1} and 10 particles per division for radius of 1 and 0.1 microns. The apparatus can be sued for high concentrations by reducing the gain of the amplifier so that the upper limit depends not on the apparatus but on the scattering process. When the concentration in the aerosol is high, secondary scattering occurs and results can no longer be simply interpreted.

VIII.4.3 Stability of the apparatus.

The duration of an experiment was of the order of 30 to 40 minutes and the apparatus was required to give consistent readings during that time.

There was no appreciable change in the sensitivity of the amplifier over a period of one hour, provided that the batteries

were in good condition and steady conditions had been attained after switching on. However, there were frequent fluctuations and shower variations in the voltage of the mains which affected the intensity of the arc. Also, the hot-spot on the electrodes of the mercury arc moved about rapidly and caused variations in the intensity of the light falling on slit S_1. Random movements of about 5% of the needle of the ammeter occurred necessitating replication of all readings.

VIII.4.4 Stray light in the apparatus.

Even though the interior of the apparatus was painted dead black, an appreciable amount of light was reflected when it was wetted by the aerosol liquid. At the beginning of each experiment, this light was measured with the cell filled with filtered nitrogen and this reading was deducted from subsequent readings taken with an aerosol in the cell. However, it was not possible to correct for light which was scattered by the aerosol and then reflected by the cell walls.

VIII. 5. The experimental procedure.

VIII. 5.1 Setting the apparatus.

Before measurements were made with the photometer, the optical system was aligned using the methods described in section VIII.3.3.4. The sensitivity of the photometer was adjusted by means of the voltage applied to the photomultiplier and by

varying the gain of the amplifier. A fince adjustment of the response of the apparatus could be achieved by varying the width of the slit S_1.

VIII. 5.2. Determination of particle size.

When a small particle of isotropic dielectric material is illuminated by a beam of parallel light, the intensity I, of the light scattered at an angle θ to the incident light is given by the relation discussed in chapter II;-

$$I_\gamma = \frac{\lambda^2}{4\pi^2}(i_1 + i_2) \quad \text{watts/unit solid angle/watt.cm}^2 \text{ incident light.} \quad (2)$$

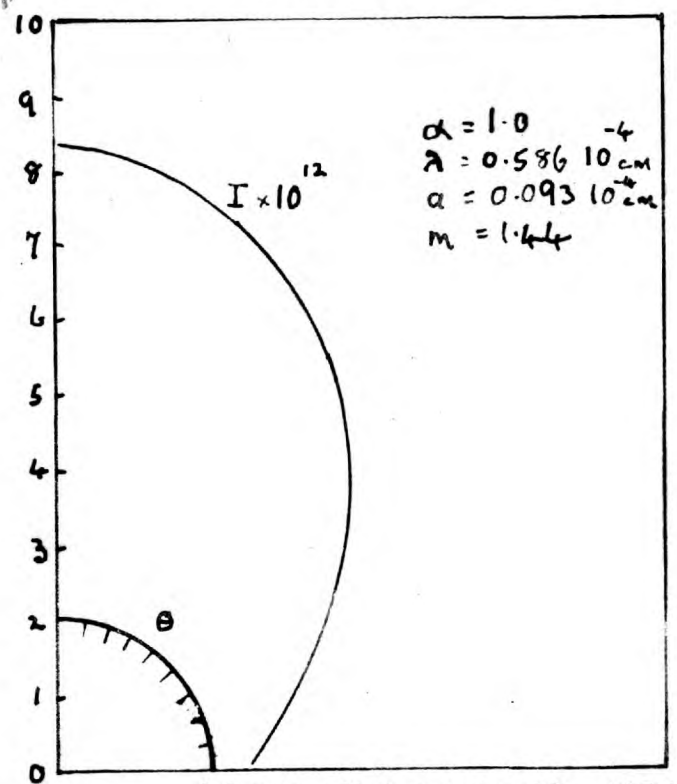
where $\gamma = \pi - \theta$

The functions i_1 and i_2 are complex but have been tabulated at 10° intervals in the range $0.5 < \frac{\lambda}{a} < 6$. by Lowan (1949) whose tables were used in the measurements described below. The incident light was assumed to be unpolarized. Examples of the angular inten sity distribution are given in figure 8.7.

With the aerosol flowing through the cell the intensity distribution was determined at intervals of 10°. It was necessary to correct these readings for the relection of light from the walls, and a preliminary determination was made of the I when filtered nitrogen was flowing.

Since absolute values of the intensity of the scattered

ANGULAR INTENSITY DISTRIBUTIONS.



FROM TABULATED VALUES

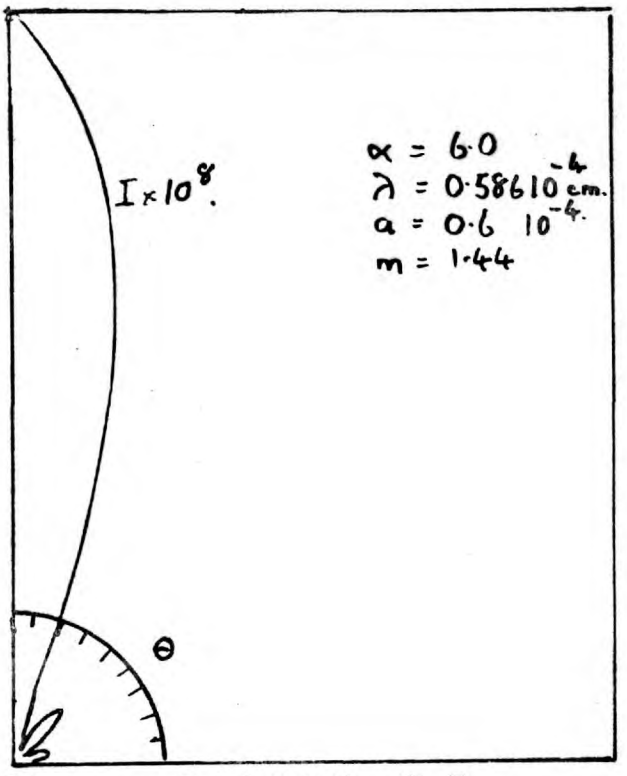
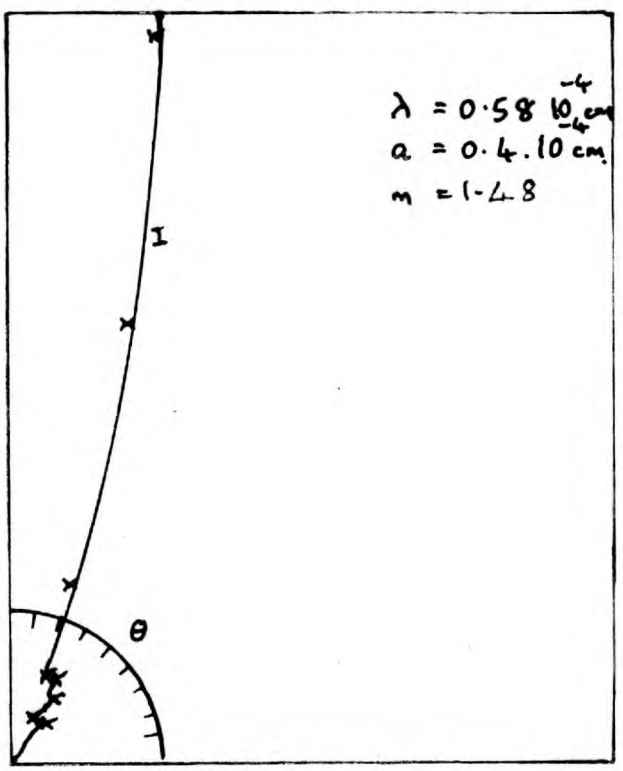


FIGURE 8·7



EXPERIMENTAL VALUES.

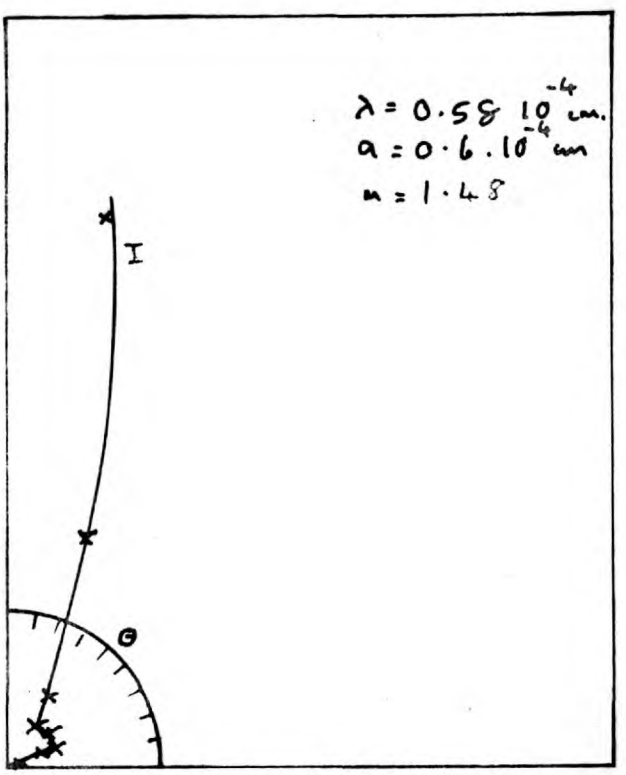


FIGURE 8·8

light were not required, the meter readings were plotted directly. Consequently, the apparatus could be used only in the range where the response was linear. Figure 8.8 shows some typical values obtained.

When the position of the maxima of the intensity distribution had been determined, then particle size could be obtained from a graph (figure 8.9) of the position and number of maxima plotted against radius; this graph was obtained from the tables of the functions i_1 and i_2.

VIII. 5.3 Determination of the initial concentration.

If a parallel beam of light of intensity I_0 is incident on an ensemble of n particles, the intensity of the transmitted light I is given by the relation

$$\frac{I}{I_0} = \exp\left[-n\ K(a)\pi\ a^2\ L\right] \qquad (3)$$

where $K(a)$ is the scattering area coefficient and has been tabulated - Lowan (1949)

L is the length of path through the aerosol.

Consequently the initial numerical concentration can be determined by placing the photometer in such a position that the incident light passed through the cell and fell directly into the photomultiplier (i.e. at $\theta = 0$). A reading of I' was then obtained and this was proportional to the intensity of the

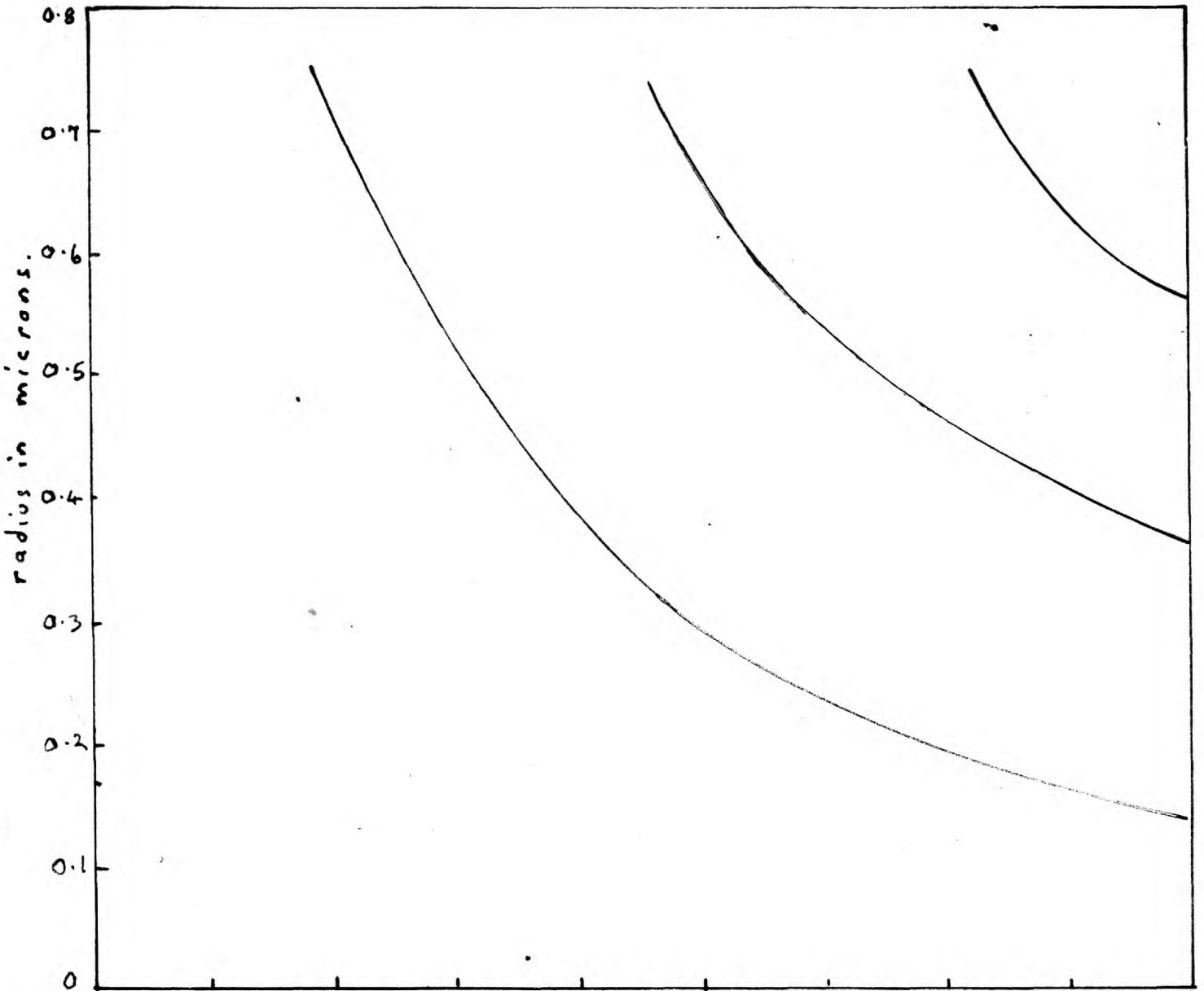


FIGURE 8·9 ANGULAR DISRIBUTION.

incident light I_o. A corresponding value of I" was obtained with an aerosol flowing through the cell.

Now $$\frac{I}{I_o} = \frac{I''}{I'} \qquad (4)$$

and since the radius a was known, K(a) could be obtained from tables and

$$n = \frac{-\ln\left(\frac{I''}{I'}\right)}{\pi a^2 K(a) L} \qquad (5)$$

VIII. 5.4 Determination of the relative concentration.

The concentration changes in the aerosol were determined by a procedure similar to the photographic method described earlier. The photometer was set to receive light at an angle corresponding to one of the maxima of the angular intensity distribution (figure 8.8) and the variations with time in the meter reading I'(t) were recorded.

The background illumination I" was determined after the cell had been swept out with filtered nitrogen and the slide closed.

The changes in concentration were followed by the following procedure. The cell was filled in the manner described in section VII.4.3. and after the photometer slit S_5 had been

set to receive light from one of the regions of the cell, the slides were closed and the photometer reading was recorded at five second intervals until the deflection had been less than one percent of the initial reading. If the initial value were I'(0) then the relative concentration c is given by

$$c = \frac{I'(t) - I''}{I'(0) - I''} \qquad (6)$$

I'(0), I'(t) and I" were determined for each of the 10 horizontal regions of the observation cell. Typical results for the variation of I'(t) - I" and c with time and position in the cell are shown in figure 8.10 and 8.11.

VIII.6. Discussion of results.

Results obtained with the photometric apparatus were compared with those obtained under identical conditions by the photographic method.

VIII.6.1 Particle size.

Particle sizes in several aerosols were determined by the photometer which was then replaced by the camera and track lengths were measured in the photomicrographs obtained. Some values obtained appear in table 8.1

The measurements were not sufficiently accurate and several improvements in accuracy could be made but they would require

Table 8.1

	Photometric measurement Radius in microns	Photographic measurement Radius in microns
1.	0.7	0.64
2.	0.6	0.51
3.	0.55	0.56
4.	0.45	0.42

The concentration was 10^5 to 10^6 particles. cm^{-3}.

modification of the apparatus.

Since the intensity of the light scattered by particles of radii greater than 0.5 microns radius varies from maximum to maximum by a factor of 10^3, a photometer having a logarithmic response would be more suitable and a method of obtaining this is discussed in section VIII.7.

The values of the theoretical functions are tabulated at intervals of 10 degrees, and this was found to be insufficient.

An increased accuracy could be obtained if further values were interpolated using the method described by Van der Hulst (1949). The curves shown in figure 8.9 could be plotted as the position of the maximum values of the ratio $\frac{I_g}{I_y}$

where I_g is the intensity of the light scattered when the aerosol was illuminated by the mercury green line - of wavelength 5461 angstroms and I_y that scattered from an incident illumination by the yellow line 5784 angstroms.

VIII. 6.2 Measurement of the initial concentration.

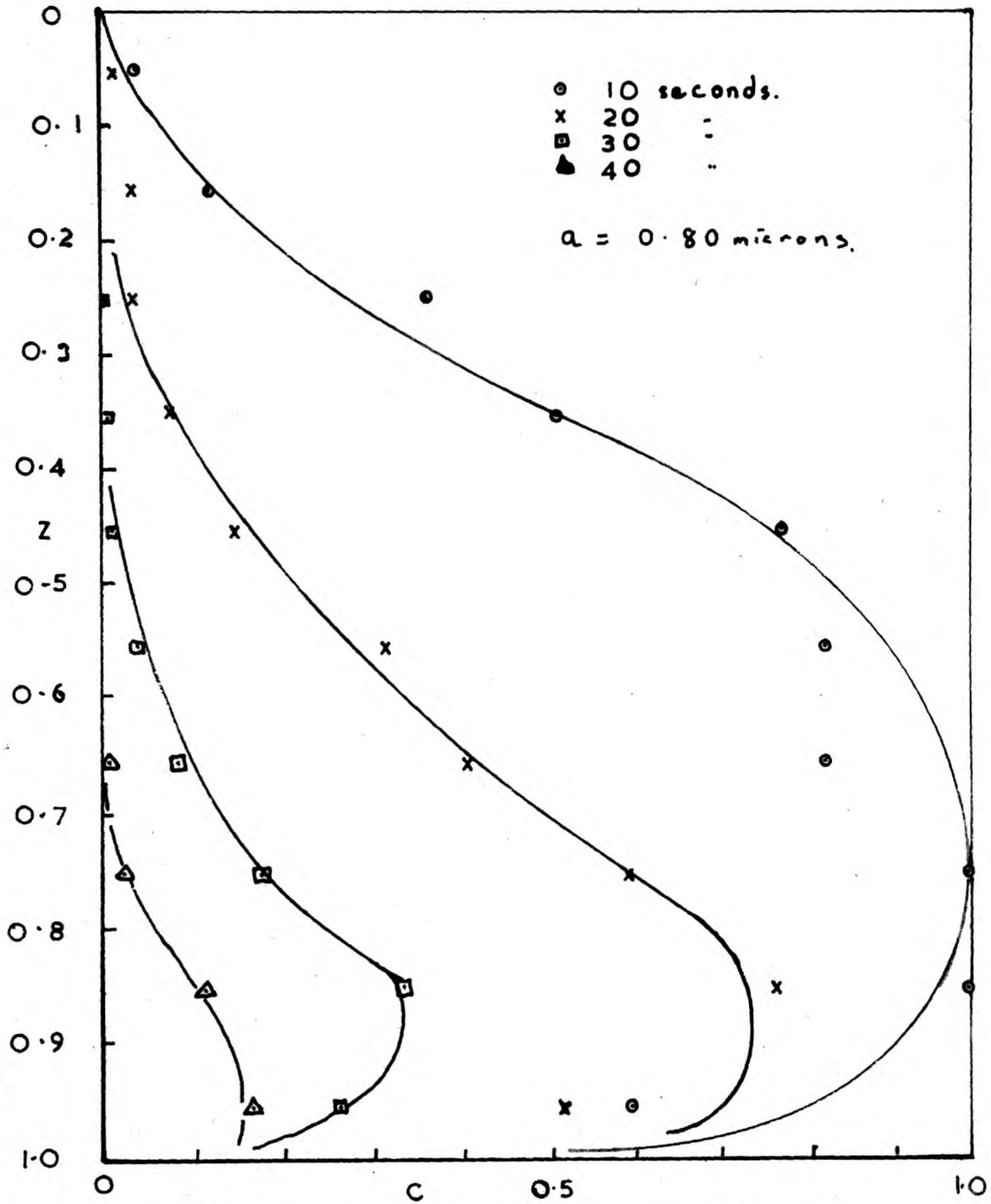
The photometric method has been developed for the investigation of aerosols of high concentration. The initial concentration was obtained in terms of the transmission $\frac{I}{I_o}$ of the aerosol from relation (5) and it can be seen that the method could be unsatisfactory at low concentrations since $\frac{I}{I_o}$ would then be the ratio of two nearly equal quantities.

Concentrations of 10^6 to 10^7 particles $cm.^{-3}$ were determined by this method and these results are comparable with the results obtained by means of the photographic method.

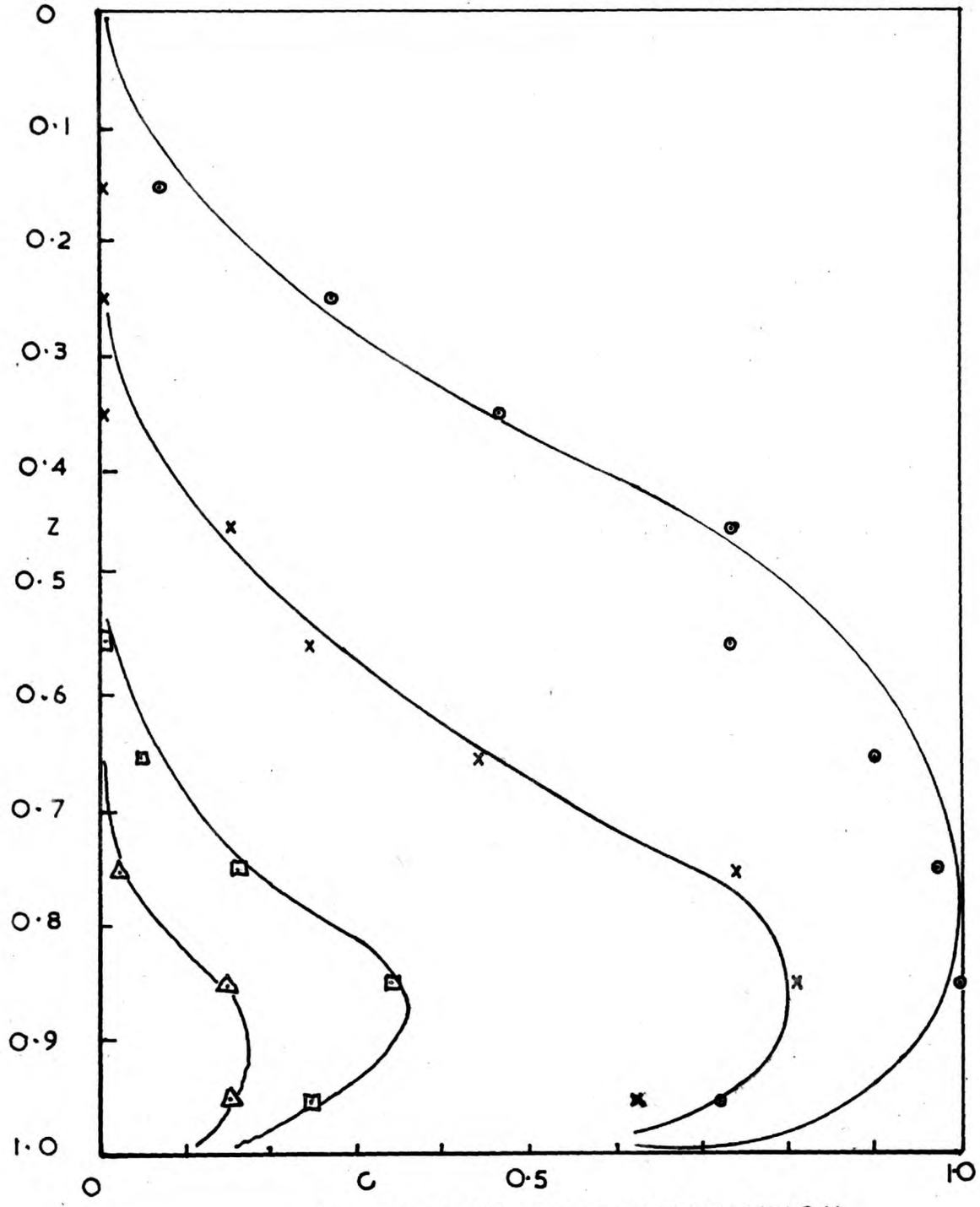
VIII.6.3 Determination of the relative concentration.

The relative concentration in a given aerosol was determined as a function of time and position in the cell by means of both the photometric and the photographic technique. The results are presented in figure 8.10 and it can be seen that they are in good agreement with one another.

The accuracy of the measurement is indicated in figure 8.11, where the concentration determinations are plotted as a function of



OBSERVED CONCENTRATION IN AEROSOL.
PHOTOMETRIC DETERMINATION.



PHOTOGRAPHIC DETERMINATION.
FIG. 8·10.

time and the standard errors of eight determinations are indicated. The range of error was between 2% at the initial value to 10% at the final reading.

Since the method was sufficiently rapid to permit concentration measurements at 5 second intervals, the mean of four readings was calculated and the distribution was plotted with a time interval of 20 seconds. This mean value was much more accurate since the standard deviation was reduced by $\frac{1}{2}$.

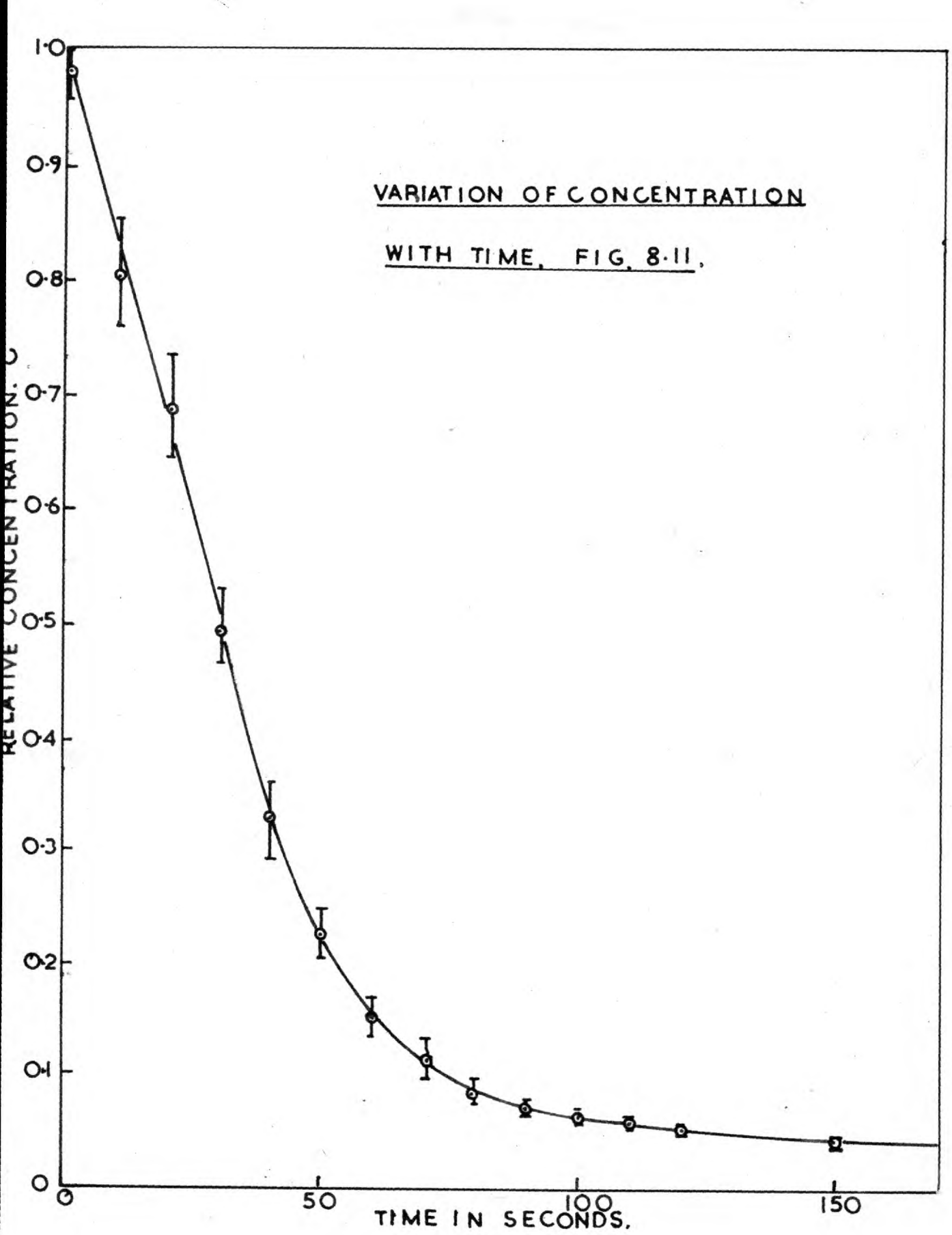
VIII.7. Conclusions.

The photometric technique described in this chapter was applied to the investigation of concentration changes in several aerosols with concentrations in the range 10^6 to 10^8 particles cm^{-3}, which were higher than those which could be measured in the photographic experiments.

Since the method was more rapid, a larger number of observations of the aerosol could be made and the results were consequently more reliable.

The measurement of particle size was not affected in any way by the Brownian motion which limited the range and the accuracy of the photographic determinations.

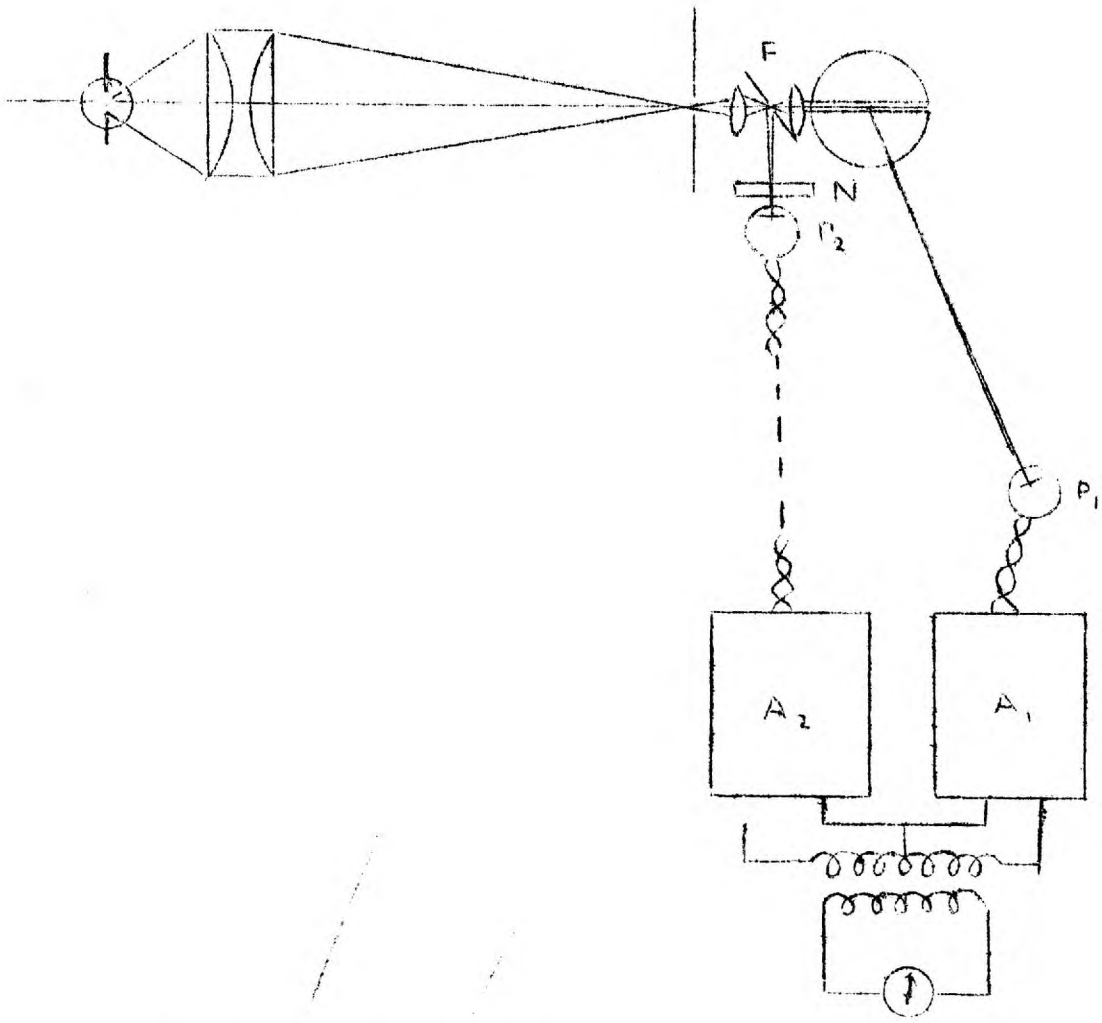
Values of the coagulation parameter γ of the order of 0.1 or 1 could be obtained by this method since it was possible to measure concentrations of 10^8 or 10^9 particles $cm.^{-3}$.


VARIATION OF CONCENTRATION
WITH TIME. FIG. 8·11.
RELATIVE CONCENTRATION. C
1·0
0·9
0·8
0·7
0·6
0·5
0·4
0·3
0·2
0·1
0
0
50
100
150
TIME IN SECONDS.

The apparatus could be improved by compensating for the fluctuations of the arc. If a small fraction of the light were made to fall on to a second photomultiplier P_2 (figure 8.12) and the current from the amplifier (A_2) supplied to a transformer in opposite phase to the circuit from the first photomultiplier, no current would flow in the transformer when the luminous energy falling on both photomultipliers was the same. The condition could be achieved by means of a neutral wedge N placed in front of the second photomultiplier.

The transmission of the neutral filter could then be used to determine the ratio $\frac{I}{I_o}$. The advantage of the arrangement is that the filter might have a linear or a logarithmic characteristic.

The sensitivity could also be improved by using a photomultiplier in which the random emission of electrons was less.



MODIFIED PHOTOMETER.

FIGURE 8·12

CHAPTER IX.

MEASUREMENT OF MASS CONCENTRATION.

IX.1.

Measurements of mass concentration of the aerosol were required for comparison with values calculated from measurements of particle size and numerical concentration and for calibrating the generator.

The method employed consisted of weighing the material filtered from a known value of aerosol. To verify that no significant quantity of liquid passed the filter, a condensation coil was connected in series with the filter (see figure 9.1)

IX.2. The filter medium.

Sintered glass filters were finally selected after several different media including asbestos wool, glass wool, slag wool, cotton wool and filter paper has been tested; and the results are shown in table 9.1. the media were dried and the increase in weight was determined after they had remained for 24 hours in an atmosphere 95% relative humidity at 15°C.

Filters formed by packing one gram of material into a tube of 2 cms. diameter were shaken vigorously and the loss in weight determined.

The same filters were used to determine the mass concen-

duration in a given polydisperse aerosol and their efficiencies compared with that of asbestos wool.

In the last test the reflux of each filter was examined for particles by means of an ultramicrscope. It was found that sintered glass filters responded most satisfactorily to these tests and that they had added advantage of being available in the most convenient form.

IX.3. The apparatus.

The apparatus is shown in the diagram (figure 9.1). By means of a pump C, a measured stream of aerosol was withdrawn near the observation cell E and passed through the filter A and a condensation coil B. A trap F was fitted to prevent liquid running down the walls of the tubes leading to the observation cell and filter. A filter G prevented aerosol entering the laboratory atmosphere.

The condensation coil was of the type described by La Mer et al (1950) and consisted (figure 9.2) of four rectangular turns of 5 mm. bore glass tubing. The upper portions were wound with a heater element and the lower part was immersed in liquid nitrogen. The heater vaporized the droplets in the aerosol and the vapour condensed on the cold walls of the tube. The process was effective since the diffusivity of the vapour molecules is much greater than that of the droplets.

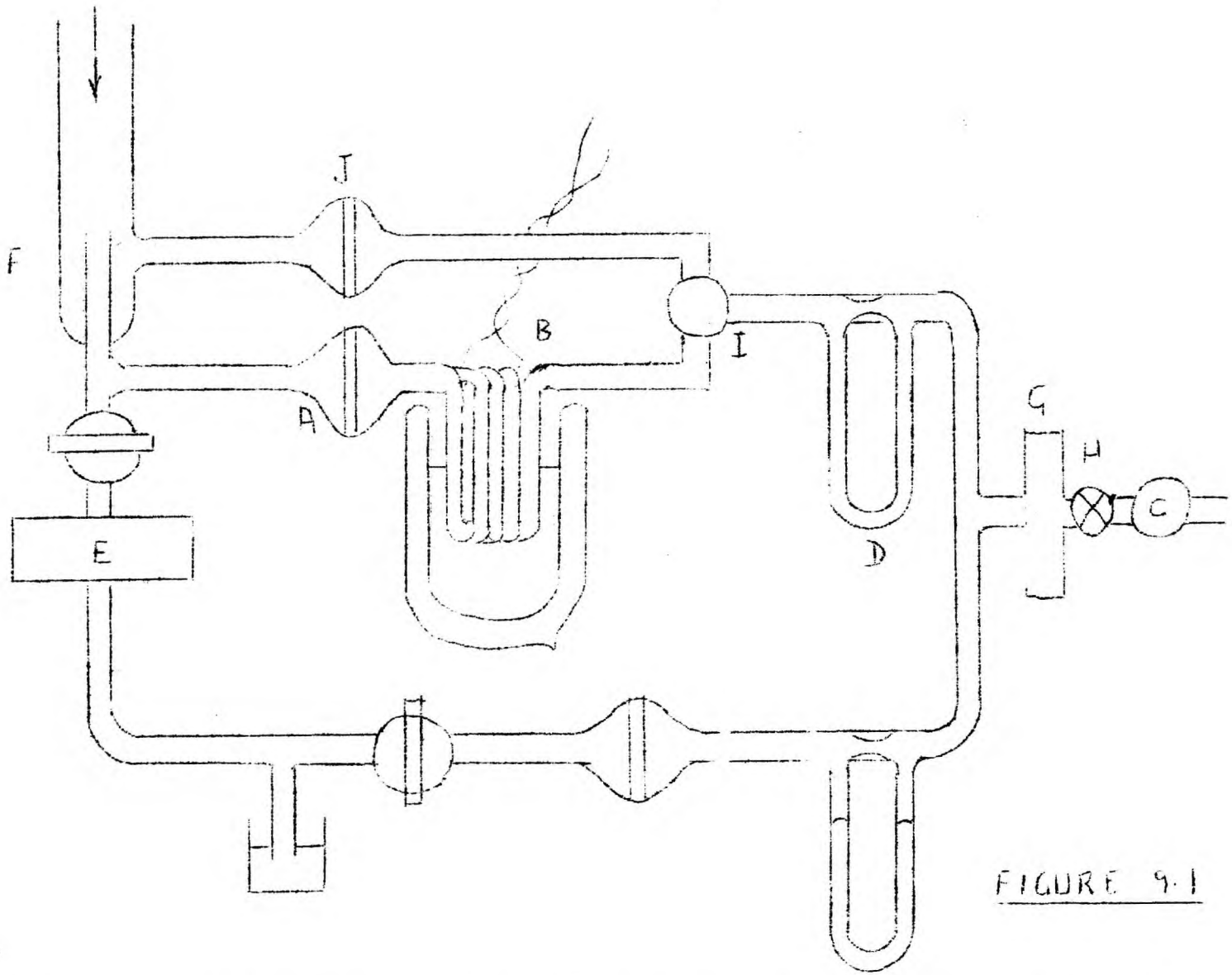
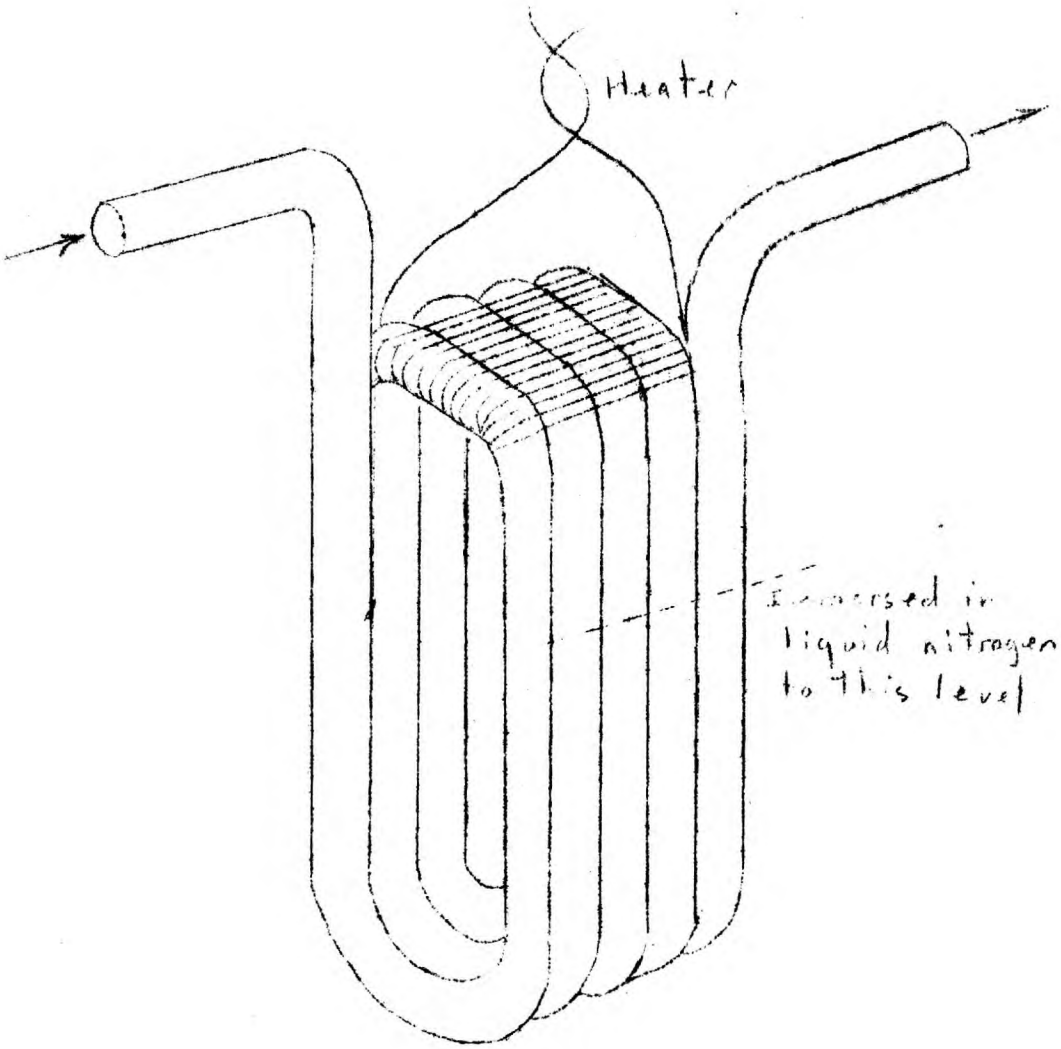


FIGURE 9·1

APPARATUS FOR DETERMINATION OF MASS CONCENTRATION

Table 9.1 Examination of filter media.

Medium	Moisture absorbed	Loss on shaking	Relative efficiency	Observation with U.M.	Advantages	Disadvantages.
Asbestos wool	3.4% by weight	fine dust	100	Nothing visible	Efficient	Changes in weight
Slag wool	0.4%	Dust Grit Short fibres	97.5			Weight not constant
Cotton wool	15.5%	None	91			Forms channels
Glass wool	2.9%	Short fibres	51			Forms channels
Filter paper		None				High pressure drop
Sintered glass	0.2%	None	100	Nothing visible	Available in 5 grades of porosity. Can sealed into any Pyrex glass apparatus	Thin disc is soon saturated with filtered material.



CONDENSATION COIL. FIGURE 9.2.

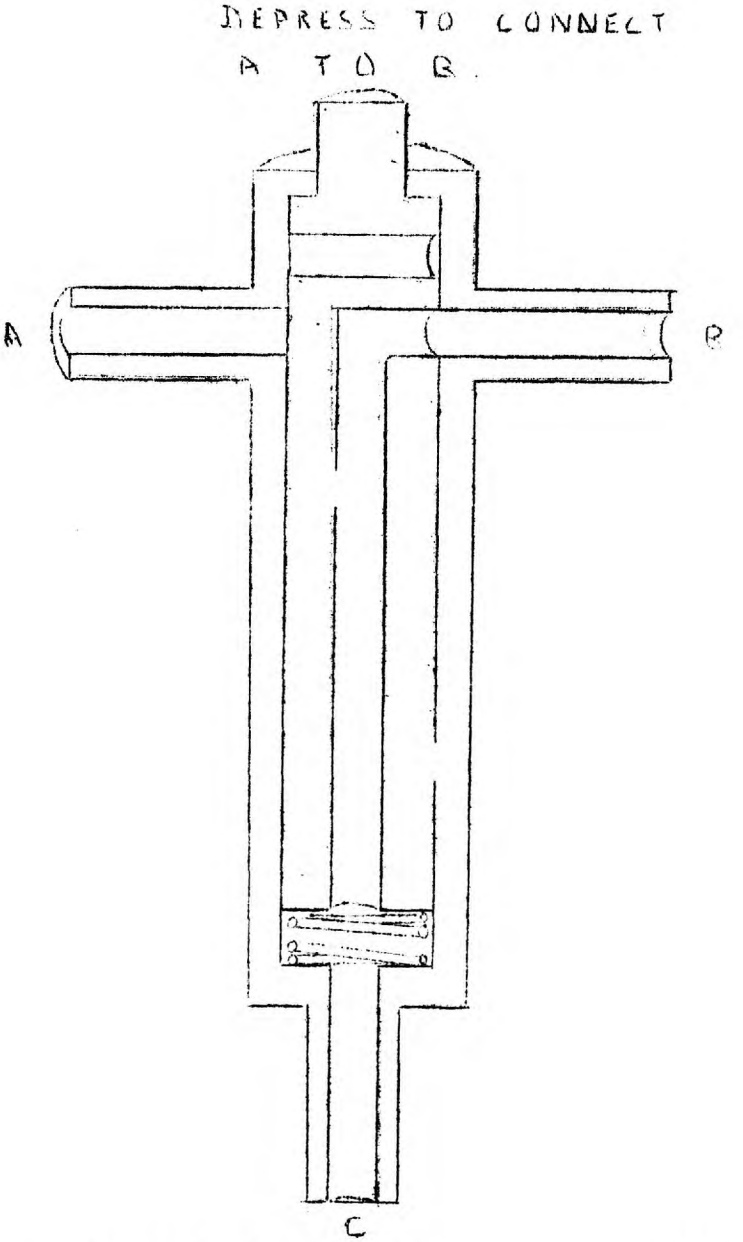
IX.4. Procedure.

Before the aerosol was filtered, the rate of flow was adjusted while the aerosol was passing through a second filter J having the same resistance to flow as filter A. The flow could then be rapidly diverted to filter A at the beginning of a determination and shut off at the end by means of a quick-release valve I (figure 9.3) which was the type described by May (1945). By this means the delay in attaining the required rate of flow was made negligible and the flow could then be maintained constant by adjustment of the needle valve H.

The ground glass joints were sealed with silicone grease to prevent leaks but this was removed with ether before weighing the filter and the coil.

To remove any moisture which condensed on the outside of the filter and condensation coil, they were heated to 120°C for 5 minutes. The evaporation of dimonyl phthalate during this time was negligible.

Any experiment in which the increase in weight of the condensation coil was greater than 5% of the increase in weight of the filter was rejected since this was accepted as evidence that the filter was saturated or that there was a leakage of air into the apparatus. Moisture could easily be detected in the condensation coil as the droplets did not wet the walls.



QUICK RELEASE VALVE

FIGURE 9 3

IX. 5. Performance of the apparatus.

Experimental values of the mass concentration were compared with those calculated from the vapour pressure assuming complete saturation at the temperature of the evaporator. They were found to differ by a factor of one tenth due to incomplete saturation and dur to deposition of aerosol on the walls of the condensation tube.

IX. 6. Accuracy of the measurements.

The accuracy fo the method depends on the accuracy of weighing, measuring the flow rate and time of collection. The balance used to weigh the filters was subject to an error of ± 0.1 mgm., the filters were found to be constant to ± 0.2 mgm., and the total increase in wieght was of the order of 0.1 gms. The maximum error of the flow gauge was 0.5 $cm^3.sec.^{-1}$ at a flow rate of 20 $cm^3 sec^{-1}$ and the stopwatch was found to have an error of ± 0.2 seconds by comparison withthe Post Office telephone clock (TIM) over a period of 1 hour.

The standard deviation $\sigma(m)$ of the measurements of mass concentration (m) is given by

$$\sigma(m) = m\left[\frac{V(w)}{w^2} + \frac{V(f)}{f^2} + \frac{V(t)}{t^2}\right]^{\frac{1}{2}} \qquad (1)$$

where V(w) etc. stands for the variance of w etc.

w is the increase in weight of the filters

f is the volume of gas measured

t is the time of observation.

The standard deviation of the measurements of mass concentration varied from 0.5 % at 10^{-4} gm. cm.$^{-3}$ to 2 % at 5.10^{-6} gm. cm.$^{-3}$.

CHAPTER X.

THE THEORY OF COALESCENCE.

X.1.

In discussing coagulation, it has been assumed that coalescence always occurs as the result of binary collision. The theoretical discussion which follows indicates that this assumption may be untrue and that coalescence occurs only under certain conditions.

Derjaguin (1935) observed that when charged particles struck a plane surface some of them rebounded and Tunitsky (1939) derived an expression for the coagulation coefficient of charged particles. It is proposed to use a rather different approach and to derive a more general expression.

X.2. The general theory.

In chapter V., the problem of diffusion in a field of force was discussed with special reference to the earth's gravitational field. The Smoluchowski equation (1) can be used when the force is no longer constant.

Now $$\frac{\partial \omega}{\partial t} = \mathrm{div}_r\left(\frac{q}{\beta^2}\,\mathrm{grad}_r\,\omega - \frac{K}{\beta}\,\omega\right) \qquad (1)$$

where ω is the probability that the particle has co-ordinate $\underline{r}$ at a time t.

$$q = \frac{\beta kT}{m}$$

$$\beta = \frac{6\pi\eta aF}{m}$$

$\underline{K}$ is the acceleration per unit mass caused by the field of force.

The force may be due to a potential V where

$$\underline{K} = -\text{grad}_r\ V$$

Such a force may be due to the following causes :-

1. Free electric charges on the particles.
2. Intermolecular forces - the Van der Waals forces.
3. The momentum of evaporating molecules.
4. The momentum of gas molecules leaving the surface of the drop. c.f. the radiometer effect.
5. Radiation pressure; this is in general a negligible force.

Now $$\frac{\partial}{\partial}\frac{w}{t} = -\text{div}_r\ j \qquad (2)$$

where j was a steady diffusion current per unit area

and

$$j = \frac{K}{\beta} w - \frac{g}{\beta^2}\text{grad}_r\ w \qquad (3)$$

If the diffusion current is replaced by a flux F

then

$$j = \frac{\partial F}{\partial s}$$

where s represents area.

Consider one stationary particle, radius a, and others diffusing towards it, then the flux into unit solid angle is constant

i.e. $\frac{\partial F}{\partial \varphi} = \text{constant}$

where φ is a solid angle

Hence

$$j = \frac{1}{r^2} \frac{\partial F}{\partial \varphi} \tag{5}$$

where r is the modulus of the radius vector.

Substitute the potential V in equation (3) then :-

$$j = -\left[\omega \frac{\text{grad}_r V}{\beta} + \frac{q}{\beta^2} \text{grad}_r \omega \right]$$

which may be rearranged to give

$$j = -\frac{q}{\beta^2} \exp.\left(\frac{\beta V}{q}\right) \text{grad}\left[\omega \exp.\left(\frac{\beta V}{q}\right)\right]$$

hence $$j \exp\left(\frac{\beta V}{q}\right) = -D \text{ grad}_r\left[\omega \exp.\left(\frac{\beta V}{q}\right)\right] \tag{6}$$

since $\frac{q}{\beta} = D$

Substitute from (5)

$$\frac{1}{r^2} \frac{\partial F}{\partial \varphi} \exp\left(\frac{\beta V}{q}\right) = -D \text{ grad}_r\left[\omega \exp\left(\frac{\beta V}{q}\right)\right] \tag{7}$$

and $$\int_R^\infty \frac{\partial F}{\partial \varphi} \frac{1}{r^2} \exp\left(\frac{\beta V}{q}\right) dr = \int_\infty^R D \text{grad}_r\left[\omega \exp \frac{\beta V}{q}\right] dr \tag{8}$$

where R is the sphere of influence of the stationary sphere and R = 2a

Then since $\frac{\partial F}{\partial \varphi}$ is not a function r,

$$\frac{\partial F}{\partial \varphi} = \frac{\int_\infty^R D \text{ grad}_r\left(\omega \exp \frac{\beta V}{q}\right) dr}{\int_R^\infty \frac{1}{r^2} \exp\left(\frac{\beta V}{q}\right) dr} \tag{9}$$

The flux over the whole surface of thesphere, assuming symetry is given by

$$F = \frac{4\pi D \, w \exp \frac{\beta V}{q} \Big]_R^\infty}{\int_R^\infty \frac{1}{r^2} \exp \frac{\beta V}{q} \, dr} \qquad (10)$$

Now the boundary condition when complete absorption occurs at the surface of the sphere is

$$w_R = 0$$

Take $w_\infty = w_0$, the average value of the probability density at a distance from the sphere (11)

Also, in general $V_\infty = 0$

Then $$F = \frac{4\pi D w_0}{\int_R^\infty \frac{1}{r^2} \exp \frac{\beta V}{q} \, dr} \qquad (12)$$

When the problem of two diffusing particles a_1 and a_2 is considered, the relative diffusivity D_{12} must replace D where :-

$$D_{12} = D_1 + D_2 \qquad (13)$$

$$= 2D \text{ when particles are identical.} \qquad (14).$$

Hence $$F = \frac{8\pi D w_0}{\int_R^\infty \frac{1}{r^2} \exp \frac{\beta V_{12}}{q} dr}.$$

where V_{12} is the potential of one particle with respect to the other.

When an aerosol of numerical concentration n is considered, there are $\frac{n}{2}$ such possibilities of collisions, and the rate of

coagulation is

$$\frac{dn}{dt} = \frac{4\pi D n^2}{\int_{2a}^{\infty} \frac{1}{r^2} \exp \frac{V_{12} m}{RT}} \qquad (15)$$

putting $R = 2a$

and $\frac{\beta}{q} = \frac{m}{kT}$

Several examples are considered below.

X.3.1 The coalescence of particles having an electric charge.

Consider two particles having charges e_1 and e_2, then the potential V is given by the relation

$$V = \frac{e_1 e_2}{r} \qquad (16)$$

when the separation is r

Then $$\frac{dn}{dt} = \frac{4\pi D n^2}{\int_{2a}^{\infty} \frac{1}{r^2} \exp \frac{e_1 e_2}{r kT} dr}$$

Now put $r = \frac{1}{x}$

and $\xi = \frac{e_1 e_2}{kT}$

Then $$\frac{dn}{dt} = \frac{4\pi D n^2}{\int_{0}^{\frac{1}{2a}} \exp \xi x \, dx}$$

$$= \frac{4\pi D n^2}{\varepsilon^{-1}\left[\exp \varepsilon x\right]_0^{\frac{1}{2a}}}$$

$$= \frac{4\pi D n^2}{\varepsilon^{-1}\left[\exp \frac{\varepsilon}{2a} - 1\right]} \qquad \text{(c.f. Tunitsky 1939)}$$

$$= \frac{4\pi D n^2}{\frac{1}{2a}\left[1 + \frac{1}{2!}\frac{\varepsilon}{2a} + \frac{1}{3!}\left(\frac{\varepsilon}{2a}\right)^2 + \cdots\right]}$$

$$\simeq \frac{8\pi a D n^2}{\left[1 + \frac{\varepsilon}{4a}\right]} \qquad (17)$$

Now consider several examples of this. When the drops are uncharged

ε is zero

and $\frac{dn}{dt} = 8\pi Dn^2$

i.e. $\frac{dn}{dt} = Kn^2$ (18)

the value obtained by Smoluchowski.

When the drops have charges of equal magnitude and opposite sign

$$e_1 = -e_2 = e$$

$$\varepsilon = -\frac{e^2}{kT} \qquad \text{i.e. is negative}$$

$$\frac{dn}{dt} > Kn^2 \qquad (19)$$

When the drops have charges of equal magnitude and the same sign

$$e_1 = e_2 = e$$

$$\frac{dn}{dt} < Kn^2 \qquad (20)$$

The magnitude of the effect may be seen if $\mathcal{E}$ is evaluated.

$$\mathcal{E} = \frac{e_1 e_2}{kT}$$

$$= 1.42. \frac{e_1 e_2}{a} . 10^{-3}$$

where e_1 and e_2 are in units of electron charge

a is in microns.

Hence the expansion used to obtain relation (17) is legitimate provided

$$\frac{e_1 e_2}{a} < 10$$

When the particle size is of the order of 1 micron, charges of 10 electron units will have an appreciable effect on the rate of coagulation.

In an aerosol of concentration n particles $cm.^{-3}$ in which a fraction p of the particles have a positive charge, q a negative charge and s = (1 - p - q) are uncharged, the fraction of collisions between particles of like charge is g , between particles of unlike charge h and between uncharged particles is i, then the fraction of each type of collision is given in table 10.1

The number of collisions which can occur between one set of unlike particles, e.g. pq, is :-

(21)

$$\sum_{k=0}^{np} (np-k)(nq-k) \qquad \text{and} \quad p < q \quad k = 0, 1, 2, 3, \ldots\ldots np$$

or $\sum_{K=0}^{nq} (np - K)(nq - K)$ $\qquad p > q$ $\qquad (22)$

Between like particles the number of collisions is :-

$$\sum_{K=0}^{np/2} (np - 2K)(np - 2K - 1) \qquad (23)$$

Table 10.1 Fraction of each type of collision

Type of collision	Participating fraction	Fraction of collisions
Unlike charges	pq $(p > q)$	$g = \frac{1}{n^2} \sum_{K=0}^{nq} (np-K)(nq-K)$
Like charges	pp	$h = \frac{1}{n^2} \sum_{K=0}^{p/2} (np-2K)(np-2K-1)$
	qq	$+ \frac{1}{n^2} \sum_{K=0}^{q/2} (nq-2K)(nq-2K-1)$
Uncharged particles	ps $(p > s)$	$i = \frac{1}{n^2} \sum_{K=0}^{ns} (np-K)(ns-K)$
	qs $(q > s)$	$+ \frac{1}{n^2} \sum_{K=0}^{ns} (nq-K)(ns-K)$
	ss	$+ \frac{1}{n^2} \sum_{K=0}^{s/2} (ns-2K)(ns-2K-1)$

The rate of coagulation is then

$$\frac{dn}{dt} = 8\pi a D n^2 \left[\frac{g}{1 - \frac{\varepsilon}{4a}} + \frac{h}{1 + \frac{\varepsilon}{4a}} + i \right] \qquad (24)$$

A collision between a charged and uncharged particle is considered to be identical with a collision between uncharged particles provided the material is nonpolar so that a charge distribution over the surface of a particle is not induced.

This theory is applicable for only a short time because collisions of particles alter the particle size and charge distributions in the aerosol. Also, if a particle participates in one type of collision, a fraction is then removed and the factors g, h, i, overestimate the fraction of each type of collision.

The changes in the charge distribution have been discussed by Tunitsky (1939).

M. 3.3 Evaporating droplets.

If a droplet of radius a is maintained in an atmosphere of its own vapour which is just saturated, evaporation occurs if

$$\frac{p}{p_\infty} > 1$$

Two droplets about to collide will be influenced by the evaporating molecule. They must pass through a potential barrier due to the energy of these molecules and the potential and its effect on the rate of coagulation are calculated below.

The molecules which evaporate from the droplet have energy 3/2 kT. This will be lost on collision with a molecule or with another particle.

If the mean free path of the vapour molecule is λ, a particle which collides with the one under consideration will encounter the molecules in a volume $\pi a^2 \lambda$.

Hence the potential distribution about the evaporating droplet is $V(r)$where

$$V(r) = \frac{3}{2} \pi c(r) a^2 \lambda kT \qquad (24)$$

where $c(r)$ is the number of molecules per unit volume at a distance r. The distribution of molecules diffusing from a spherical surface is given by equation (17) chapter V. It is :-

$$c = c_0 \left[1 - \frac{R}{r} + \frac{R}{r} erf \frac{r-R}{2(Dt)^{\frac{1}{2}}} \right] \qquad (25)$$

As before $\underline{K} = - grad_r V \qquad (26)$

and equation (15) is written

$$\frac{dn}{dt} = \frac{4\pi D n^2}{\int_R^\infty \frac{1}{r^2} exp \frac{V(r)}{RT} dr}$$

The integration would present considerably difficulty and the following assumptions are made to facilitate a solution of the problem. Provided that the mass which evaporates in a time t defined by

$$(Dt)^{\frac{1}{2}} = r - R \qquad (27)$$

is a negligible proportion of the droplet the distribution of molecules is approximately c so that

$$V \doteq \frac{3}{2}\pi c_0 a^2 \lambda kT \qquad (28)$$

The molecules which evaporate lose their original energy at a distance of one mean free path from the surface of the droplet and it can be assumed that :-

$$\left.\begin{aligned} V &= \tfrac{3}{2}\pi c_0 a^2 \lambda kT \quad \text{in the range } R < r < R + \lambda \\ \text{and } V &= 0 \quad \text{at } r > R + \lambda \end{aligned}\right\} \qquad (29)$$

Consequently

$$\int_R^\infty \frac{1}{r^2} \exp \frac{V}{RT}\, dr = \int_R^{R+\lambda} \frac{1}{r^2} \exp \frac{V}{RT}\, dr + \int_{R+\lambda}^{\infty} \frac{1}{r^2} \exp \frac{V}{RT}\, dr$$

$$= \frac{1}{R(R+\lambda)} \left[R + \lambda \exp \tfrac{3}{2}\pi c_0 a^2 \lambda \right] \qquad (30)$$

When two droplets collide, the concentration of evaporating molecules is effective at a distance 2λ not λ.

$$\frac{dn}{dt} = \frac{4\pi R D n^2 (R + 2\lambda)}{\left[R + 2\lambda \exp \tfrac{3}{2}\pi c a^2 \lambda\right]} \qquad (31)$$

If coalescence occurs when the two droplets are just in contact R = 2a and

$$\frac{dn}{dt} = \frac{8\pi a D n^2 (a+\lambda)}{\left[a + \lambda \exp \frac{3}{2}\pi c a^2 \lambda\right]} \qquad (32)$$

This equation is valid if the particle size does not change appreciably due to evaporation during the time considered.

If no evaporation occurs, then equation (32) is identical with Smoluchowski's coagulation equation. For example, consider 0.1 micron droplets of dinonyl phthalate at 20°C. Then the numerical concentration of the vapour molecules is of the order of 10^{5} cm.$^{-3}$ and the exponent is of the order of exp. 10^{-10} which is negligible. However, for water droplets of the same size the exponent becomes exp. (10^{5}) and the coagulation rate would then be negligible.

X.3.2. The effect of Van der Waals forces.

Tikhomirov et al (1942) state that due to van der Waal's forces the rate of coagulation is increased by a factor

$$\frac{1}{2\int_{2R}^{\infty} \frac{R^2}{r^2} \exp \frac{E}{RT} \frac{dr}{R}} \qquad (33)$$

of equation (14).

No derivation is given but the forces are stated to cause an attraction

$$\frac{-Q \frac{m_1}{\rho} \frac{m_2}{\rho}}{r^6} \qquad (34)$$

London (1930) has calculated the interaction energy between two atoms. The potential is :-

$$V = -\frac{3}{4} h \nu_0 \frac{P^2}{r^6} \qquad (35)$$

where ν_0 is a characteristic frequency

h is Planck's constant

P is the polarizability of the atoms

r is the separation of the atoms.

He also assumed that these forces are additive.

X.4. Discussion.

The theory developed in this section indicates that coagulation occurs at a rate which is different from that calculated by Smoluchowski and the examples given indicate that the variation may be considerable under certain conditions. The problem of calculating the changes in particle size distribution and charge distribution has been briefly discussed and certain relevant relations have been indicated.

In deriving the theory, it was assumed that coalescence would occur immediately if two particles made contact. However there is the possibility of films being adsorbed on the surface of the drops when the energy of cohesion of the liquid in the two droplets might be affected so that coalescence is hindered. In such a case colliding droplets would require suffieient energy to enable the surface to increase and to disrupt the film.

Two drops approaching one another sweep away gas molecules in their paths. When their separation is small, the resistance β will be increased since the gas molecules can no longer move freely. (c.f. e.g. Chapter II.)

In this section, a number of factors influencing coalescence have been considered. The relation produced initially is sufficiently general to enable other factors to be considered but difficulty may be encountered in calculating the potential barrier which must be penetrable for coalescence to occur.

CHAPTER XI.

CONCLUSIONS.

The purpose of this investigation was to obtain information concerning the concentration changes which occur in an aerosol. The aerosols examined consisted of liquid droplets of radii in the range 0.08 to 2 microns and in concentrations up to 10^7 particles per cubic centimetre.

Many of the previous studies have been made without sufficient control of the variables and without an adequate theoretical investigation. One of the more rigorous investigations was carried out by Gillespie et al (1947) and (1953) who examined the changes which occurred in the concentration of an aerosol enclosed in a cube having a volume of 0.2 cubic metres. They showed that the rate of change in concentration could be represented by the equation

$$\frac{dn}{dt} = -kn^2 - \beta n \qquad (1)$$

The coagulation parameter k and the surface loss parameter β varied by a factor of 10 for aerosols of similar size distribution.

In the present work, it has been shown that the concentration changes in dilute aerosols can be represented by

the partial differential equation :-

$$\frac{\partial c}{\partial T} = \alpha \frac{\partial^2 c}{\partial Z^2} - \frac{\partial c}{\partial Z} \qquad (2)$$

This was derived on the assumption that there was no mass motion in the aerosol, that the particles were involatile and that the effects of coagulation were negligible. In chapter V. the following equation was derived to account for the effects of coagulation in addition :-

$$\frac{\partial c}{\partial T} = \alpha \frac{\partial^2 c}{\partial Z^2} - \frac{\partial c}{\partial Z} - \gamma c^2 \qquad (3)$$

This was derived on the assumption that every collision between two particles resulted in coalescence and this assumption was discussed in more detail in chapter X. The effects of electric charges on the particles and of evaporation of the droplets were considered.

The experimental work was carried out using a monodisperse aerosol produced by a generator similar to that used by La Mer. The interpretation of the experimental results was thereby simplified. Three methods of determining particle size and concentration in an aerosol were employed. In the

preliminary experiments, a sedimentation cell was used to take samples of the aerosol but the method was shown to be unreliable. Subsequently, the aerosol was examined while enclosed in a special cell. At low concentrations, the photographic method was found to be adequate, but when the concentration was sufficiently high for the photographic images to overlap, a photometric method was used.

The La Mer generator was used since the information available indicated that aerosols of low dispersions could be produced. The ratio of the standard deviation to the mean of the particle radius was used by La Mer as a criterion of dispersion: an aerosol being termed monodisperse if the ratio were less than 0.1. There are no published data with which to compare the dispersion obtained but the values were slightly larger than 0.1.

The ranges of particle sizes (0.08 to 2 microns) and concentrations (10^3 to 10^7 particles per cubic centimetre) produced by the generator were adequate for this work but the control of the apparatus was not as rigid as might be desired. The characteristics of the aerosol being produced could easily be changed but the magnitude of the change was rather indefinite so that the required setting was ultimately obtained by trial and error. To obtain aerosols of lower dispersion would require very

accurate control of the temperature of the apparatus, removal of all gaseous ions which might form and perhaps fractionation of the nuclei.

With the photographic technique the individual particles could be observed on the photomicrographs obtained and it was found possible to measure particles of radius 0.08 to 2 microns with an error of $\pm$ 2% and on concentrations of 10^4 to 10^7 particles per cubic centimetre.

The range of application of the technique is limited for very small particles by the effect of Brownian motion and for large particles by the short time taken to settle out completely. Concentrations up to 10^7 particles per cubic centimetre could be determined without the error due to overlap becoming appreciable. The lower limit was imposed by the statistical errors becoming appreciable when less than 10 particles were visible in the photomicrographs.

The values of the parameter α which were obtained from over twenty measurements of concentration were in good agreement with theoretical values provided that the effect of statistical fluctuations in concentration had been smoothed out.

Since the measurements of concentration involved very much smaller errors than the measurement of particle size, the method would appear suitable for the determination of the ultramicroscopic

particles.

The photometric technique used a method of analysis dependant on optical scattering measurements which are applicable in the range 0.1 to 1 micron. Concentrations in the range 10^3 to 10^9 particles per cubic centimetre can be measured but it is expected that the accuracy is diminished at higher concentrations due to the effect of secondary scattering.

The method is at present limited to the study of aerosols of low dispersion but it would appear possible to develop it for the study of polydisperse aerosols if measurements are made of the light scattered in various directions.

In chapter V. two theories relating to concentration changes in an aerosol were discussed. Davies' transformation of Smoluchowski's equation has been shown as a result of the present experimental investigation to give an accurate description of the changes occurring in a dilute aerosol. The experimental and theoretical values of the parameter λ were in good agreement with one another as seen in figure 7.25 but there is a discrepancy when the aerosol is disperse since λ is a function of the cube of the radius.

The second equation which is applicable to the changes in a concentrated aerosol, has been developed by the author but cannot be appraised until further measurements have been made. The values of the coagulation parameter can then be used to

examine the coalescence theory developed in chapterX.

A numerical analysis was used in the calculation of the parameter α. Since the measurements of concentration were subject to statistical fluctuations, considerable smoothing of many readings was carried out to obtain a single value of the parameter.

With the photometric determination however, a larger volume was examined, more readings were obtained and consequently the results were much more consistent and it should be possible to utilize them without further treatment.

The equations derived in chapter V for the rate of change of concentration due to sedimentation, diffusion and coagulation in an aerosol is applicable to other systems. For example in certain flames, molecules(or radicles) are produced, diffuse migrate and recombine. In a spark, ions are formed, diffuse and migrate in an electric field and there is the possibility of recombination of positive and negative ions. In a wet film of paint, which contains several pigments which are initially well mixed, the colour changes considerably as particles of different pigments diffuse to the air-paint interface, and to the paint-substrate surface and also settle, float or form aggregates.

The future development of the theory would appear to require consideration of mass motion. Indeed, the next step might well

be accomplished by replacing the diffusivity of a particle by the eddy diffusivity but it could no longer be assumed that complete absorption of particles occurred at the surface of the enclosure. The sedimentation velocity might be modified to account for mass motion produced by convection.

The Brownian motion of particles has several other effects in addition to the diffusion of the aerosol.

In particular an uncertainty of $(2Dt)^{\frac{1}{2}}$ is attached to the determination of the position of a particle, at any time. If the time t of observation is made long enough for it to be measured accurately the position of the particle becomes uncertain. This principle is of fundamental importance in all measurements made with instruments of such high resolution that molecular phenomena become observable.

The photometer described in chapter VIII needs modification. Compensation must be made for the flicker of the arc and the response should be made logarithmic. Further, tabulation of the scattering functions is required at smaller intervals and this can be achieved by interpolation using the present tables. It should then be possible to obtain the required data for comparison of the calculated and experimental values of the coagulation parameter and to test the coagulate theory developed in chapter X.

The initial problem to be investigated concerned the changes in concentration of an aerosol which was completely enclosed. A certain aspect of this problem has been investigated when the environment of the aerosol was rigorously controlled. This leads the way to a more detailed understanding of the phenomena occurring in an aerosol. The next steps should be the investigation of changes in aerosols of very much higher concentrations, and should be extended to aerosol which are in mass motion or which are produced from volatile materials.

Appendix 1.

Relaxation solution of the equations derived in chapter V.

A solution of equation (26) was attempted using relaxation methods. It was seen that this equation could be expressed in terms of finite differences instead of in differentials.

i.e. $$0 = -\gamma c_o^2 - \frac{2\alpha}{h^2} c_o + \left(\frac{\alpha}{h^2} - \frac{1}{2h}\right) c_1 + \left(\frac{\alpha}{h^2} + \frac{1}{2h}\right) c_3 - (c_2 - c_4) \frac{1}{2h^2} \quad (1)$$

The right hand side of this equation is zero when the equation contains the true values of c. For an approximation to c, there is a residual R and the equation may be written

$$R = -\gamma c_o^2 - \frac{2\alpha}{h^2} c_o + \left(\frac{\alpha}{h^2} - \frac{1}{2h}\right) c_1 + \left(\frac{\alpha}{h^2} - \frac{1}{2h}\right) c_3 - (c_2 - c_4) \frac{1}{2h^2} \quad (2)$$

The relaxation technique may be used to obtain a solution of the equation (i.e. when R = 0) by assuming numerical values of c at intervals of Z and T, and calculating the residual. Using the network of values of c in the Z T plane, as shown in figure 1, values of c are assumed and the residual R is calculated at each point in the network. Then by the operation represented in figure 2

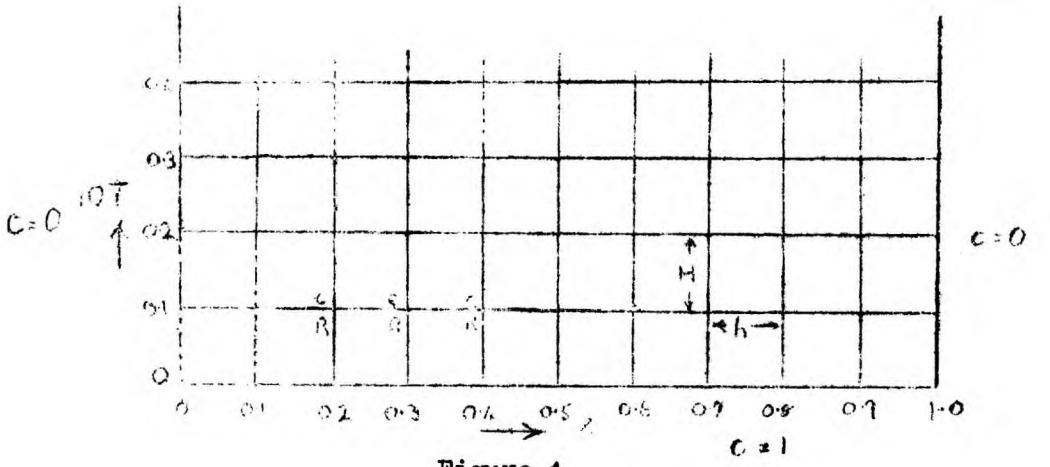


Figure 1.

the residual at each point is made zero.

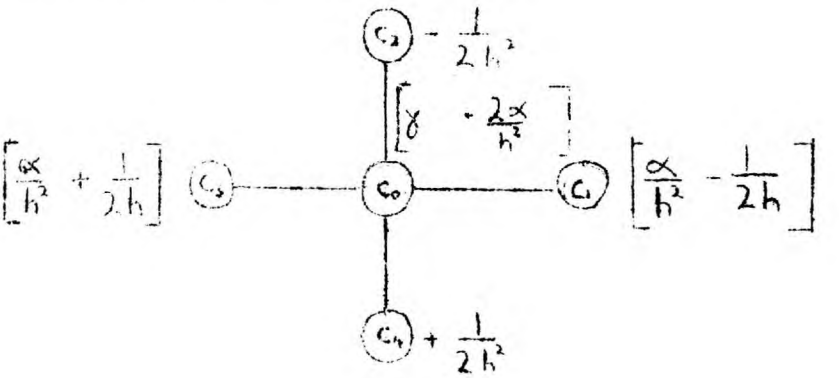


Figure 2.

(N.B. This operator is non-linear)

As an example consider the point Z = 0.3, T = 0.3 where the value of c can be represented by c (3.3) and take an interval h = 0.1.

Then a unit operator decreases c (3.3) by $(\gamma + \frac{2\alpha}{0.01})$ and the effects on the other four values of c are

c_0	$c(3.3)$	Increment to c = -1	Increment to residual = $-(\chi + \frac{2\alpha}{0.01})$
c_1	$c(4.3)$	0	$= + (\frac{\alpha}{0.01} - \frac{1}{0.2})$
c_2	$c(3.4)$	0	$- \frac{1}{0.02}$
c_3	$c(2.3)$	0	$+(\frac{\alpha}{0.01} + \frac{1}{0.2})$
c_4	$c(3.2)$	0	$+ \frac{1}{0.02}$

By repeated operations, it is possible to make the residuals zero at each node of the network and the correct values of c have thus been obtained.

The solution of the sedimentation-diffusion equation was attempted by this method (i.e. when $\chi = 0$) but it was found that the solutions converged very slowly, rounding-off errors and arithmetical mistakes accumulated so that the method was rejected.

The differential equations may be considered as two problems. A 'jury' problem in the Z direction, where c is defined at the boundaries $Z = 0$ and $Z = 1$ and the values of c must be found between the two boundaries, and a 'marching' problem in the T direction where c is defined at $T = 0$ and the rate of change $\frac{\partial c}{\partial T}$ must be used to obtain values of c at subsequent values of T. The 'marching' problem is more difficult to solve and probably causes the slow convergence of the solutions.

Appendix 2. Sedimentation in a Polydisperse Aerosol.

If the particle size in the aerosol follows a Gaussian distribution then $c(a)$ represents the fraction of particles having radii in the interval a to $a + da$

$$c(a) = \frac{2}{\sigma\sqrt{2\pi}} \exp. - \frac{|a - \bar{a}|^2}{2\sigma} da \qquad (1)$$

Then the fraction of particles having radii greater than a_1 is

$$c(a > a_1) = \text{erf}\frac{a_1 - \bar{a}}{\sigma} \qquad (2)$$

In sedimentation a particle of radius a_1 initially at $z = 0$ will reach a position z_1 in a time t, so that the sedimentation velocity v_1 of the particle is given by

$$v_1 = \frac{z_1}{t_1} \qquad (3)$$

This velocity is approximately proportional to the square of the radius :-

$$\text{i.e. } v_1 = b\, a_1^2 \qquad (4)$$

If z and t are written in terms of the reduced co-ordinates Z and T (see chapter V.)

$$Z = \frac{z}{L}$$

$$T = t\frac{\bar{v}}{L}$$

$$\frac{z_1}{t_1} = \frac{Z_1}{T_1}\,\bar{v} \qquad (5)$$

Then from equations (3), (4) and (5) it can be shown that

$$a_1 = \frac{Z_1}{T_1}\left(\frac{\bar{v}}{b}\right)^{\frac{1}{2}} \qquad (6)$$

Since equation (4) can be used to determine the r.m.s. radius $(\bar{a}^2)^{\frac{1}{2}}$, equation (6) can be rewritten as :-

$$a_1 = \frac{Z_1}{T_1}^{\frac{1}{2}}\,(\bar{a}^2)^{\frac{1}{2}} \qquad (7)$$

If at a time T_1 all particles of radius a_1 have just fallen below the co-ordinate Z , the concentration of all particles at Z_1 is given by the relation

$$c\,(Z_1 T_1) = \operatorname{erf}\left[\left(\frac{Z_1}{T_1}\frac{\bar{a}^{-2}}{}\right)^{\frac{1}{2}}\frac{1}{\sigma} - \frac{1}{\sigma}\right] \qquad (8)$$

where σ is the dispersion $\frac{\sigma(a)}{\bar{a}}$

Nomenclature.

Where ambiguity may arise symbols are defined in the text.

A	collision area for gas and vapour molecules.
a	radius of a particle
$\bar{a}$	arithmetic mean radius.
α	coefficient of accommodation for molecules on a surface.
α	the parameter in the equation of diffusion and sedimentation $= \frac{D}{v L}$
b	breadth of beam
β	dynamical friction experienced by a particle/unit velocity $= \frac{6\pi\eta r}{m}$
c	velocity of light
c_o	numerical concentration of vapour molecules.
c	numerical concentration of vapour over a plane surface at saturation.
c	relative concentration of particles $= \frac{n}{n_o}$
γ	parameter in the equation of diffusion, sedimentation and coagulation $= \frac{Kn_o L}{v}$
γ	rate of cooling of vapour in degrees centigrade per unit time.
γ	angle

D	diffusivity of a particle.
D_r	diffusivity of a molecule
$\mathcal{D}$	dispersion of radii of particles or coefficient of variation of radius $= \frac{\sigma(a)}{\bar{a}}$
d	length of particle track
e	exposure time - of photograph
e	electric charge
E	electric field intensity
$\mathcal{E}$	error due to overlap
ϵ	dielectric constant
f	frequency
F	the slip factor for a particle moving in a fluid
F	flux of energy or of particles
g	acceleration due to the force of gravity
η	viscosity
h	interval ΔZ used in difference equation
H	interval ΔT used in difference equation
I	luminous intensity of scattered light
I_o	intensity of incident light
j	a diffusion current
k	Boltzman's constant
K	scattering area coeffident.
K	the coagulation coefficient $= \frac{4}{3}\frac{kT}{\eta}F$
$\underline{K}$	force exerted on unit mass in a field
L	a length

L	depth of observation cell
λ	mean free path of gas molecules
λ	wavelength of light
m	mass of a droplet
m_1	mass of a molecule
m	refractive index
M	magnification of a photograph
n	numerical concentration expressed as particles per cubic centimetre.
N	Avagadro's number.
P	atmospheric pressure
p	vapour pressure
p_a	vapour pressure at a plane surface
p_n	radiation pressure
p_r	vapour pressure at surface of radius r
q	$\frac{\beta kT}{m}$ where $\beta = \frac{6\ r}{m}$
R	a radius
R	sphere of influence of a particle
R	the gas constant
r	radius vector
ρ	density of material of particle
ρ_o	density of gas
S	Poynting's vector
s	surface area
σ (a)	standard deviation of a
γ	surface tension

τ	element of volume
θ	angle
t	time
T	reduced time co-ordinate
T	absolute temperature
u	velocity
v	sedimentation velocity (unless specified)
V(a)	variance of a
V	volume of particles per cubic centimetre of aerosol
V	potential
ϕ	solid angle
w	width of beam
x,y,z	spatial co-ordinates
X,Y,Z	reduced spatial co-ordinates
ω (ru)	probability of particles having co-ordinates ru.

BIBLIOGRAPHY.

GENERAL.

Electronics.

Terman, F.E. (1947). Radio Engineering. 3rd Edtn. McGraw Hill Book Co. Inc. N.Y.& London.

Microscopy.

Martin, L.C. and Johnson, B.K(1931). Practical Microscopy. 1st. Edtn. Blackie & Son Ltd. London & Glasgow.

Mathematics. General.

Margenan, H. and Murphy, G.M. (1943). The Mathematics of Physics and Chemistry. 1st. Edtn. Van Norstrand Co. Inc. N.Y.

Pipes, L.A. (1946). Applied Mathematics for Engineers and Physicists. 1st. Edtn. McGraw Hill Book Co. Inc. N.y. & London.

Operational Methods.

Churchill, R.V. (1944). Modern Operational Mathematics in Engineering. 1st. Edtn. McGraw Hill Book Co. Inc. N.Y. & London.

Numerical Analysis.

Hartree, D.R. (1952). Numerical Analysis. 1st. Edtn. The Charendon Press, Oxford.

Relaxation Methods.

Fox, L. (1948). Q Journal Mech, and Appl. Mathematics. 1, 253

Statistics.

Kendall, M.G. (1943). The Advanced Theory of Statistics. Vol. I. 1st. Edtn. Griffin.

Stochastic Processes.

Chandrasekhar, S. (1943). Rev. Mod. Phys. 15, 34

Optics.

Monk, G.S. (1937). Light Principles and Experiments. 1st. Edtn. McGraw Hill Book Co. Inc. N.Y. & London.

Photography.

The Ilford Manual of Photography. Ed. Mitchell, J. 1944. 3rd. Edtn. Ilford Ltd., London.

REFERENCES.

Armitage, P. 1949. Biometrika 36, 257.

Beckers, R. and Döring, W. 1935, Ann. Phys. Lpz. 24, 719

Bergers. 1942. Nederl. Ark. v. Wetenschappen Proc. 45, 126

Birks, J. and Bradley, R.S. 1949. Proc. Roy. Soc. A198, 226

Born, H.J. and Zimmes, K.G. 1940. Naturwiss 28, 447

Bradley, R.S., Evans, M.G. and Whytlaw-Gray, R.W. 1946, Proc. Roy. Soc. A186, 368

Bradley, R.S. and Shellard, A.D. 1949. Proc. Roy. Soc. A198, 239

Chandrasekhar, S. 1943. Rev. Mod. Phys. 15, 1

Cunningham . 1910. Proc. Roy. Soc. A83, 357

Dady. 1947. Comptes Rendues Acad. Sci. Paris. 225, 1349

Davies, C.N. 1947. Trans. Inst. Chem. Eng. Symposium on Particle Size Analysis. 25, 12

Davies, C.N. 1949. Proc. Roy. Soc. A200, 100

Dimmock, N.A. 1950, Nature, London. 66, 686

Einstein, A. 1905. Ann. der Physik. 17, 549; 1906, 19, 371

Engstrom, R.W. 1947, J. Opt. Soc. Amer. 37, 420

Fairs, G.L. 1943. Chemistry and Industry. 62, 374

Fick, A. 1855. Phil. Mag. 10, 30

Findeisen, W. 1932. Gerlands Beiträge zdr Geophysik. 35, 295

Fuchs, N. 1935. Acta Physicochim URSS. 3, 61

Fürth, R. 1917. Arn. der. Phys. 53, 177

Gillespie (1947) - Langstroth, G.O. and Gillespie, T. 1947. Canad. J. Res. B25, 455

Gillespie 1953. Proc. Roy. Soc. A216, 569

Hopper, V.D. and Grant. 1948. Aust. J. Sci. Res. A1, 28

Hopper, V.D. and Laby, T.N. 1941. Proc. Roy. Soc. A178, 243

Jost, W. 1952. Diffusion in solids, liquids and gases. 1st. Edtn. Academic Press Inc. N.Y.

Jander and Wygash. 1938. Kolloid. Zeits. 85, 1

Jones, F.W. 1941. J. Sci. Instr. 18, 157

Joos, G. 1934. Theoretical Physics. 1st. Edtn. Blackie & Son Ltd.

Knudsen and Weber. 1911. Ann. Phys. Lpz. 36, 982

Lqdenburg. 1907. Ann. der. Phys. 22, 287

London, F. 1930. Physikal Z. 60, 491; 63, 245

Lowan, A.N. 1949. Tables of scattering functions for spherical particles. N. Bur. of Standards. Appl. Maths. Series 4 U.S. Gov. Printing Office Washington.

La Mer, V.K. Private Communication. (1952)

La Mer, V.K., Inn. E.C.Y and Wilson, I.B. 1950. J. Coll. Sci. 5, 471

La Mer, V.K. and Sinclair, D. 1949. Chem. Rev. 44, 261

Mason, M. and Weaver, W. 1924. Phys. Rev. 23, 412

May, K.R. 1945. J. Sci. Instr. 22, 177

May, K.R. 1949. J. Appl. Phys. 20, 932

Merrington, A.C. and Richardson, E.G. 1947. Proc. Phys. Soc. London, 59, 1.

Mie, G. 1908. Ann. der Physik. 25, 377

Millikan, R.A. 1913. Phys. Rev. 2, 109

Patterson, H.S., Whytlow-Gray, R. and Cawood, R. 1927. Proc. Roy. Soc. A116, 540

Patterson, H.S., Whytlow-Gray, R. Cawood, R. 1929. Proc. Roy. Soc. A 124, 502

Patterson, H.S. and Cawood, R. 1932. Proc. Roy. Soc. A136, 538

Perrin, J. 1916. Atoms, London. Constable.

Lord Rayleigh, 1903. Scientific Papers 4, 400. Cambridge University Press.

Reiss, H. 1951. J. Chem. Phys. 19, 482

Schwechendeck. 1950. Z. Natur. Forsch. 5a, 153

Sinclair, D. 1950. Handbook on aerosols. p.81. U.S. Atomic Energy Commission Washington, D.C.

Small, P.A., Small, K.W. and Cowley, P. 1948. Trans Faraday Soc. 44, 810

von Smoluchowski, M. 1915. Ann. der. Physik. 48, 103

von Smoluchowski, M. 1916. Phys. Zeit. 17, 557; 17, 587

von Smoluchowski, M. 1917. Z. Physik. Chem. 92, 129

Stull, D.R. 1947. Ind. Eng. Chem. 39, 517

Sturtevant, J.M. 1947. Rev. Sci. Instr. 18, 124

Swinbank. 1947. Nature London, 159, 849

Thomson, J.J. 1903. Conduction of Electricity through Gases. 1st. Edtn. Cambridge University Press.

Thomson, W. 1881. Phil. Mag. 42, 448

Tikhomirov, Tunitsky and Petrjanov. 1942. Acta Physicochim. 17, 185

Tunitsky. 1939. J. Phys. Chem. Moscow. 13, 1141

Weil, R. 1947. Phil. Mag. 37, 643

Westgren, A. 1916. Arkiv fur Matematik Astronomi och Fysik. 11, Nos.8 & 14 1918, 13, No. 14

Wright. 1936. Proc. Phys. Soc. 48, 675

Van der Hulst, H.C. 1946. The Optics of Spherical Particles. Recherches Astronomique de L'Observatoire d'Utrecht, 11, Pt.1

Van der Hulst, H.C. 1949. J. Coll. Sci. 4, 79

Zsigmondy and Siedentopf. 1903. Ann. der. Physik. 10, 1.